

DISS ETH NO. 20753

**SEDIMENTARY LIPID BIOMARKERS AND TRACE METALS AS
INDICATORS FOR PAST HYPOXIA AND EUTROPHICATION**

A dissertation submitted to

ETH ZURICH

for the degree of

DOCTOR OF SCIENCES

presented by

SEBASTIAN NÄHER

Dipl.-Geol., Johannes Gutenberg University of Mainz, Germany

born on July 26th, 1984

citizen of Germany

accepted on the recommendation of

Prof. Dr. Rolf Kipfer, examiner

Dr. Carsten J. Schubert, co-examiner

Prof. Dr. Bernhard Wehrli, co-examiner

2012

Dedicated to my family

“All our dreams can come true, if we have the courage to pursue them.”

(“Alle Träume können wahr werden, wenn wir den Mut haben, ihnen zu folgen.“)

Walt Disney

Contents

Summary.....	9
Zusammenfassung	11
Chapter 1: Introduction	13
1.1 Background and objectives.....	13
1.1.1 Definitions of hypoxia and anoxia in lakes and oceans.....	13
1.1.2 Causes and consequences of hypoxia and eutrophication	14
1.1.3 Organic proxies – lipid biomarkers	16
1.1.4 Inorganic proxies – iron and manganese	19
1.2 Outline	19
Chapter 2: Impact of recent lake eutrophication on microbial community changes as revealed by high resolution lipid biomarkers in Rotsee (Switzerland).....	25
Abstract.....	25
2.1 Introduction	26
2.2 Material and methods	27
2.2.1 Study site and sample collection.....	27
2.2.2 Age model.....	30
2.2.3 Bulk parameters	30
2.2.4 Biomarker analysis	30
2.2.5 XRF core scanning	32
2.2.6 Diatom analysis	32
2.2.7 Definition of BIT _{CH} index.....	32
2.3 Results and discussion	33
2.3.1 Sedimentation rate and age model.....	33
2.3.2 Eutrophication and sewage input history of Rotsee	34

2.3.3	Terrestrial OM sources	38
2.3.4	Input and degradation of sedimentary OM	42
2.3.5	Impact of eutrophication on microbial community changes	42
2.3.5.1	<i>Primary producers</i>	42
2.3.5.2	<i>Bacteria and Thaumarchaeota</i>	45
2.3.5.3	<i>Diatoms</i>	46
2.3.5.4	<i>Methanogenic and methanotrophic archaea</i>	49
2.4	Summary and conclusions	51
2.5	Acknowledgements	52

Chapter 3: Maleimides in recent sediments – Using chlorophyll degradation products for palaeoenvironmental reconstructions 53

Abstract	53
3.1 Introduction	54
3.2 Methods	56
3.2.1 Study sites and sample collection	56
3.2.2 Sample preparation	57
3.2.2.1 <i>Lipid biomarkers and pigments</i>	57
3.2.2.2 <i>Free and oxidised maleimide analysis</i>	58
3.2.2.3 <i>Chromic acid oxidation of methyl pyropheophorbide a</i>	59
3.2.2.4 <i>Instruments</i>	60
3.2.3 Definition of Me,Me and Me,Et indices	61
3.3 Results and discussion	61
3.3.1 Me,vinyl and Me,Et maleimides in the free and oxidised fraction from Rotsee samples.....	61
3.3.2 Me,H and Me,Me maleimides in the free and oxidised fraction from Rotsee samples.....	67
3.3.3 Maleimides and photic zone euxinia in Rotsee	69
3.3.4 Sources of other maleimides in the oxidised fraction from Rotsee samples	72
3.3.5 Maleimides in samples from the Romanian Black Sea Shelf.....	73
3.3.6 Factors responsible for chlorophyll degradation and maleimide formation	76
3.3.7 Maleimide degradation indices	77
3.4 Conclusions	79

3.5	Acknowledgements	80
3.6	Appendix	81
Chapter 4: Tracing bottom water oxygenation with sedimentary Mn/Fe ratios in Lake Zurich, Switzerland.....		87
	Abstract.....	87
4.1	Introduction	88
4.2	Materials and methods.....	91
4.2.1	Study site	91
4.2.2	Developments of bottom water oxygenation in Lake Zurich	92
4.2.3	Core retrieval and age model.....	92
4.2.4	XRF core scanning	93
4.3	Results.....	94
4.3.1	Ca, Mn and Fe seasonality.....	94
4.3.2	Mn/Fe ratios along a core transect.....	96
4.3.3	Mn/Fe ratios as a proxy for bottom water oxygenation.....	97
4.4	Discussion	102
4.4.1	Bottom water oxygen reconstructions based on Mn/Fe ratios.....	102
4.4.2	Indication of diagenetic alteration of the Mn/Fe ratio	103
4.4.3	Oxygen concentrations in the early 20th century in Lake Zurich	105
4.5	Conclusions	105
4.6	Acknowledgements.....	106
Chapter 5: Environmental variations in a semi-enclosed embayment (Amvrakikos Gulf, Greece) – reconstructions based on benthic foraminifera abundance and lipid biomarker pattern		107
	Abstract.....	107
5.1	Introduction	108
5.2	Regional setting.....	110
5.3	Methods	111

5.4	Results	113
5.4.1	Sediment cores and age model	113
5.4.2	Benthic foraminifera	114
5.4.3	Bulk parameters and biomarkers	117
5.5	Discussion	121
5.5.1	Benthic foraminifera abundance	121
5.5.2	Benthic foraminifera clusters.....	121
5.5.3	Eutrophication, productivity and OM sources.....	124
5.5.4	Impact of eutrophication on benthic foraminifera and bacteria – Hypoxia reconstructions in the gulf	126
5.5.5	Impact of climate on stratification and oxygen replenishment.....	129
5.6	Conclusions	131
5.7	Acknowledgements	132
 Chapter 6: Conclusions and Outlook		133
 Acknowledgements		139
 Bibliography		141
 Curriculum vitae		171

Summary

Climate change and eutrophication are main reasons for large-scale alterations of aquatic ecosystems. Dramatically increased or persistent appearances of hypoxia and anoxia have caused mass mortality events or even species extinction. More specifically, human induced eutrophication since the industrial revolution has been a major driver for a dramatic decline of hypolimnetic oxygen concentrations in lakes. Although water treatment and remediation efforts have largely reduced nutrient levels and eutrophication, oxygen depletion still exists. The goal of this thesis was to reconstruct past oxygen depletion and eutrophication with sedimentary proxies. These reconstructions help to understand factors and processes that lead to oxygen depletion, which is a basis for the development of remediation strategies and the assessment of future impacts. Sedimentary proxies were studied in selected Swiss lakes (Rotsee, Lake Zurich), Amvrakikos Gulf (Greece) and the Black Sea (Romanian Shelf).

The eutrophication history of Rotsee was reconstructed using lipid biomarkers. The high resolution analysis of these markers revealed short-term environmental changes during the last 150 years of lake history, including changes in composition and abundance of microbial communities. The diatom species *Stephanodiscus parvus*, *Cyclotella radiosa* and *Asterionella formosa* were dominant sources of specific diatom biomarkers. Variations of methanogenic archaeal cell densities during the lake history and lipid cell contents could be estimated based on isoprenoidal glycerol dialkyl glycerol tetraethers (GDGTs). A new proxy for terrigenous OM input was proposed (BIT_{CH} index).

In the recent sediments of Rotsee and the Black Sea, maleimides (1*H*-pyrrole-2,5-diones) were studied, whereas most previous studies focused on ancient deposits. Most of the maleimides were formed in the sediments under the absence of oxygen. 2-Methyl-3-ethyl-maleimide (Me,Et) and 2-methyl-3-vinyl-maleimide (Me,vinyl) mainly originate from chlorophyll *a*, 2-methyl-maleimide (Me,H) might be derived from chlorophyll-related compounds, which have lost ring E. 2-Methyl-3-*n*-propyl-maleimide (Me,*n*-Pr) and 2-methyl-3-*iso*-butyl-maleimide (Me,*i*-Bu) traced the presence of phototrophic sulphur bacteria (Chlorobiaceae), which indicated photic zone euxinic and anoxic conditions in Rotsee during the last 150 years and throughout the last ca. 9-10 ka in the Black Sea, which includes the

limnic phase of the Black Sea (Unit 3). Novel maleimide degradation indices are proposed to estimate the degree of OM degradation and are applicable on longer timescales than conventional indices.

The manganese to iron ratio was explored to reconstruct semi-quantitatively bottom water oxygenation in Lake Zurich. The redox dynamics of Mn were resolved with precise sediment core age models, monthly long-term oxygen monitoring data (1936-2010) and high-resolution XRF core scanning. Distinct Mn maxima coincided with annual maximum deep-water O₂ concentrations in spring, whereas the Fe signal is mainly the result of calcite dilution. However, sedimentological factors and geochemical and sediment focusing can limit the application of this proxy.

Benthic foraminifera and lipid biomarkers were used to examine the causes and impacts of eutrophication on the living biomass in Amvrakikos Gulf. During the last decades, productivity and bacterial biomass increased, benthic assemblages shifted towards opportunistic and tolerant species with a lower species density. Increased surface water temperatures and eutrophication led to decreased water column mixing and the development of seasonal photic zone euxinia throughout the gulf.

Zusammenfassung

Klimawandel und Eutrophierung sind Hauptgründe für grossräumliche Veränderungen aquatischer Ökosysteme. Vor allem die dramatische Abnahme der Sauerstoffgehalte wird zunehmend als Grund für das häufigere Auftreten von Massen- und Artensterben erkannt. In Seen hat durch Eutrophierung seit der industriellen Revolution eine dauerhafte Abnahme der Sauerstoffgehalte im Hypolimnion stattgefunden. Obwohl Abwasserreinigungs- und Sanierungsmassnahmen zu einer Reduktion der Nährstoffgehalte geführt haben, haben sich die Sauerstoffgehalte nicht wie erhofft erhöht. Das Hauptziel dieser Dissertation war die Rekonstruktion von Gewässereutrophierung und Sauerstoffverarmung mithilfe sedimentärer Indikatoren. Hierzu wurden sedimentäre Indikatoren in den Schweizer Seen Rotsee und Zürichsee, sowie im Ambrakischen Golf und dem Schwarzen Meer untersucht.

Die Eutrophierungsgeschichte des Rotsees wurde durch Biomarker (Lipide) rekonstruiert. Mittels Biomarker wurden Veränderungen in Zusammensetzung und Häufigkeit verschiedener mikrobieller Gemeinschaften während der letzten ca. 150 Jahre hochaufgelöst bestimmt. Zusätzlich konnten die Diatomeen *Stephanodiscus parvus*, *Cyclotella radiosa* und *Asterionella formosa* als dominante Quelle bestimmter Biomarker erkannt werden. Die zeitlichen Änderungen der Zelldichte methanogener Archaeen, sowie deren durchschnittlicher Lipidzellgehalt konnte mithilfe isoprenoidalen Glycerol-dialkyl-glycerol-tetraether (GDGTs) abgeschätzt werden. Es wird ein neuer Indikator für den Eintrag terrigenen organischen Materials vorgeschlagen (BIT_{CH} index).

Im rezenten Sediment des Rotsees und des Schwarzen Meeres wurden Maleinsäureimide (1*H*-Pyrrol-2,5-Dione) untersucht. 2-Methyl-3-Ethyl-Maleinsäureimid (Me,Et) und 2-Methyl-3-Vinyl-Maleinsäureimid (Me,vinyl) stammen hauptsächlich von Chlorophyll *a*, 2-Methyl-Maleinsäureimid (Me,H) von Chlorophyllen nach Verlust vom Ring E. 2-Methyl-3-*n*-Propyl-Maleinsäureimid (Me,*n*-Pr) und 2-Methyl-3-*iso*-butyl-Maleinsäureimid (Me,*i*-Bu) deutete auf phototrophe Schwefelbakterien (Chlorobiaceae) und somit auf anoxische und euxinische Bedingungen in der photischen Zone hin. Diese Bedingungen wurden sowohl während der letzten 150 Jahre im Rotsee als auch während der letzten 9000-10000 Jahre im Schwarzen Meer festgestellt und damit auch während der limnischen Phase (Sedimenteinheit 3). Neue

Maleinsäureimid-basierte Indikatoren wurden zur Abschätzung des Abbaugrades von organischem Material in Sedimenten entwickelt. Diese sind über längere Zeiträume anwendbar als konventionelle Indices.

Das Verhältnis von Mangan zu Eisen im Sediment des Zürichsees konnte für semi-quantitative Rekonstruktionen des Sauerstoffeintrags im Bodenwasser genutzt werden. Die Redoxdynamik von Mn im Seesediment konnte mithilfe präziser Altersmodelle, monatlichen Sauerstoffdaten (1936-2010) und hochaufgelöster Röntgenfluoreszenzmessungen nachvollzogen werden. Mn-Maxima korrelierten mit jährlichen Höchstkonzentrationen von Sauerstoff im Bodenwasser im Frühling, wogegen das Fe-Signal hauptsächlich durch Calcitverdünnung beeinflusst ist. Allerdings kann die Anwendung dieses Indikators durch sedimentologische Faktoren und geochemische und sedimentäre Fokussierungsprozesse eingeschränkt sein.

Einflüsse und Auswirkungen von Eutrophierung und Umweltveränderungen wurden durch benthische Foraminiferen und Biomarkern im Ambrakischen Golf untersucht. Während der letzten Jahrzehnte stieg die Produktivität und es folgte Übergang zu Opportunisten, Foraminiferengemeinschaften mit einem hohen Akzeptanzbereich hinsichtlich der vorliegenden Umweltbedingungen und einer niedrigen Speziesdichte. Höhere Oberflächenwassertemperaturen und Eutrophierung führten zu einer stabileren Schichtung der Wassersäule und zur Entwicklung von saisonal auftretenden euxinischen Bedingungen im Tiefenwasser, die auch die photische Zone erfassten.

Chapter 1: Introduction

1.1 Background and objectives

This introduction sets a general frame for the PhD thesis and gives a general overview over causes and implications of oxygen depletion and eutrophication in aquatic ecosystems. In order to provide basic background, oxygen depletion patterns in lakes and oceans are reviewed and defined. It is followed by an overview about the importance and implications of low oxygen conditions in these settings. Then, a summary of eutrophication as a major factor of oxygen decline is described. It is illustrated that sedimentary proxies are needed for palaeoxygen reconstructions and that there is still a need for high resolution records. Furthermore, a general introduction of the proxy groups used in this thesis is provided, which comprise lipid biomarkers and trace metals. Finally, the outline consists of an introduction to the different chapters, which summarises the achievements of this thesis.

1.1.1 Definitions of hypoxia and anoxia in lakes and oceans

Low oxygen conditions in aquatic settings have classically been categorised as “hypoxic” and “anoxic”, but no consistently used terminology, values and units exist (Canfield and Thamdrup, 2009; Gooday et al., 2009; Hofmann et al., 2011). The term “hypoxia” ($<63 \mu\text{M O}_2$; $<2 \text{ mg O}_2 \text{ l}^{-1}$; $<1.4 \text{ ml O}_2 \text{ l}^{-1}$; e.g. Middelburg and Levin, 2009) was originally used to describe internal stress on biota under low oxygen conditions (Piiper, 1982; Gray et al., 2002). However, tolerance thresholds depend on the considered species and its life stages (e.g. Pihl et al., 1991; Gray et al., 2002; Levin et al., 2009). “Anoxia” is used to describe severe oxygen depletion with conditions below $10 \mu\text{M O}_2$ ($<0.5 \text{ mg O}_2 \text{ l}^{-1}$; $<0.2 \text{ ml O}_2 \text{ l}^{-1}$; e.g. Gooday et al., 2009).

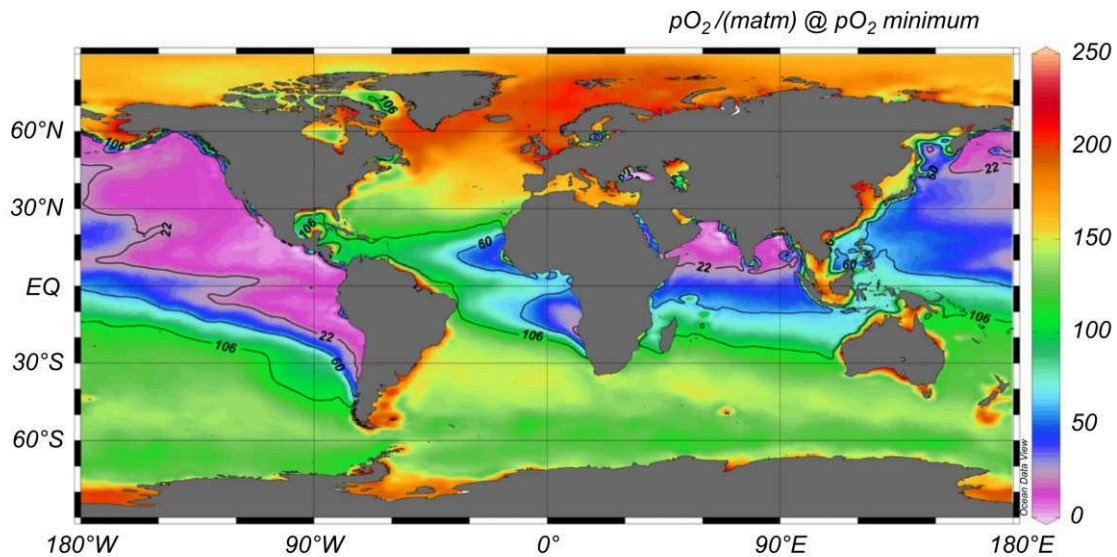


Fig. 1.1. Global map of oxygen minimum zones with minimum oxygen partial pressure (pO_2/matm , top panel). From Hofmann et al. (2011) after Garcia et al. (2010). Hypoxia ($<63 \mu\text{M O}_2$; $<2 \text{ mg O}_2 \text{ l}^{-1}$; $<1.4 \text{ ml O}_2 \text{ l}^{-1}$) corresponds to values $<60 pO_2/\text{matm}$ (blue and purple colour in top panel).

1.1.2 Causes and consequences of hypoxia and eutrophication

Oxygen determines the health of aquatic ecosystems, because it can be a limiting factor for organisms for which oxygen is essential (Diaz and Rosenberg, 2008; Keeling et al., 2010). Terrestrial and aquatic ecosystems have been strongly altered due to climate change and eutrophication (Smith et al., 1999; Diaz and Rosenberg, 2008; Gooday et al., 2009; Keeling et al., 2010). Although oxygen depletion phenomena in marine systems have occurred throughout earth history, the number, duration and spatial extent of oxygen depletion events have increased dramatically across the globe (Fig. 1.1) (Diaz, 2001; Diaz and Rosenberg, 2008; Gooday et al., 2009; Gilbert et al., 2010; Zhang et al., 2010; Hofmann et al., 2011).

Oxygen depletion can cause mass mortality events (Fig. 1.2), species extinction and irreversible ecosystem decline (Lancelot et al., 2002; Mee et al., 2005; Diaz and Rosenberg, 2008). This means that hypoxia has crucial impacts on biodiversity, food webs and biogeochemical cycles (Joyce, 2000; Diaz and Rosenberg, 2008; Conley et al., 2009). Shifts towards more tolerant, often invasive species are observed, but especially persistent oxygen-poor conditions result in the establishment of dead zones (Lancelot et al., 2002; Mee et al.,

2005; Diaz and Rosenberg, 2008). For the last 50 years, dead zones have been described from more than 400 coastal marine systems, which comprise a total area of more than 245000 km² (Diaz and Rosenberg, 2008). Therefore, oxygen depletion is a key stressor in marine and limnic ecosystems and might be caused or influenced by eutrophication, stratification, climate change, and upwelling (Livingstone, 1997; Diaz, 2001; Livingstone, 2003; Diaz and Rosenberg, 2008; Müller et al., 2012). Apart from natural consequences, hypoxia can lead to large economic damage in fisheries and aquacultures (Diaz, 2001; Zhang et al., 2010).



Fig. 1.2. Dead fish at the beach of Constanta (Romania) in summer 2010 after hypoxia affected the Romanian Black Sea shelf due to an interplay of eutrophication and stratification at that time (Photo: Adrian Teaca, GeoEcoMar, Constanta)

Since the industrial revolution, eutrophication has been a major driver for dramatic hypolimnetic oxygen decline in lakes (Vitousek et al., 1997; Smith et al., 1999). The mechanisms of eutrophication are quite well understood today (reviewed by Smith et al., 1999). Elevated nutrient levels fuel productivity and lead to increased organic matter (OM) accumulation and OM mineralisation, which more dramatically deplete oxygen in the

hypolimnion. Despite the reduction of nutrients by water treatment and remediation, oxygen deficiency in the hypolimnion remains persistent in deep, stratified lakes due to high rates of sedimentary OM remineralisation, which in turn results in resupply of nutrients to the water column (Smith et al., 1999; Matzinger et al., 2010; Müller et al., 2012).

Another consequence of more persistent hypoxia is the enhanced emission of greenhouse gases, which implies a positive feedback to global climate change (Keeling et al., 2010). One of these gases is methane, which is the second most important greenhouse gas after carbon dioxide since although its concentration in the atmosphere is much smaller it has a 25 times higher global warming potential over a 100-year period (IPCC, 2007). Aquatic environments can represent a significant natural source of methane (Bastviken et al., 2004). In a changing climate, rising water temperatures can lead to increased stratification (Livingstone, 1997; Adrian et al., 2009; Rempfer et al., 2009; Foley et al., 2012). The reduced mixing hinders oxygen replenishment to deeper waters (Keeling et al., 2010).

Environmental changes due to oxygen depletion and eutrophication can result in fragile ecosystem state transitions, so called 'tipping points' (Scheffer, 2009; Scheffer, 2010). Based on complex, still not understood feedback processes, environmental alterations may lead to mass mortality events and ecosystem decline (Scheffer, 2010). However, the understanding of such mechanisms is often hampered by lack of historical data. Therefore, there is still a need for high resolution and long-term proxy based reconstructions of environmental changes. For this purpose, sedimentary proxies are needed for qualitative and quantitative reconstructions of oxygen in lakes and oceans. Such indicators help to understand past processes and developments. Sedimentary proxies are valuable for deducing information on past causes, drivers and effects of low oxygen concentrations and eutrophication, including the role of human impact. Such information is indispensable to develop strategies for improvement measures, to reduce oxygen depletion and its diverse negative impacts.

1.1.3 Organic proxies – lipid biomarkers

Lipid biomarkers (Fig. 1.3) are organic compounds, which originate from formerly living organisms (Peters et al., 2006). They can provide information on OM sources (aquatic vs.

terrigenous origin) and fate, microbial community changes, environmental conditions during deposition and diagenesis, biodegradation, climate and age (e.g. summarised by Peters et al., 2006; Bianchi and Canuel, 2011). The complex structure of biomarkers reveals more information about their origins than other compounds like methane and graphite, which can be generated from many different organic compounds (Peters et al., 2006).

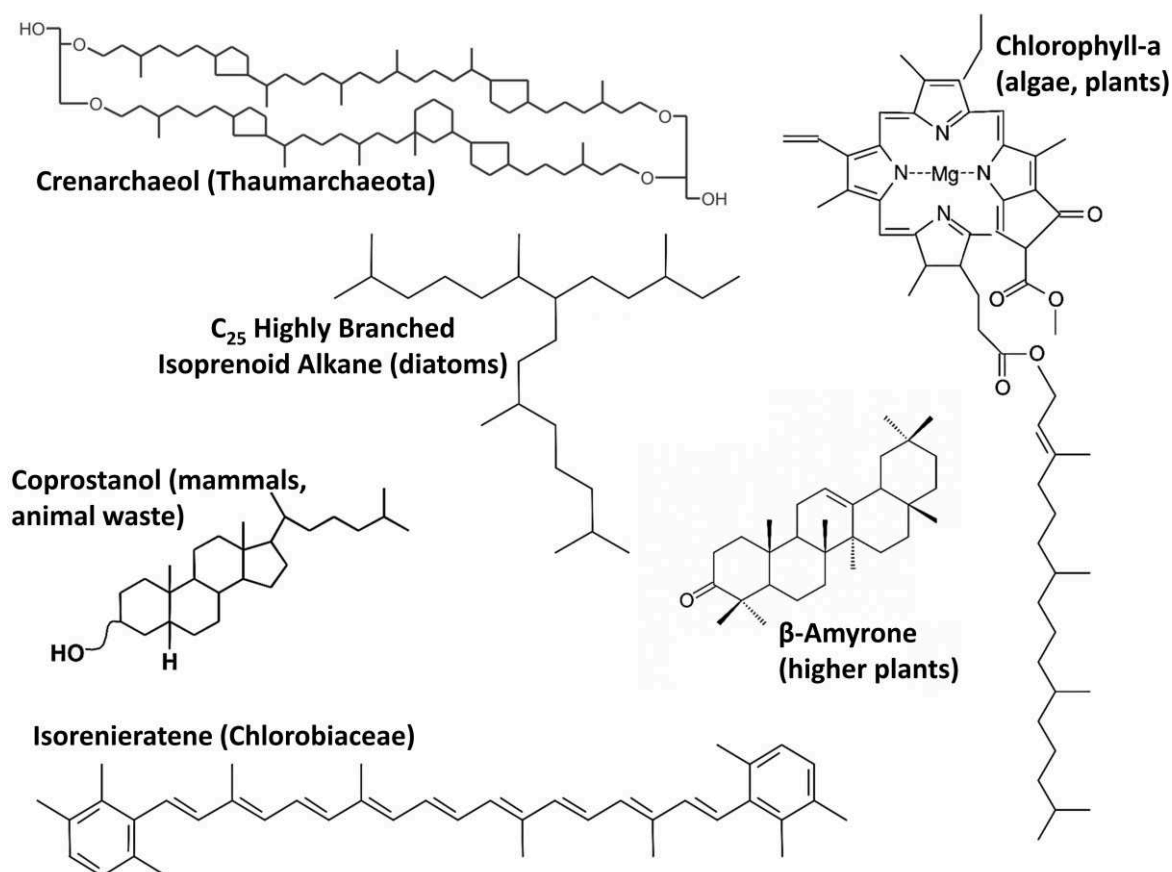


Fig. 1.3. Sample structures of lipid biomarkers (adapted from Peters et al., 2006). Origin of these lipids in brackets.

Biomarkers have also been used repeatedly to trace anoxic conditions in present and ancient water columns of lakes, inland seas and oceans (Brocks et al., 2005; Hebting et al., 2006; van Bentum et al., 2009). Hypoxia indicators like the carotenoids isorenieratene and okenone are only produced by phototrophic sulfur bacteria belonging to the Chromatiaceae and

Chlorobiaceae (Schaeffer et al., 1997; Brocks and Summons, 2003). Because of the limited oxygen tolerance of these organisms and their dependence on light and free hydrogen sulphide, these compounds are robust markers for photic zone anoxia and euxinia (Brocks and Summons, 2003; Brocks et al., 2005).

Biomarkers also trace alterations of the abundance and composition of their source organisms (i.e. microbial communities), which can be caused by eutrophication (e.g. Meyers and Ishiwatari, 1993; Schouten et al., 2001; Peters et al., 2006; Bechtel and Schubert, 2009). Eutrophication leads to the increase of primary producers and these changes can be traced by biomarkers (Meyers and Ishiwatari, 1993). More specific indicators such as coprostanol and epicholestanol have been used as proxies for the supply of untreated sewage to aquatic systems and to reconstruct eutrophication (Mermoud et al., 1985; Bull et al., 2002; Wu et al., 2009).

However, there is still a need for biomarkers, which allow the reconstruction of past oxygen levels. Furthermore, the responsible processes for oxygen depletion must be examined in the studied systems, also in the context of system state transitions and remediation measures. The advantages and disadvantages of the applicability of biomarkers for oxygen reconstructions are discussed and evaluated in this thesis.

An important prerequisite for reliable palaeoenvironmental reconstructions is the knowledge on lipid sources, for instance the differentiation between aquatic and terrigenous OM. For instance, one biomarker based proxy for terrigenous OM supply to lakes and oceans is the branched and isoprenoid tetraether index (BIT index, Hopmans et al., 2004). But it has been found that its interpretation can be misleading, hence a multi-proxy approach is generally recommended to better estimate the origin of OM in aquatic systems (c.f. Fietz et al., 2011). Previous work showed that the BIT index was often uncorrelated to other terrestrial organic matter input proxies (Fietz et al., 2011). Therefore, there is a need to develop new proxies, which better identify the origin of sedimentary OM. Furthermore, OM degradation also affects biomarker records in the sediment. Only if these parameters are known, biomarkers can be used as robust indicators for palaeoenvironmental reconstructions. Therefore, it was an objective of this thesis to better distinguish between aquatic and terrigenous sources and to better evaluate the effects of degradation on sedimentary biomarker records.

1.1.4 Inorganic proxies – iron and manganese

Transition metals, such as iron (Fe) and manganese (Mn), have received much attention in the last decades due to their redox-sensitive behaviour in the environment. Because of the low solubility of Fe and Mn in oxic waters, deposits are formed when anoxic waters with reduced, dissolved species of Fe and Mn are oxygenated (Davison, 1993; Calvert and Pedersen, 2007). Especially in lakes seasonal redox changes result in Fe and Mn cycling (Stumm, 1985; Sigg et al., 1987; Davison, 1993). Dissolved Fe and Mn species in the water column precipitate after oxygenation at the chemocline or during lake mixing, after which they can also be deposited and preserved in the lake sediment (Davison, 1993; Schaller and Wehrli, 1996).

However, it was not possible so far to use these transition metals for quantitative lake bottom water oxygen reconstructions. Therefore, Mn and Fe redox dynamics were studied in the Swiss Lake Zurich. The correlation of data from high resolution x-ray fluorescence (XRF) core scanning and long-term oxygen monitoring improved the understanding of short-term transport and enrichment of these redox-sensitive elements in deeper lake waters.

1.2 Outline

This thesis presents the results of biomarker and trace metal studies carried out on sediment cores obtained from Swiss lakes (Rotsee and Lake Zurich), Amvrakikos Gulf (Greece) and the Black Sea (Romanian Shelf). It is divided into the four following chapters after this introduction.

Chapter 2: Impact of recent lake eutrophication on microbial community changes as revealed by high resolution lipid biomarkers in Rotsee (Switzerland)

Rotsee is an ideal example of an anthropogenically altered ecosystem. The lake underwent eutrophication mainly due to untreated sewage input, leading to high productivity events, which culminated in the 1920s and 1960s. The increased productivity led to changes in microbial community assemblages, which were traced by biomarkers. Historical remediation measures had direct implications for productivity and microbial biota, leading to variations in community composition and abundance. In this study, we reconstructed local environmental change during the last 150 years.

Apart from the biomarker proxy based palaeoenvironmental reconstructions, the diatom *Stephanodiscus parvus* was found to be the dominant source of dinosterol and 24-methylcholesterol, whereas *Cyclotella radiosa* and *Asterionella formosa* were the predominant source organisms of specific fatty acids (FA). The lipid content and lipid cell density of methanogenic archaea was estimated based on the sedimentary glycerol dialkyl glycerol tetraether without cyclopentane moieties (GDGT-0) profile. Furthermore, an improved BIT index (BIT_{CH}) is proposed. Confirmed by detrital trace metal profiles, this indicator better described changes in terrigenous OM supply to the lake compared to the traditional BIT index.

Chapter 3: Maleimides in recent sediments – Using chlorophyll degradation products for palaeoenvironmental reconstructions

Maleimides (1*H*-pyrrole-2,5-diones), transformation products of chlorophylls and bacteriochlorophylls, were studied in the recent sediments from the Swiss lake Rotsee and the Romanian Black Sea Shelf to investigate chlorophyll degradation, the role of oxygen in maleimide formation, and to identify their sources. Maleimides have so far been mostly studied in ancient deposits (e.g. Grice et al., 1996). An exception is the observation of 2-methyl-3-ethyl-maleimide (Me₂Et maleimide) in recent sediments from Tokyo Bay (Kozono et al., 2002). Maleimides and other transformation products of chlorophylls (chlorins, porphyrins) can serve as proxies for palaeoenvironmental reconstructions.

Naturally occurring (i.e. “free”) maleimides and maleimides obtained after chromic acid oxidation of sediment extracts were analysed. 2-Methyl-maleimide (Me,H maleimide), 2,3-dimethyl-maleimide (Me,Me maleimide), 2-methyl-3-vinyl-maleimide (Me,vinyl maleimide), Me,Et maleimide and traces of 2-methyl-3-*iso*-butyl-maleimide (Me,*i*-Bu maleimide) occur naturally in the sediment with a large predominance of the Me,Et homologue. Based on chromic oxidation of methyl pheophorbide it was found that Me,Et and Me,vinyl maleimides mainly originate from Chlorophyll *a*. While the source of Me,Me maleimide still remains unknown, Me,H maleimide seems to be derived from chlorophyll-related compounds, which have lost ring E. In agreement with the presence of isorenieratene in Rotsee and isorenieratene and chlorobactene in the Black Sea, 2-Methyl-3-*n*-propyl-maleimide (Me,*n*-Pr maleimide) and Me,*i*-Bu maleimide traced the presence of phototrophic sulphur bacteria (Chlorobiaceae). The results indicated photic zone euxinic and anoxic conditions in Rotsee during the last 150 years and during the last 9-10 ka in the Black Sea (including the limnic phase, Unit 3). Other obtained maleimides originate from bacteriochlorophylls with specific alkylation patterns, but their sources remain unknown.

Free maleimides were mainly formed under the absence of oxygen in the sediment. Novel maleimide degradation indices are proposed to estimate the degree of OM degradation (OM freshness/degradability). These proxies are applicable on longer timescales than e.g. the chlorin index.

Chapter 4: Tracing bottom water oxygenation with sedimentary Mn/Fe ratios in Lake Zurich, Switzerland

Iron and manganese records were studied concerning their potential for palaeoxygen reconstructions in Lake Zurich. Sediment cores were analysed in high resolution using x-ray fluorescence (XRF) core scanner. Together with a well-established age model based on half-year lamination pattern with calcium maxima in summer (light layer) and minima in winter (dark layer), the metals could be studied in seasonal resolution since 1895 (Fig. 1.4). The iron (Fe) signal is mainly the result of calcite dilution as indicated by a good negative correlation between Fe and calcium (Ca) XRF data, whereas manganese (Mn) peaks matched with monthly oxygen (O₂) monitoring data reaching back until 1936.

The Mn/Fe ratio in the core from the maximum lake depth (137 m; Fig. 1.4) revealed a good correlation with O₂ measurements in the lake bottom water confirming the successful application of the Mn/Fe ratio to semi-quantitatively reconstruct bottom water oxygenation in the lake. Mostly low ratios were observed between 1895 and the mid-1960s as a result of eutrophication. However, geochemical and sediment focusing and other sedimentological factors can reduce the applicability of the Mn/Fe ratio for reconstructions of annual O₂ concentrations in the bottom water of lakes.

Chapter 5: Environmental variations in a semi-enclosed embayment (Amvrakikos Gulf, Greece) – reconstructions based on benthic foraminifera abundance and lipid biomarker pattern

The recent developments of eutrophication and environmental change in Amvrakikos Gulf were studied by benthic foraminifera and lipid biomarkers in the sediment. These proxies revealed that during the last decades the gulf has exhibited a transition towards a fluctuating and increasingly stressful environment. The productivity increased together with bacterial biomass. Benthic foraminifera assemblages shifted towards opportunistic and tolerant species, whereas the species density decreased.

Benthic foraminifera assemblages appeared to be more diversified under less severe conditions in the area of influence of the Preveza Strait, which connect the gulf

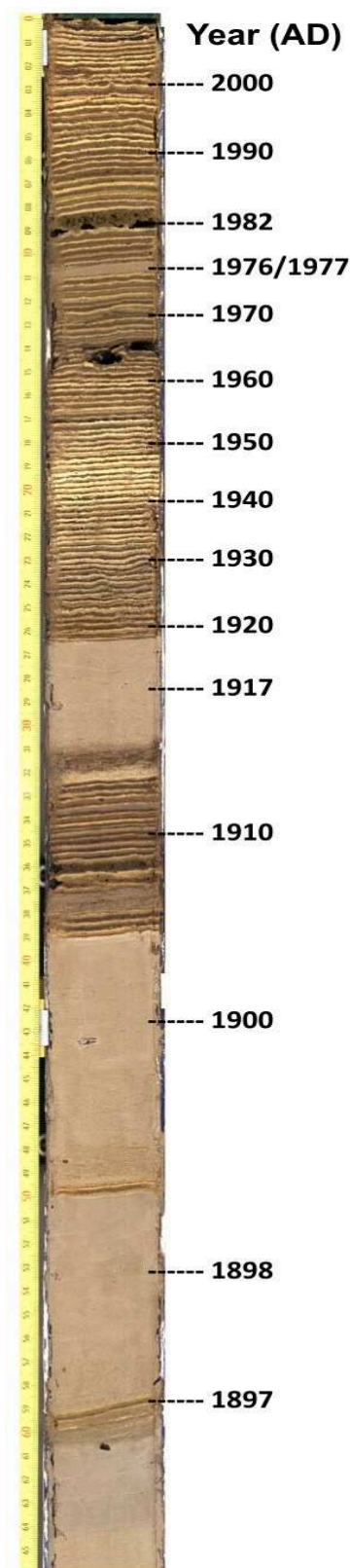


Fig. 1.4. Sediment core obtained from 137m in Lake Zurich (max. depth).

with the Ionian Sea. However, isorenieratane, chlorobactane and lycopane traced photic zone euxinic and anoxic conditions throughout the gulf. The increase in surface water temperatures and eutrophication led to a reduction in water column mixing and oxygen replenishment to deeper waters. Because of the similarity to causes and processes of eutrophication, oxygen depletion, circulation patterns and ecosystem decline on the Romanian Black Sea Shelf, Amvrakikos Gulf can be considered to be a Black Sea analogue.

Chapter 2: Impact of recent lake eutrophication on microbial community changes as revealed by high resolution lipid biomarkers in Rotsee (Switzerland)

Sebastian Naeher, Rienk H. Smittenberg, Adrian Gilli, Emiliya P. Kirilova, André F. Lotter, Carsten J. Schubert

Published in Organic Geochemistry, Volume 49, 2012, Pages 86-95

<http://dx.doi.org/10.1016/j.orggeochem.2012.05.014>

Abstract

The effects of eutrophication on short term changes in the microbial communities were investigated using high resolution lipid biomarker and trace metal data for sediments from the eutrophic Rotsee (Switzerland). The lake has been strongly influenced by sewage input since the 1850s and is an ideal site for studying an anthropogenically altered ecosystem. Historical remediation measures had direct implications for productivity and microbial biota, leading to community composition changes and abundance shifts. The higher sewage and nutrient input resulted in a productivity increase, which led predominantly to a radiation in diatoms, primary producers and methanogens between about 1918 and 1921, but also affected all microorganism groups and macrophytes between about 1958 and 1972. Bacterial biomass increased in 1933, which might have been related to the construction of a mechanical sewage treatment plant. Biomarkers also allowed tracing of fossil organic matter/biodegraded oil

contamination in the lake. *Stephanodiscus parvus*, *Cyclotella radios*a and *Asterionella formosa* were the dominant sources of specific diatom biomarkers. Since the 1850s, the cell density of methanogenic archaea (*Methanosaeta* spp.) ranged within ca. $0.5\text{--}1.8 \times 10^9$ cells g⁻¹ dry sediment and the average lipid content of Rotsee archaea was ca. 2.2 fg iGDGTs cell⁻¹. An altered BIT index (BIT_{CH}) indicating changes in terrestrial organic matter supply to the lake is proposed.

2.1 Introduction

Due to human activity such as land clearing, agriculture, forestry and urbanisation, nutrient cycling in ecosystems has been intensively altered, especially since the industrial revolution. The impact, along with climate change (Keeling et al., 2010), has profoundly altered natural biological communities in limnic, marine and terrestrial ecosystems (e.g. Vitousek et al., 1997; Smith et al., 1999). It has been estimated that human induced eutrophication has altered one third to one half of the land surface (Vitousek et al., 1997).

Today, the mechanisms of lake eutrophication are quite well understood (for an overview see Smith et al., 1999), with high nutrient loading fuelling productivity and biomass accumulation. Another factor is increased water column stratification, which leads more rapidly to O₂ depletion in the hypolimnion, which can even result in dead zones and mass mortality of species (Diaz and Rosenberg, 2008). The O₂ deficiency enhances the release of nutrients from the sediment, further increasing nutrient cycling and bioavailability.

Because of the negative impact of eutrophication, water sewage treatment has had a dramatic improvement over the last decades, resulting in a general increase in surface water quality (Smith et al., 1999; Matzinger et al., 2010). At the same time, efforts to remediate affected water bodies have been less successful and have not always worked out as foreseen. For example, Matzinger et al. (2010) showed that the decrease in nutrient supply to lakes did not strongly reduce O₂ consumption rate in the water column because of remineralisation of organic matter (OM) in the sediment.

Another aspect is that complex system changes from chemical, physical and biological feedback mechanisms, that rule the system ecology of lakes, may result in 'tipping points' (Scheffer, 2010). These are critical transitions indicating the fragility of an ecosystem, resulting in dramatic changes in the abundance and composition of inhabiting organisms, either (algal) blooms or the extinction of species and the 'point of no return' (Scheffer, 2010). However, increased understanding of these mechanisms is often hampered by lack of historical data - investigations have typically only been started after severe cases of eutrophication, while hardly any prior physicochemical and biological data are available (Stadelmann, 1980; Scheffer, 2010). This lack is particularly for microbiological data, yet such biota play a central role during eutrophication. There is therefore a need for high temporal resolution reconstruction of microbial communities to improve the understanding of the 'natural' state, the onset and development of eutrophication, and subsequent remediation measures.

The aim of this study was to reconstruct the eutrophication history and the response of microbial biomass, using organic and inorganic proxies, in a small eutrophic Swiss lake. The relationship between biomarker concentration change and shift in microbial abundance was constrained, partly down to the species level, being supported by results from previous work on diatoms (Lotter, 1989) and methanogenic archaea (Falz et al., 1999). Finally, we reevaluated the effectiveness of recovery activity and the implications for microbial communities after intensive sewage input to this ecosystem.

2.2 Material and methods

2.2.1 Study site and sample collection

Rotsee is a small (0.46 km²) prealpine, monomictic and eutrophic lake with a maximal depth of 16 m (Fig. 2.1, Table 2.1). It formed after the retreat of the Reuss glacier after the last interglacial (Frey, 1907). Currently, it has a stable stratified water column with a strong chemocline between ca. 6 and 10 m and an anoxic hypolimnion for most of the year (Schubert

et al., 2010). During the Holocene, the lake was mostly eutrophic and only partly mesotrophic, according to the past algal flora (Züllig, 1985a).

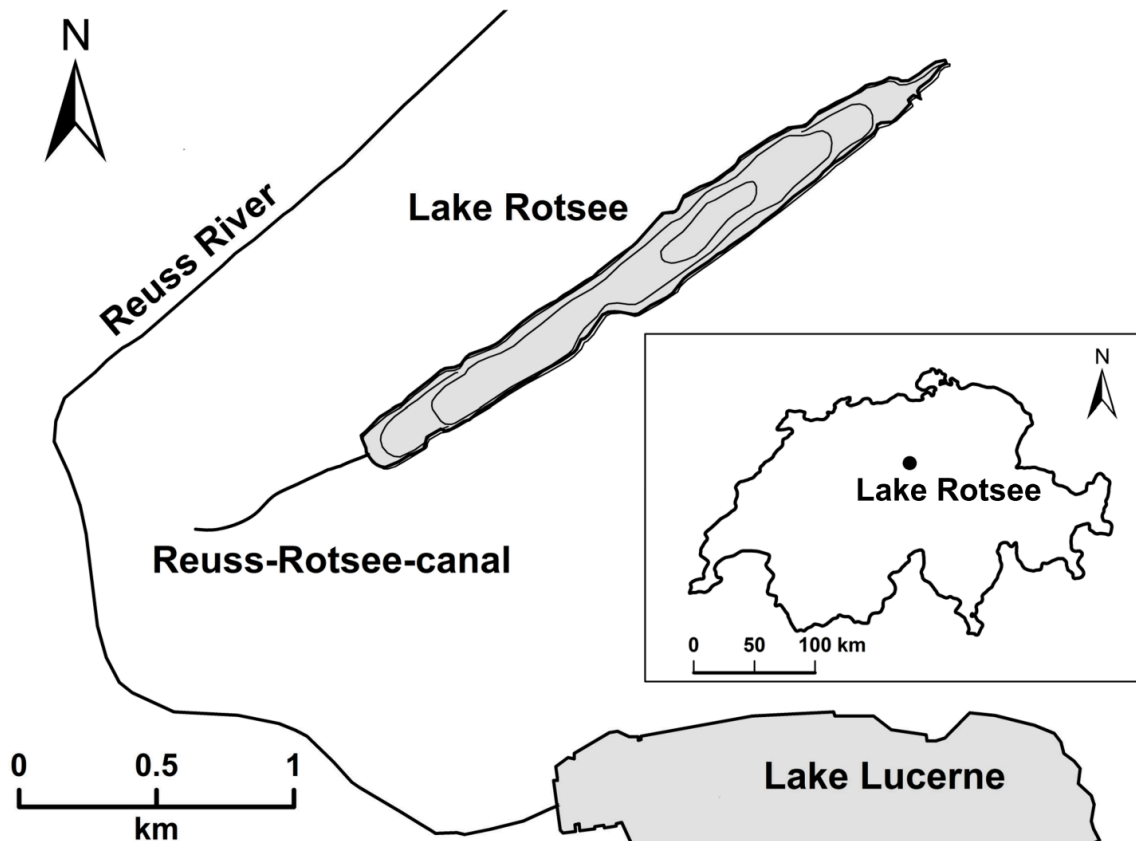


Fig. 2.1. Map with Rotsee, the Reuss River and its connection with Rotsee by the Reuss-Rotsee-canal (partly below ground level) and the northwest corner of Lake Lucerne. Insert map shows location of Rotsee.

The combination of the geographical and hydrological characteristics, together with the forested catchment, favours natural eutrophication (Bloesch, 1974), on which the anthropogenic nutrient enrichment since the 19th century (Stadelmann, 1980) has been profoundly superimposed. Since ca. 1850, the trophic state increased through sewage input and in 1920 the lake was classified as polytrophic (Bloesch, 1974; Stadelmann, 1980), leading to numerous blooms of *Oscillatoria rubescens* (today: *Planktothrix rubescens*, in German “Burgunderblutalge”), which turned the lake water red (Züllig, 1985a). As a consequence of a canal construction from the Reuss River in the south-west corner of the lake in 1922 (Fig.

2.1), freshwater input increased (Kohler et al., 1984) and the water renewal time dropped from 3-4 to 0.4 yr (Lotter, 1989). However, recovery measures were unsuccessful because of continued nutrient supply from a nearby disposal site, temporal drying of the canal and the inability of the water inflow from the canal to initiate mixing (Bachmann, 1931; Stadelmann, 1980). After the completion of construction of an interceptor sewer in 1969 and a sewage treatment plant in 1974, the lake started to recover slowly (Stadelmann, 1980).

Table 2.1: Hydrographical and limnological parameters of Rotsee (Bloesch, 1974; Kohler et al., 1984; Schubert et al., 2010; Züllig, 1985a)

Parameter	Value	Unit
Drainage area	4.6	km ²
Surface area	0.46	km ²
Volume	0.0039	km ³
Max. depth	16	m
Mean depth	9	m
Residence time	0.44	yr
Trophic state	Eutrophic	
Lake mixing	Monomictic, holomictic (winter)	
Chemocline	6-10	m

A 56 cm long sediment core was recovered with a gravity corer in October 2009 from the centre of the lake at 16 m depth (GPS position N 47° 4.251 E 8° 18.955, WGS84). The core was sliced in continuous 1 cm intervals and frozen at -20°C until analysis. Another 63 cm core was obtained from the same location in August 2010 for elemental analysis.

2.2.2 Age model

For core dating, ^{137}Cs and ^{210}Pb in freeze-dried and ground sediment were measured via γ spectrometry with a high purity Ge detector (Canberra GCW-3523) using the γ energy at 46.5 keV for ^{210}Pb and 661.7 keV for ^{137}Cs . Based on the Chernobyl accident and nuclear bomb test peaks in ^{137}Cs and a constant rate of supply (CRS) model, sedimentation (Appleby and Oldfield, 1978) and accumulation rates (Niessen et al., 1992) were calculated.

2.2.3 Bulk parameters

Total carbon (TC) and total nitrogen (TN) were measured on freeze-dried samples with a Thermo Quest CE Instrument NC 2500. Total organic carbon (TOC) was measured on decalcified samples. Total inorganic carbon (TIC) was calculated as the difference between TC and TOC. The errors for TC and TOC were ± 0.1 wt.% and ± 0.2 wt.% for TN. Additional TIC measurements with a Coulomat 5011 coulometer indicated that the method led to 0.5 wt.% higher TIC values, corresponding to 0.5 wt.% lower TOC values. C and N isotopic compositions ($\delta^{13}\text{C}$ and $\delta^{15}\text{N}$) of the OM were obtained with a GV Instruments IsoPrime isotope ratio mass spectrometry (IRMS) instrument, using the same run as for TOC and TIC. The $\delta^{13}\text{C}$ [‰ Vienna Peedee Belemnite (VPDB)] and $\delta^{15}\text{N}$ (‰ air) errors were up to ± 0.3 ‰. The chlorin index (CI) and total chlorin concentration were determined according to Schubert et al. (2005). The analytical precision of the method was ca. 5% (Schubert et al., 2005).

2.2.4 Biomarker analysis

Ca. 5 g thawed sediment was extracted (x 3) by way of ultrasonication with MeOH and dichloromethane (DCM): 1x10ml MeOH, 1x10ml MeOH:DCM (1:1, v:v), 1x10ml DCM. For quantification, a known mixture of 5 α -cholestane, C₁₉ *n*-alcohol and C_{19:0} fatty acid (FA) was added to the extract. Water was removed in a separation funnel with NaCl (20 ml, 5%). The extract was run over a Cu column to remove elemental S and over a column filled with

Na₂SO₄ to remove traces of water. Samples were saponified (3 h, 80 °C) with 6% KOH in MeOH. Neutrals were extracted (x 3) with hexane and dried with Na₂SO₄ while the acid fraction was extracted from the aqueous phase after the addition of 6M HCl. The neutrals were divided into apolar and polar fractions via liquid chromatography over NH₂ columns (Hinrichs et al., 2003). The polar fraction was derivatised [1 h, 80 °C with N,O-bis(trimethylsilyl)trifluoroacetamide (BSTFA, Supelco)]. FAs were derivatised with 14% BF₃/MeOH (Sigma Aldrich) to produce the methyl esters (FAMES). To identify multiple bond positions in FAs, an aliquot was derivatised with 2-amino-2-methylpropanol to form 2-alkenyl-4,4-dimethoxyloxazoline (DMOX) derivatives (Spitzer, 1997).

The resulting fractions were examined using gas chromatography with flame ionisation detection [GC-FID; Carlo Erba HRGC 5160 Mega Series, VF-5 column (60 m x 0.25 mm inner diameter (i.d.) x 0.25 µm film thickness (f.t.), He carrier gas flow of 1.0 ml/min)]. The samples were also examined using a gas chromatography mass spectrometer (GC-MS; GC8000Top Finnigan Voyager, electron impact ionisation, Agilent HP-5 column, 30 m x 0.32 mm i.d. x 0.25 µm f.t., He carrier gas flow of 1.0 ml/min).

Glycerol dialkyl glycerol tetraethers (GDGTs) were analysed using a fraction of the total extract, dissolved in hexane/isopropanol (1:1, v:v) and filtered with 0.45 µm PTFE filters prior to analysis via high performance liquid chromatography (HPLC) in a manner similar to that described by Hopmans et al. (2000). For quantification, a synthesized C₄₆ GDGT standard was added to each sample prior to analysis (Huguet et al., 2006). Analysis was performed with a Thermo Surveyor LC system coupled to an LCQ Fleet ion trap mass spectrometer, as described by Bechtel et al. (2010). Isoprenoid GDGTs (isoGDGTs) were named according to (Schouten et al., 2009) and for branched GDGTs (brGDGTs) the nomenclature from Weijers et al. (2007) was used. Ethers in the polar fraction were cleaved prior to carbon isotopic analysis (Kohnen et al., 1992; Blumenberg et al., 2004). No derivatisation was necessary. For compound specific carbon isotopic analysis of the cleaved ethers, an Agilent GC 6890N with a combustion furnace using copper oxide coupled to a micromass IsoPrime mass spectrometer (Restek Rxi-5ms column, 60 m x 0.32 mm i.d. x 0.25 µm FT) was used. The GC oven temperature programme was: 70°C to 130°C at 20°C min⁻¹, then to 320°C (held 20 min) at 4°C min⁻¹. He was the carrier gas with 1.0 ml min⁻¹.

The precision of the biomarker analysis was 10%, whereas the error for GDGTs was within 15%. The analytical error of compound specific $\delta^{13}\text{C}$ values were 1–2‰.

2.2.5 XRF core scanning

Relative elemental concentration was determined for the 2010 core, which was cut lengthwise and the surface was allowed to dry at room temperature for 24 h. One half of the core was measured with the AVAATECH X-Ray Fluorescence Core Scanner at the ETH Zurich, Switzerland, at excitation energy 10 and 30 kV with a resolution of 0.3 mm for 30 s at each point (Richter et al., 2006). The units are XRF counts (peak area). The precision was ca. 2–3%, dependent on the element.

2.2.6 Diatom analysis

Diatom samples were prepared from 2–4 cm intervals using standard techniques including processing with H_2O_2 (30%) and HCl (10%). Between 300 and 400 valves were counted and identified for each sample and diatom accumulation rate was calculated using the evaporation tray technique (Battarbee et al., 2002).

2.2.7 Definition of BIT_{CH} index

A changed branched and isoprenoid tetraether index (BIT_{CH} index) was defined as:

$$\text{BIT}_{\text{CH}} = \text{brGDGTs} / \text{isoGDGTs} = ([\text{GDGT-III}] + [\text{GDGT-II}] + [\text{GDGT-II-b}] + [\text{GDGT-II-c}] + [\text{GDGT-I}] + [\text{GDGT-I-b}] + [\text{GDGT-I-c}]) / ([\text{GDGT-0}] + [\text{GDGT-1}] + [\text{GDGT-2}] + [\text{GDGT-3}] + [\text{crenarchaeol}] + [\text{crenarchaeol regio isomer}])$$

with:

(a) brGDGTs (Weijers et al., 2007):

[GDGT-III]: $m/z=1050$; [GDGT-II]: $m/z=1036$; [GDGT-II-b]: $m/z=1034$; [GDGT-II-c]: $m/z=1032$; [GDGT-I]: $m/z=1022$; [GDGT-I-b]: $m/z=1020$; [GDGT-I-c]: $m/z=1018$

(b) isoGDGTs (Schouten et al., 2009):

[GDGT-0]: $m/z=1302$; [GDGT-1]: $m/z=1300$; [GDGT-2]: $m/z=1298$; [GDGT-3]: $m/z=1296$; [crenarchaeol]: $m/z=1292$; [crenarchaeol regioisomer]: $m/z=1292$

2.3 Results and discussion

2.3.1 Sedimentation rate and age model

A precise age model is a prerequisite for a high resolution biomarker and trace metal record of Rotsee sediment. Since the core was only rarely laminated and mostly uniform brown-black in colour, radionuclides, i.e. ^{137}Cs and ^{210}Pb , were used for dating (Fig. 2.2). The former showed increased activity at 9-10 cm and 18-19 cm corresponding to the Chernobyl accident in 1986 and the peak in nuclear bomb tests in 1963, respectively. The resulting sedimentation rate was calculated as 0.40 cm yr^{-1} using ^{137}Cs . Using ^{210}Pb dating, a similar sedimentation rate of 0.35 cm yr^{-1} was found. Using an average sedimentation rate of 0.38 cm yr^{-1} , the core contained ca. 150 yr of lake history. The age model (Fig. 2.2) could be calibrated with higher TOC concentration at 33-34 cm via the high productivity event before 1922 (Lotter, 1989). The match with the age model of Lotter (1989) supports the high precision of the age model. Hence, biomarker sampling resolution of 1 cm gave a resolution of ca. 4 yr.

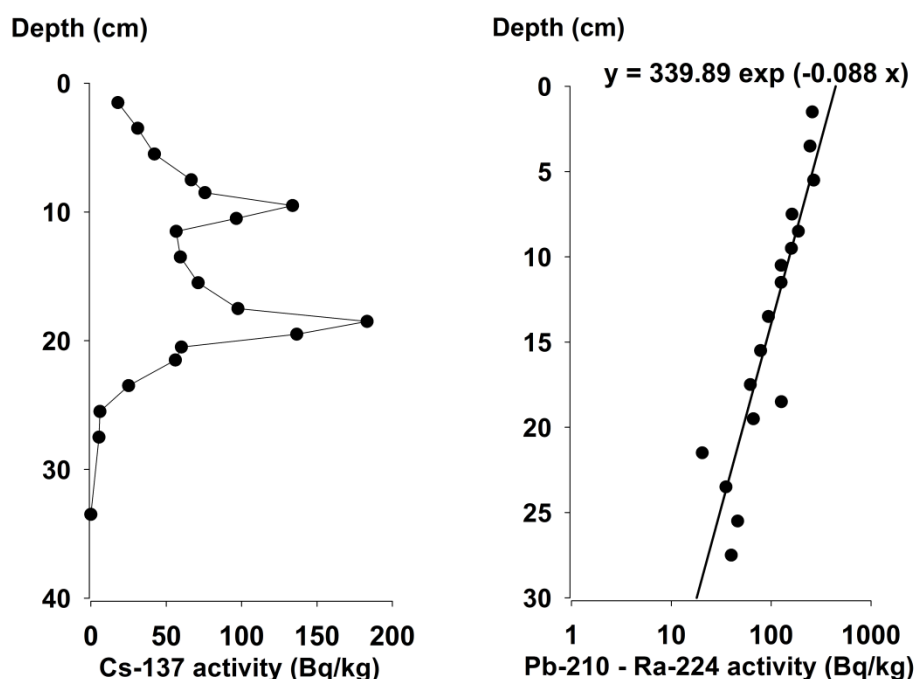


Fig. 2.2. Age models of Rotsee based on ^{137}Cs (left) and ^{210}Pb (right) with the specific activity (Becquerel kg^{-1} freeze-dried ground sediment) on x-axis vs. sediment depth.

2.3.2 Eutrophication and sewage input history of Rotsee

TOC varied down the core, ranging between 4.3 and 6.8 wt.%, with accumulation rate between 3.1 and 4.9 $\text{g cm}^{-2} \text{yr}^{-1}$ (Fig. 2.3). At ca. 33-34 cm (1918-1921) and 15-18 cm (1961-1969), TOC accumulation rate maxima indicated times of higher productivity. The peak at 33-34 cm seemed to be a result of a nutrient supply induced trophic regime shift before the canal construction in 1922 (Lotter, 1989). The change became evident from reanalysis of phytoplankton samples from Bachmann (1931) in Lotter (1989), so the connection to the Reuss River was not the main driver of the higher productivity.

At the beginning of the 1960s, eutrophication peaked. The decreasing productivity since the end of the 1960s was a direct result of the construction of an interceptor sewer, preventing direct sewage supply to the lake from the surrounding urban area (Stadelmann, 1980). However, Reuss River water was still rich in nutrients, but this ended in 1974 after the construction of a sewage treatment plant (Stadelmann, 1980). Between 3 and 14 cm (1972-2001), TOC accumulation remained stable and decreased only in the recent lake sediment.

Two explanations are likely: Non-point source input of nutrients from agriculture, which continued to fuel productivity or redissolution and resuspension of nutrients and OM. The latter explanation implies that, although the nutrient input to the lake was reduced, nutrient redissolution from the lake sediment still fuelled productivity, similar to observations for other Swiss lakes (Matzinger et al., 2010). The continued nutrient supply explains the still conspicuous eutrophic character of the lake.

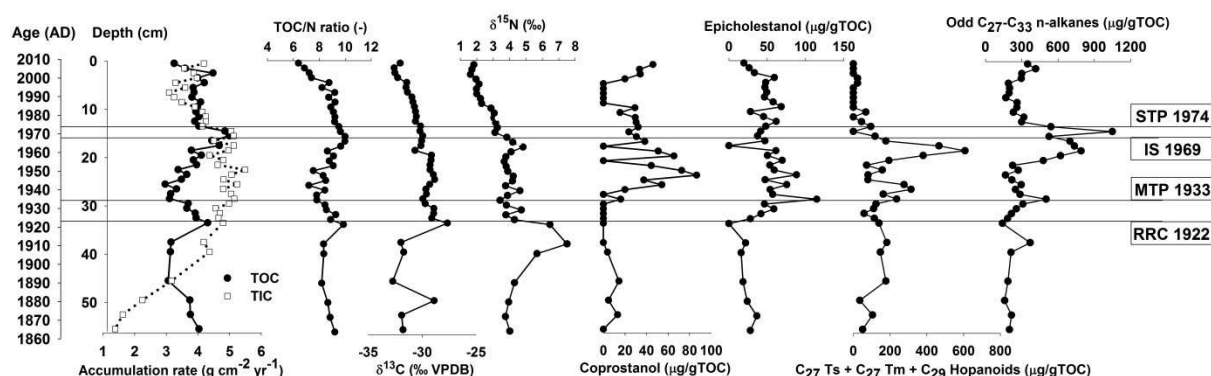


Fig. 2.3. Bulk parameters for core and profiles of coprostanol, epicholestanol, sum of C₂₇ Ts, C₂₇ Tm and C₂₉ hopanoids and sum of odd C₂₇-C₃₃ *n*-alkanes, plotted vs. sediment depth and age (AD). RRC, Reuss-Rotsee-canal; MPT, mechanical sewage treatment plant; IS, interceptor sewer; STP, sewage treatment plant (in all cases with the time of completed construction).

TIC increased consistently from the lower end of the core (1.4 g cm⁻² yr⁻¹), towards ca. 33-34 cm (4.8 g cm⁻² yr⁻¹, Fig. 2.3) and remained almost constant to 17-18 cm (4.3-5.1 g cm⁻² yr⁻¹). Above this, TIC decreased to ca. 3.1 g cm⁻² yr⁻¹ at 5-6 cm, before reaching 4.2 g cm⁻² yr⁻¹ at the top of the core. The higher TIC values between ca. 17 and 34 cm (1918-1964) are in agreement with the elevated trophic state (Bloesch, 1974; Lotter, 1989). Bloesch (1974) and Lotter (1989) showed that TIC (and therefore carbonate precipitation) was related to productivity. Use of accumulation rate prevents potential bias of the TOC as a result of dilution by way of enhanced carbonate deposition (Stein, 1991).

TN, between 0.5 to almost 1.0 wt.%, coincided with the TOC profile, with higher values at ca. 17-20 cm and 29-34 cm. The much higher TOC (4.3-6.8 wt.%) and TN (0.5-1.0 wt.%) values

(Fig. 2.3) vs. other Swiss lakes (Bechtel and Schubert, 2009) such as the oligotrophic Lake Brienz (0.4–1 wt.% TOC, <0.1 wt.% TN) and the eutrophic Lake Lugano (1.1–3.2 wt.% TOC, 0.1–0.4 wt.% TN) may be explained by Rotsee's higher nutrient input, higher productivity, shallow maximum depth and anoxic hypolimnion.

The $\delta^{13}\text{C}$ values for TOC were mostly $<-31\text{‰}$ before the beginning of the 1920s (Fig. 2.3) and increased to -27.6 at ca. 33–34 cm (1918–1921), which might related to the increased productivity, leading to more enriched $\delta^{13}\text{C}$ values at that time. Since they have remained quite constant, likely due overall to the high extent of eutrophication. However, the values decreased again since the 1960s/1970s, until reaching -32.0‰ in the surface sediment (Fig. 2.3), possibly related to a continuous recovery from eutrophication. The carbon isotope signal therefore also traces the trends in eutrophication and recovery during the lake's history. One complication in using $\delta^{13}\text{C}$ values with sediments is the so-called Suess effect. Burning $\delta^{13}\text{C}$ depleted fossil fuel in conjunction with industrialisation led to a shift in the isotopic ratio for atmospheric CO_2 , which rose to -1.7‰ in 2004 compared with preindustrial values (McCarroll and Loader, 2004). Carbonate and OM deposited after the beginning of industrialization could therefore be influenced. Hence, if a lake is in equilibrium with the atmosphere, like e.g. the Great Laurentian Lakes, this has to be taken into account since it would decrease the $\delta^{13}\text{C}$ value of the deposited OM (Meyers, 2006). However, Lake Rotsee is not in equilibrium with the atmosphere due to the mixing into the surface water of liberated dissolved inorganic carbon derived from OM degradation. Additionally, other factors like variation in the extension of blooms and precipitation of calcareous nanoplankton has a much stronger influence on the isotopic signal in the productive zone. We therefore think that the Suess effect is of minor importance in Lake Rotsee and have therefore not corrected the $\delta^{13}\text{C}$ TOC values.

The $\delta^{15}\text{N}$ values (Fig. 2.3) increased from the bottom of the core (4.0‰) to a clear maximum between 33 and 38 cm (max. 7.5‰), then decreased again upwards to the sediment surface (1.8‰). The values are within the range (Heaton, 1986; Hoefs, 2009) for soil OM (0 to $+9\text{‰}$), fertilizer (-4 to $+4\text{‰}$) and manure and septic waste (sewage, 0 to $+25\text{‰}$). Shifts in the latter potential source might in particular strongly increase $\delta^{15}\text{N}$, which might lead to large excursions in the isotopic signature. Although these different sources cannot be distinguished on the basis of $\delta^{15}\text{N}$ values alone, the decrease in $\delta^{15}\text{N}$ from the 1920s until 2009 may indicate

reduced sewage and nutrient input. In contrast, the increasing $\delta^{15}\text{N}$ values until the 1920s are indeed likely an indication of increasing sewage input, which is known to have taken place since the mid-19th century (Kohler et al., 1984). N fixation and/or denitrification might have also led to the decrease in $\delta^{15}\text{N}$ values since the 1920s. However, nitrogen fixation is low in eutrophic systems because nitrogen is not limited (Canfield et al., 2005), so it seems to have hardly affected the $\delta^{15}\text{N}$ values in Rotsee. While no isotopic data of NO_3^- are available for the water column, the values in the sediment can trace water column nitrification-denitrification. Denitrification in the sediment of lakes proceeds until completion, which results in similar nitrogen isotopic signatures in the water column and sediment, also hardly affecting the $\delta^{15}\text{N}$ composition (Lehmann et al., 2003). Therefore, source changes (especially sewage supply) are the most likely reason for the observed shifts in the $\delta^{15}\text{N}$ signal.

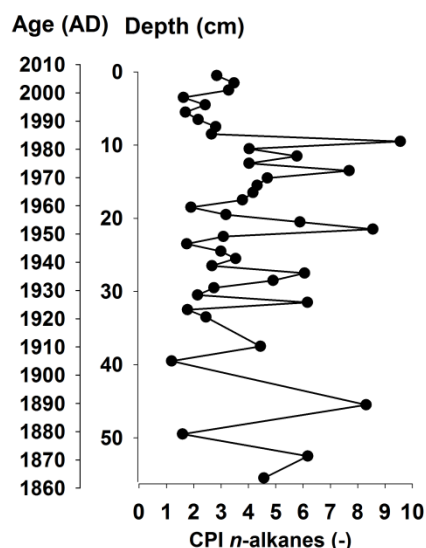


Figure 2.4. Carbon preference index (CPI; defined by Bray and Evans, 1961) of *n*-alkanes vs. sediment depth and age (AD).

Other sewage input indicators are thought to be coprostanol and epicholestanol (Mermoud et al., 1985; Bull et al., 2002), which were also found in Rotsee (Fig. 2.3). However, coprostanol can originate from mammals (Sherwin et al., 1993), so animal waste can be another source, which is likely due to surface runoff from nearby livestock farming north of the lake. Epicholestanol is more likely an indicator of bacterial alteration in the lake (Cordeiro et al., 2008), which might indicate higher bacterial activity during lake eutrophication, especially since the 1920s and culminating at ca. 1933. Sewage input began in the mid-19th century and ceased in 1974 with the construction of a treatment plant. Both markers, still observed in the surface sediment, are therefore apparently no clear sewage indicators in Rotsee.

The two C_{27} isomers Ts (18α -22,29,30-trinor-hopane) and Tm (17α -22,29,30-trinor-hopane, much less abundant than Ts) and C_{29} hopanoids (Seifert and Moldowan, 1978), tracers for petroleum contamination, were found with peaks at 25-29 cm (1932-1942) and 17-20 cm (1956-1964, Fig. 2.3). The *n*-alkane carbon preference index (CPI, defined by Bray and

Evans, 1961) also showed some lower values here (1.9-3.2, Fig. 2.4) although high maturity material like fossil OM or petroleum shows typical values close to 1 (Peters et al., 2006) which were not observed in this part of the core.

Previous studies indicate that the presence of these hopanoids together with tricyclopolyrenanes strongly suggests a contribution from fossil OM and/or biodegraded oil (Seifert and Moldowan, 1978; Behrens et al., 1998). However, the low abundance of tricyclopolyrenanes and the CPI values (>1) show that the contamination remained low. The decrease in these hopanoids at the beginning of the 1970s and the peak in the sum of odd C_{27} - C_{33} *n*-alkanes at 13-20 cm (1956-1974) indicate that the sewage treatment plant in 1974 effectively reduced the oil supply to the lake. The saturated hydrocarbons cannot be a result of the reduction in biohopanoids by H_2S such the end products of that pathway remain partially unsaturated (Hebting et al., 2006).

2.3.3 Terrestrial OM sources

Aquatic and terrestrial OM sources were distinguished on the basis of TOC/N values, specific terrigenous biomarkers, trace metal profiles and distributions of FAs, *n*-alkanes and *n*-alcohols.

The molar TOC/N ratio showed values between 6 and 10 (Fig. 2.3), indicating a predominance of aquatic OM sources (Meyers and Ishiwatari, 1993). In contrast, specific terrigenous biomarkers were detected, such as lupeol, β -amyrin and amyrenone (Brassell and Eglinton, 1983), but the concentrations were too low for quantification.

The maximum at *n*- $C_{16:0}$ FA suggests predominantly autochthonous OM input to the sediment, in line with TOC/N values <10 (Fig. 2.3). In contrast, the maxima in the C_{17} , C_{23} , C_{25} and C_{27} *n*-alkanes and C_{16} , C_{22} and C_{26} *n*-alcohols indicate both aquatic and terrestrial sources (Meyers and Ishiwatari, 1993). The high abundance of C_{23} and C_{25} *n*-alkanes and C_{22} *n*-alcohol indicate a significant contribution from submerged and/or floating macrophytes (Ficken et al., 2000).

Other proxies for terrigenous input are the relative content of Fe, K and Ti, the covariance of which indicates that these trace metals have a similar detrital source (Tribovillard et al., 2006). They show a general decrease until about 1922 (Fig. 2.5), which we interpret to be primarily the result of dilution of detrital input by an increasing input of autochthonous material resulting from eutrophication and related higher productivity. The fluxes may have remained constant over time. Ti intensity decreased to the detection limit after 1922 (Fig. 2.5).

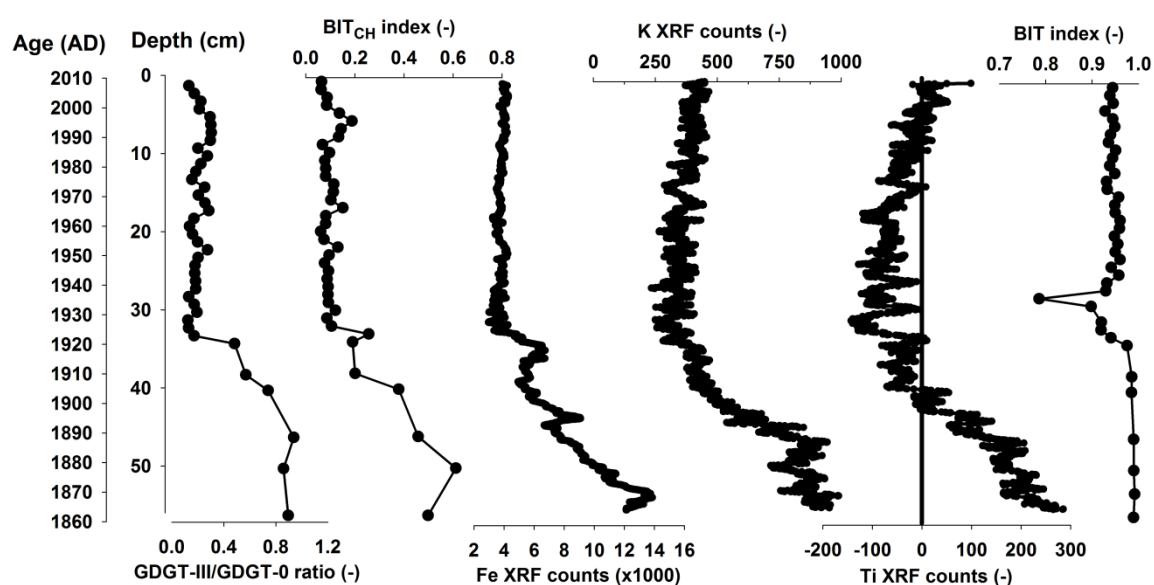


Fig. 2.5. Terrestrial input to the lake, traced via the ratio of branched GDGT-III/GDGT-0 (1050/1302), sum of branched to sum of isoprenoid GDGTs (BIT_{CH} index) and the XRF counts of Fe and K as running average of 9, XRF counts of Ti plotted as running average of 20 and BIT index according to Hopmans et al. (2004). All profiles are plotted vs. sediment depth and age (AD).

These trace metals correlate well with the ratio of branched (br) and isoprenoid (iso) GDGTs (Fig. 2.5). The correlation is in line with observations that indicate that brGDGTs originate from catchment soil, e.g. Weijers et al., 2007; Bechtel et al., 2010. Even though all the proxies indicate that most of the sediment material is of autochthonous, aquatic origin, the BIT index (Hopmans et al., 2004) would lead to a contrasting conclusion. Below 33 cm, the BIT index shows highest values between 0.98 and 1.0 and decreases to 0.9 at 28-29 cm. From 26 cm to the top of the core, the index is between 0.93-0.96. If interpreted in the classical way

(Hopmans et al., 2004), one would conclude that Rotsee sediment OM has a primarily terrigenous source. As concluded before (Bechtel et al., 2010) BIT index values can, however, be primarily ruled by the input of crenarchaeol, instead of by the input of brGDGTs. Indeed, the lower BIT value at 28-29 cm is due to a higher crenarchaeol concentration at that depth (Fig. 2.6). In lake settings, crenarchaeol is much less an indicator of aquatic archaeal input than it is in marine settings (Blaga et al., 2009), for which the BIT index was developed, and this may be especially the case in systems with a strong CH₄ cycle. The original BIT index deliberately excluded the other isoGDGTs because their source is considered more diverse, including methanogenic and methane-oxidizing archaea. If however, as is the case of Rotsee, a larger part of aquatic archaeal production is related to the CH₄ cycle, inclusion of the other isoGDGTs in the ratio should better reflect the relative input of allochthonous and autochthonous OM. Indeed, two alternative BIT indices, (i) the sum of all brGDGTs over the sum of all isoGDGTs (BIT_{CH}; definition in Section 2.2.7) or (ii) the ratio of a single brGDGT to GDGT-0, show much higher and more reasonable sensitivity to changes in the allochthonous supply from the lake catchment (Fig. 2.5).

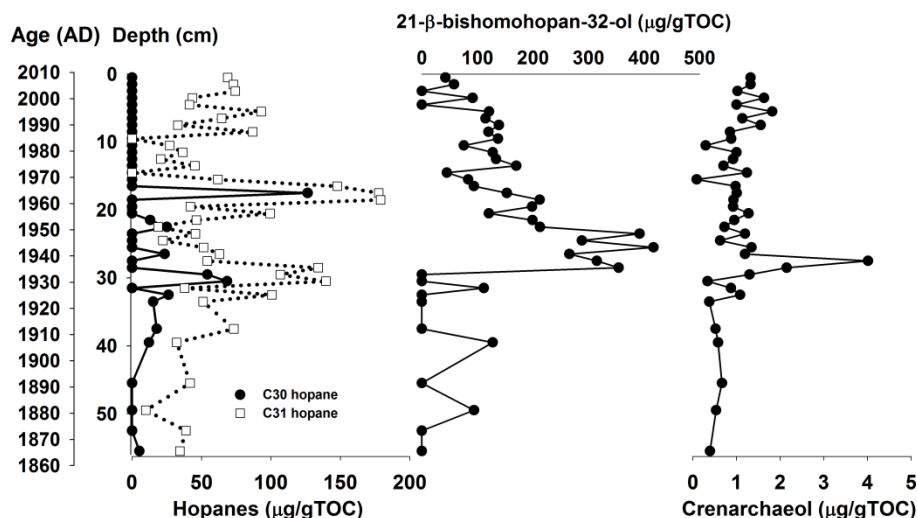


Fig. 2.6. Concentration of hopanoids and crenarchaeol vs. sediment depth and age (AD).

Besides dilution by autochthonous OM input as a cause for the relative changes in detrital input to the lake, this may of course also be caused by real changes in detrital input. Pfister (1999) observed that from 1828 to 1895 the frequency of extreme flood events in the Reuss River increased, although at that time it was not connected to Rotsee and therefore had no direct relationship. However, precipitation in the Swiss Alps was on average 28% higher during fall than the period between 1901 and 1960. In the 20th century, extreme floods decreased in abundance, which could have resulted in lower erosional input from the catchment to the lake. However, such an increase in flood events since the 1970s (Schmocker-Fackel and Naef, 2010) is not apparent from the profiles of Fe, K and BIT_{CH}, although the Ti profile may show such a signal (Fig. 2.5). We therefore conclude that these profiles most likely indicate a dilution of terrigenous detrital input by aquatic input. Profiles (Fig. 2.3, 2.7) of the sum of long chain FAs (C₂₄-C₃₀), *n*-alkanes (C₂₇-C₃₃) and *n*-alcohols (C₂₄-C₃₂) do not show a trend comparable to the Fe, K, Ti counts and BIT_{CH} (Fig. 2.5). In contrast, these compounds indicate that terrestrial input into the lake remained relatively constant.

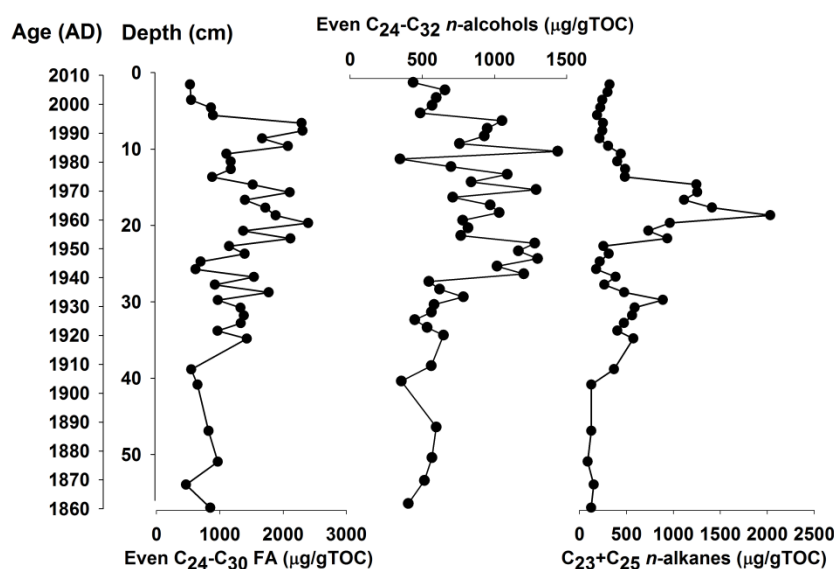


Fig. 2.7. Concentration profiles of sum of even C₂₄-C₃₀ FAs and sum of even C₂₄-C₃₂ *n*-alcohols and C₂₃+C₂₅ *n*-alkanes vs. sediment depth and age (AD).

2.3.4 Input and degradation of sedimentary OM

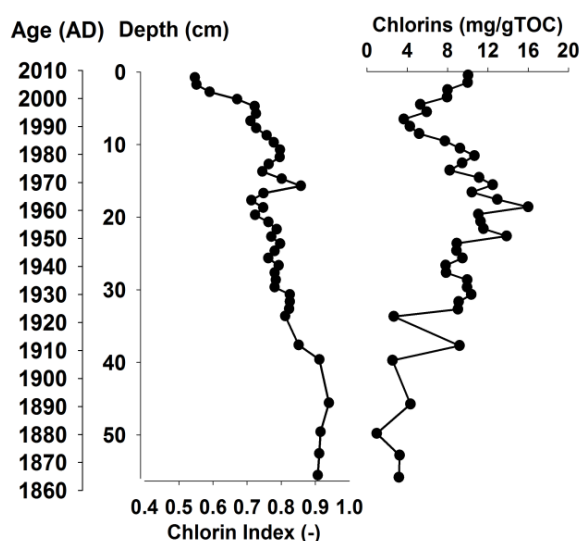


Fig. 2.8. Chlorin index and total chlorin concentration vs. sediment depth and age (AD).

The chlorin index (CI) is a qualitative parameter estimating OM “freshness” and degradation. The lowest value (0.55) was in surface sediment (Fig. 2.8), indicating relatively fresh OM (Schubert et al., 2005). However, fresh chlorophyll would show values of ca. 0.2, suggesting that chlorophylls reaching the sediment are partly degraded in the water column. With increasing sediment depth the index increased up to 0.94 (Fig. 2.8), close to that of inert material (1.0).

The concentration profile of total chlorins (Fig. 2.8) has been used to reconstruct palaeoproductivity (Schubert et al., 2005). In contrast to the TOC, there was a maximum only at 18-19 cm (16 mg/g TOC), followed by a continuous decrease with depth. Together with the strong increase in total chlorins from 6-7 cm towards the sediment surface and the rapid increase in CI values with depth, the absence of a peak at ca. 33-34 cm could be due to degradation (Fig. 2.8).

2.3.5 Impact of eutrophication on microbial community changes

2.3.5.1 Primary producers

While C₁₆ unsaturated FAs are generally related to algae and bacteria, C₁₈ unsaturated FAs originate from algae, zooplankton and cyanobacteria (Volkman et al., 1980; Wakeham et al., 2007). Despite the non-specificity of these FAs, their changing abundance indicated changes in overall productivity within the lake. Because of significant correlation with the TOC and

hopanoid profiles, the C_{16:1(9)} FA (double bond at C-9) may originate from a mixed source of primary producers (peaks at 15-20 and 32-33 cm) and bacteria (peaks at 22-25 cm and 18-19 cm), whereas C_{16:2(5,10)} FA is only related to productivity (Fig. 2.3, 2.9).

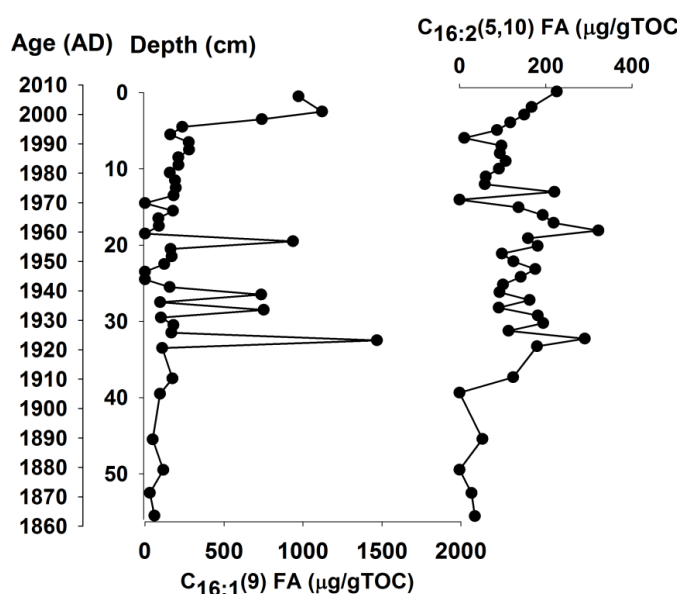


Fig. 2.9. Concentration of C_{16:1(9)} FA and C_{16:2(5,10)} FA vs. sediment depth and age (AD).

Phytol (3,7,11,15-tetramethyl-2-hexadec-2-en-1-ol), a ubiquitous marker, can originate from chlorophylls in phytoplankton, but also from land plants, bacteriochlorophylls and cyanobacterial mats (Rontani and Volkman, 2003). However, peaks in the profile trace times of higher productivity, due to the similarity with the TOC profile (Fig. 2.10).

Ergosterol (24-methylcholest-7-en-3β-ol, C_{29:1Δ7}; Fig. 2.10) has been found in fungi and yeast (Mille-

Lindblom et al., 2004), but also in low amount in algae and protozoa (Raederstorff and Rohmer, 1987). The latter source is more likely, as indicated by the similarity in the depth profile to that for phytol (Fig. 2.10). Nonetheless, fungi could thrive on phytoplankton and/or bacterial biomass in the water column and sediment. They may play a crucial role in the cycling of nutrients and carbon, but knowledge about fungi in lakes is limited (Grossart et al., 2010).

Certain steroids were very abundant between 1958 and 1972. They (Fig. 2.10 and 2.11), specifically stigmaterol (24-ethylcholesta-5,22E-dien-3β-ol, C_{29:2Δ5,22E}), stigmastanol (24-ethylcholestan-3β-ol, C_{29:0}), campesterol (24-methylcholesterol, 24-methylcholest-5-en-3β-ol, C_{28:1Δ5}), β-sitosterol (24-ethylcholest-7-en-3β-ol, C_{29:1Δ7}), dinosterol (4,23,24-trimethylcholest-22E-en-3β-ol) and dinostanol (4,23,24-trimethylcholestan-3β-ol) can be related to higher productivity between 1958 and 1972 (Fig. 2.3, 2.10, 2.11). The absence of a

peak between 1918 and 1922 may be due to bad preservation, because of their high relative lability vs. other lipids (Hoefs et al., 2002).

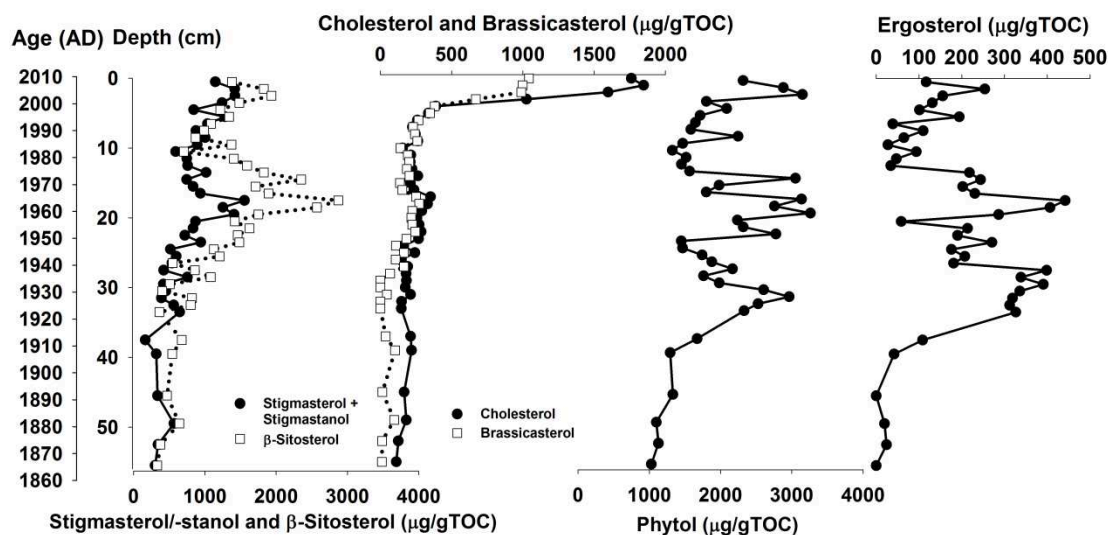


Fig. 2.10. Concentration of sterols, stanols and phytol vs. sediment depth and age (AD).

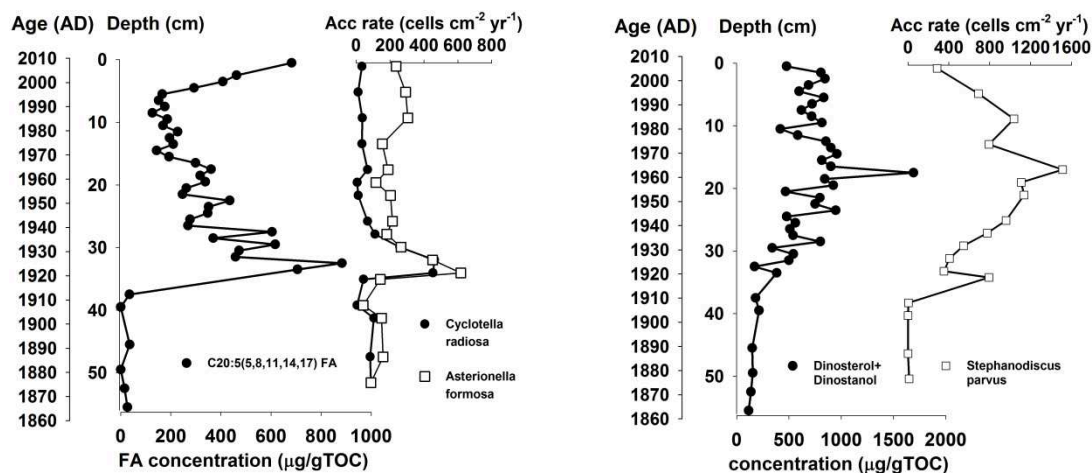


Fig. 2.11. Concentration of $\text{C}_{20:5(5,8,11,14,17)}$ FA and cell accumulation rate (acc rate) of *Cyclotella radiosa* and *Asterionella formosa* and profile of Dinosterol/stanol with accumulation rate of *Stephanodiscus parvus* vs. sediment depth and age (AD).

Because of the good match with higher TOC values between 1958 and 1972 (Fig. 2.3), stigmasterol and stigmasterol (Fig. 2.10) are interpreted as being derived mainly from phytoplankton in Rotsee, although a vascular plant source cannot be excluded (Volkman, 1986).

Similarly, brassicasterol (24-methylcholesta-5,22E-dien-3 β -ol, C₂₈:2 Δ 5,22E) and 24-methylcholesterol (Fig. 2.10) likely originate predominantly from algae (cf. Orcutt and Patterson, 1975; Volkman, 2003), but a contribution from higher plants cannot be excluded (Volkman, 2003). The match with cholesterol (cholest-5-en-3 β -ol, C₂₇:1 Δ 5), an algal/phytoplankton and zooplankton biomarker (Volkman, 1986; Volkman et al., 1998), suggests a similar origin. However, cholesterol and brassicasterol strongly decreased within the upper 5 cm, to ca. 21% and 37%, respectively (Fig. 2.10). Because of the high degree of degradation, the exact source of brassicasterol remains uncertain in Rotsee. A diatom source was not evident by comparison with diatom accumulation rate obtained in this study.

β -Sitosterol (Fig. 2.10) is the major sterol of emerged macrophytes (Ficken et al., 2000) and is often used as an indicator for higher plant input (Volkman, 1986). A high concentration peak was observed between 14 and 20 cm. The biomass of emerged aquatics probably increased as a result of the higher productivity. This is supported by the increased relative abundance of mid-chain *n*-alcohols and C₂₃ and C₂₅ *n*-alkanes at that depth (Fig. 2.7).

2.3.5.2 *Bacteria and Thaumarchaeota*

Hopanoids can be used as bacterial indicators (Rohmer et al., 1984), except for the hopanes discussed in Section 3.2.3. The peaks for C₃₀ and C₃₁ hopane at 28-31 cm (1926-1934) and 21- β -bishomohopan-32-ol between 25 and 29 cm (1932-1942) suggest a higher abundance of bacterial biomass and greater bacterial reworking of OM between 1926 and 1942 (Fig. 2.6). The higher abundance of straight and branched alkanes at 28-29 cm also indicates higher bacterial biomass at that time. Hopan-29-ol, C₃₂-bishomohopanol and C₃₁-homohopanol were detected, but could not be quantified because of the low abundance. The higher bacterial activity is further suggested by an epicholestanol peak at ca. 1933 (Fig. 2.1).

After another hopanoid maximum in the 1960s, following the primary productivity during the eutrophication maximum, the abundance decreased, which could be a combination of biomass reduction due to reduced nutrient supply and the low extent of degradation of their precursors in the upper sediment. The depth dependent differences when comparing different hopanoids suggest distinct unequal sources. Based on biomarker data alone, a clear source distinction within the bacteria is not possible.

At 27-28 cm (1934-1937) crenarchaeol is on average five times more abundant vs. the rest of the profile, with a trend of increasing concentration starting at ca. 1922 (Fig. 2.6). As crenarchaeol originates from Thaumarchaeota, (NH_4^+ oxidising archaea (Pitcher et al., 2011), the high abundance of crenarchaeol suggests a higher oxidation rate. It is not clear why Thaumarchaeota are only more abundant at this depth, because the trophic state was in general very high, at least between the 1920s and 1970s (Stadelmann, 1980; Kohler et al., 1984). However, the close match with bacteria between 1934 and 1937 suggests that a higher amount of NH_4^+ was supplied to the lake, which may have promoted Thaumarchaeota. The crenarchaeol maximum coincides with the construction of a mechanical sewage treatment plant in 1933 (Stadelmann, 1980), which would suggest a causal relationship. However, the mechanical water treatment should not have affected NH_4^+ content (Tchobanoglous et al., 2004). Either the biomass of bacteria and Thaumarchaeota might have increased due to a higher remineralisation rate for nutrients and OM during water treatment or these organisms were not removed in the treatment plant and entered the lake.

2.3.5.3 Diatoms

A description of the diatom assemblage in Rotsee was given by Bachmann (1931) and Lotter (1989). To compare the results, diatom accumulation rate was reinvestigated. In total, 71 different species were determined. Seven species *Stephanodiscus parvus*, *Cyclotella comensis*, *Asterionella formosa*, *Fragilaria crotonensis*, *Fragilaria ulna* var. *acus*, *Stephanodiscus hantzschii* and *Cyclotella comta/radiosa* represented at least 64% of all the diatoms. Several species represent the most dominant sources for certain biomarkers. It was not, however, possible to exclude other less abundant diatoms and/or other microorganisms as sources of these biomarkers.

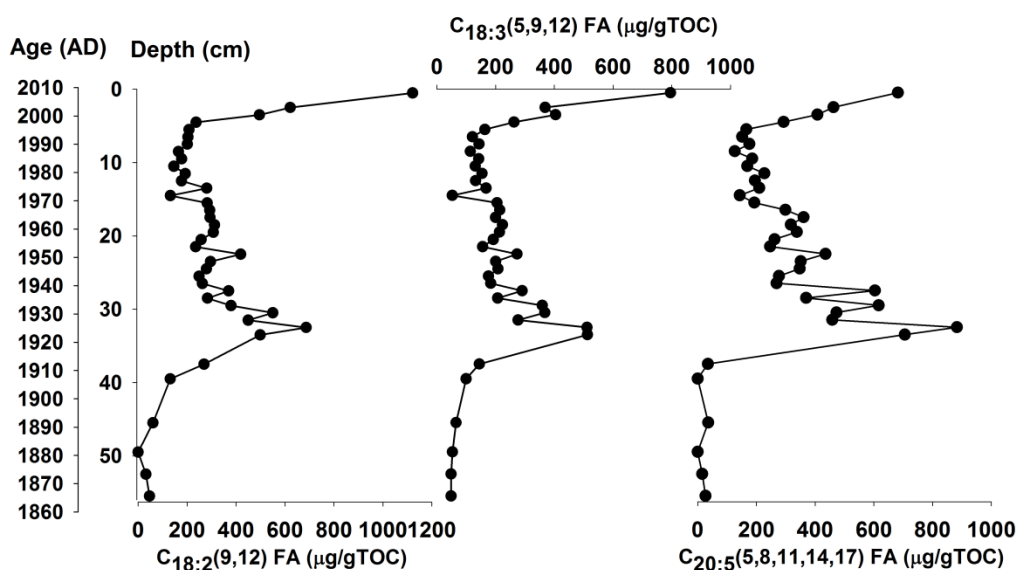


Fig. 2.12. Concentration of $C_{18:2(9,12)}$ FA, $C_{18:3(5,9,12)}$ FA and $C_{20:5(5,8,11,14,17)}$ FA, vs. sediment depth and age (AD).

The pentaunsaturated $C_{20:5(5,8,11,14,17)}$ FA (Fig. 2.11) is assumed to originate from diatoms (Volkman et al., 1998). The good correlation between the di- and tri-unsaturated FAs $C_{18:2(9,12)}$ and $C_{18:3(5,9,12)}$ with the $C_{20:5(5,8,11,14,17)}$ FA (R^2 0.69 and 0.76, respectively) suggests the same origin for all three FAs (Fig. 2.12). All three were sparse before 1918, most abundant between 1918 and 1924, and then continuously decreased (Fig. 2.12). The increase in the upper 5 cm could be a degradation pattern, as FAs are easily decarboxylated (Hoefs et al., 2002). The correlation with *Asterionella formosa* (R^2 0.46 for $C_{20:5}$, 0.37 for $C_{18:3}$, 0.48 for $C_{18:2}$) and *Cyclotella radiosa* (R^2 0.33 for $C_{20:5}$, 0.28 for $C_{18:3}$, 0.43 for $C_{18:2}$) seems to confirm them as the predominant source of these FAs. However, di- and tri-unsaturated FAs have also been referred to cyanobacteria and higher plants (Rezanka et al., 1983), which may explain the lower correlation between the diatoms and the $C_{18:2}$ and $C_{18:3}$ FAs.

The $C_{25:2}$ highly branched isoprenoid alkene ($C_{25:2}$ HBI; Fig. 2.13) is also known to be derived from diatoms (Volkman et al., 1998). In freshwater settings, only *Navicula sclesvicensis* has been reported to contain HBIs (Belt et al., 2001), but this diatom has not been found in Rotsee. The highest correlation with $C_{25:2}$ HBI could be found for *Stephanodiscus hantzschii*, but is only R^2 0.30, which suggests that other sources of this lipid need to be considered (Fig. 2.13).

Dinosterol and dinostanol were considered to be specific for dinoflagellates (Withers, 1983), but can also originate from diatoms (Volkman et al., 1993). Bachmann (1931) showed that dinoflagellates rarely occur in Rotsee and the deterministic $C_{22:6}$ FA for dinoflagellates (Volkman, 2003) is absent. Therefore, Dinosterol and dinostanol are interpreted as being of diatom origin. The Dinosterol/stanol profile matched the profiles

of *Stephanodiscus parvus*, *Fragilaria crotonensis*, *Cyclotella pseudostelligera* and *Tabellaria fenestrata* together with the productivity maximum for 1958-1961 (18-19 cm; Fig. 2.11, 2.14). However, cross plots indicate that the most dominant source seemed to be *Stephanodiscus parvus* (R^2 0.62, Fig. 2.11), also the most dominant of these diatoms in the lake since the 1920s due to the eutrophication. The low correlation for *Fragilaria crotonensis* (R^2 0.30) and *Tabellaria fenestrata* (R^2 0.28) suggests only a minor source of these lipids, while *Cyclotella pseudostelligera* (R^2 0.40) is unlikely to be a significant source because of its low accumulation rate.

24-Methylcholesterol can also be derived from dinoflagellates and diatoms (Orcutt and Patterson, 1975; Volkman, 2003). From the correlations, its main source could be *Stephanodiscus parvus* (R^2 0.45).

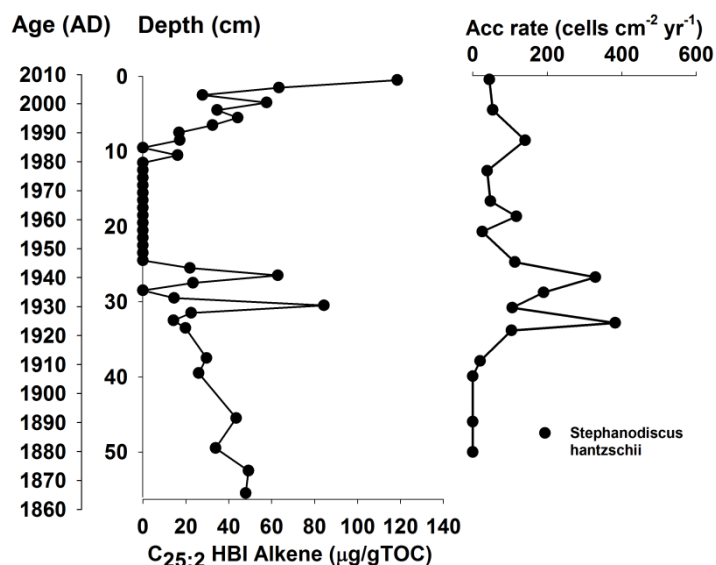


Fig. 2.13. Concentration of $C_{25:2}$ HBI alkene with cell accumulation rate (acc rate) of *Stephanodiscus hantzschii* vs. sediment depth and age (in AD).

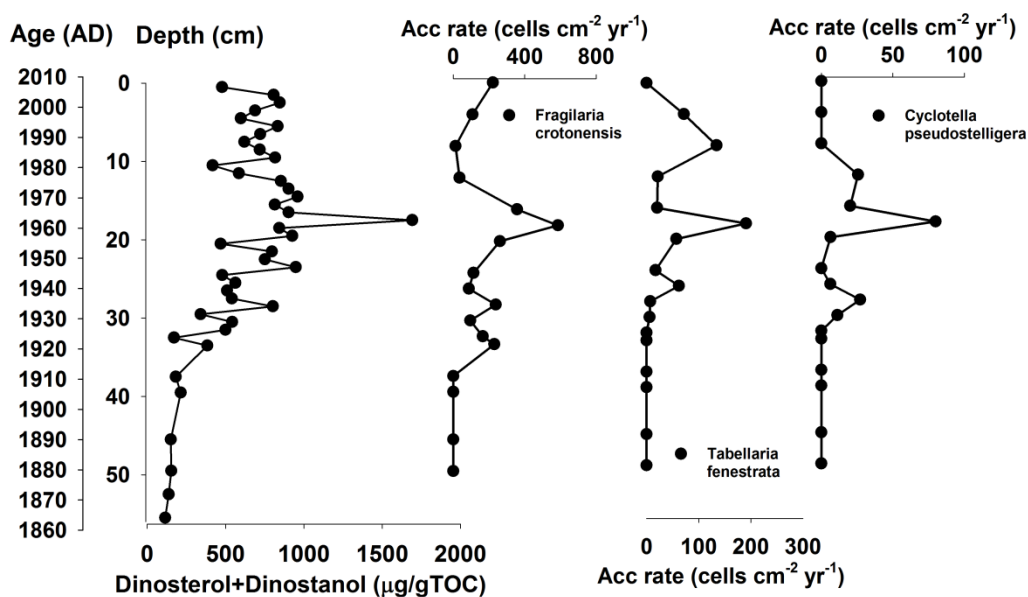


Fig. 2.14. Concentration of dinosterol + dinostanol with cell accumulation rate (acc rate) of *Fragilaria crotonensis*, *Tabellaria fenestrata* and *Cyclotella pseudostelligera* vs. sediment depth and age (AD).

2.3.5.4 Methanogenic and methanotrophic archaea

GDGT-0, the most dominant archaeal lipid, was used as a proxy for methanogenic archaea. This proposed origin is supported by the fact that ca. 98% of archaeal biomass in the lake was methanogenic with 91% consisting of *Methanosaeta* spp. (Falz et al., 1999). More evidence came from carbon isotope analysis after ether cleavage, with high $\delta^{13}\text{C}$ values between -36‰ and -21‰ for almost all ether cleaved GDGTs in the surface sediment, which is about the typical range of -35 to -22‰ for terrigenous, aquatic and also methanogenic archaeal lipids (Hinrichs et al., 2000), suggesting predominantly methanogenic sources. This is in contrast to much lower values, which can reach <-100‰ in marine settings, suggesting a predominantly methanotrophic origin (Hinrichs et al., 2000). On average, GDGT-0 showed a quite constant concentration of ca. 20 μg/g TOC, interrupted by a higher concentration during the productivity maxima, with ca. 42 and 83 μg/g TOC at 17-21 cm and 33-34 cm, respectively.

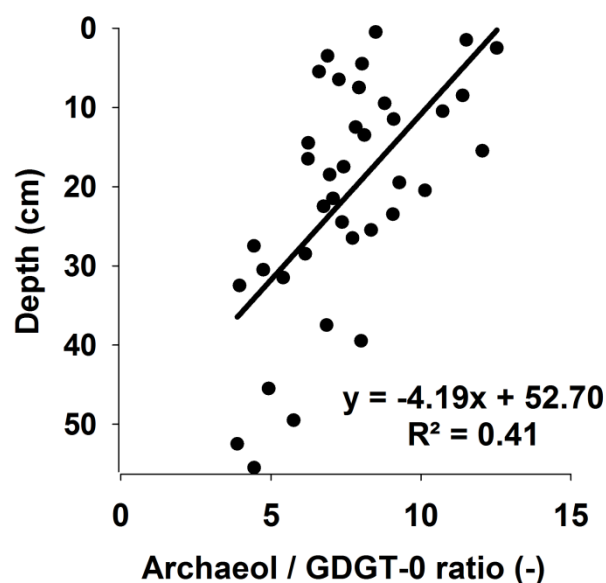


Fig. 2.15. Archaeol/GDGT-0 ratio vs. sediment depth and age (AD). The very low ratio at 33-34 cm was removed from the data, because of bias from the high GDGT-0 concentration.

ca. 9.2×10^8 cells g^{-1} dry sediment at 17-21 cm (1953-1964) and 1.8×10^9 cells g^{-1} dry sediment at 33-34 cm (1918-1921). From these estimates, it was assumed that the proportion of *Methanosaeta* spp. to all archaea in surface sediment has remained constant at 91% for the last 150 yr.

The extent to which the supply of archaeal lipids within the sediment core compensated for degradation losses remained, however, unconstrained. GDGTs and archaeol are considered to be relatively recalcitrant (Pease et al., 1998). The linear decrease in the ratio of archaeol and GDGT-0 with depth (Fig. 2.15) indicates that archaeol is more rapidly degraded than GDGT-0, suggesting slow degradation of GDGT-0 in Rotsee sediment.

Based on the results, the average cell content of GDGTs was estimated on the basis of values from the literature, with 1-3 fg intact GDGTs (iGDGTs) cell⁻¹ (Sinninghe Damsté et al., 2002; Wuchter, 2006; Huguet et al., 2010). IGDGTs consist of core GDGTs (cGDGTs) and polar head groups. In sediments, polar head groups are decomposed within days to weeks (Harvey et al., 1986; Lipp et al., 2008). A cell density in the surface sediment of 4.6×10^8 cells g^{-1} sediment (Falz et al., 1999) and 1-3 fg intact GDGTs, together with the correlation between

Based on reported data (Falz et al., 1999), GDGT-0 was used to estimate methanogen cell density in the lake sediment. The cell counts were highest at the sediment surface and decreased continuously with depth, with ca. 3x lower cell density at 10 cm vs. the sediment surface (Falz et al., 1999). Through correlation of the cores, a concentration of 4.6×10^8 cells g^{-1} dry sediment of *Methanosaeta* spp. in the surface sediment corresponded to GDGT-0 concentration of ca. 20 $\mu g/g$ TOC for most of the last 150 yr. During the productivity maxima, *Methanosaeta* spp. apparently increased up to at least

iGDGTs and cGDGTs (Huguet et al., 2010) leads to cGDGT concentration between 1.6 and 4.9 $\mu\text{g/g}$ sediment. This range is of the same order of magnitude as the measured concentration of the sum of isoGDGTs (2.0 $\mu\text{g/g}$ sediment). In the other direction, a theoretical iGDGTs/cell value for Rotsee sediment can be estimated, with a cell density of 4.6×10^8 cells g^{-1} sediment and 2.0 $\mu\text{g/g}$ sediment isoGDGTs leading to an average value of ca. 2.2 fg i-GDGTs/cell for Rotsee archaea.

2.4 Summary and conclusions

Rotsee has been shown to be an ideal site for studying an anthropogenically altered ecosystem due to eutrophication. A multi-proxy approach, using lipid biomarkers and trace metals with a high temporal resolution of 4 years, made it possible to reconstruct short term changes in the physical, chemical and biological status. A direct impact of higher sewage and nutrient input on the increase in productivity and OM accumulation was observed, which led predominantly to a radiation in diatoms, primary producers and methanogens between about 1918 and 1921 and all microorganism groups and macrophytes between about 1958 and 1972. A higher abundance of bacteria and NH_4^+ oxidising archaea was likely related to the construction of a mechanical sewage treatment plant in 1933. The decrease in OM accumulation in the lake since the end of the 1960s resulted from the construction of an interceptor sewer between 1967 and 1969. Furthermore, the decrease in fossil OM/biodegraded oil related biomarkers (C_{27} Ts/Tm and C_{27} hopanoids, long chain odd *n*-alkanes) is a clear indication for the achievement by the sewage treatment plant construction in 1974. The $\delta^{15}\text{N}$ of bulk OM, in contrast to coprostanol and epicholestanol, traced the eutrophication and recovery during the past 150 years.

Based on the correlation of trace metals (Fe, Ti, K) with br/iso GDGTs, terrestrial input could be reconstructed. We propose an altered BIT index, BIT_{CH} , as the sum of all brGDGTs/the sum of all isoGDGTs, the ratio better reflecting the balance between all aquatic archaea, including those related to the methane cycle, and soil-derived brGDGTs than the original BIT index.

The impact of eutrophication on microbial assemblage changes could be traced. Also based on previous microbial studies, the sources of certain biomarkers could be partly identified down to the species level. The C_{18:2(9,12)}, C_{18:3(5,9,12)} and C_{20:5(5,8,11,14,17)} FAs likely originated mainly from the diatoms *Cyclotella radiosa* and/or *Asterionella formosa*. The C_{25:2} HBI originated from mixed sources and a clear source distinction between diatom species was not possible. *Stephanodiscus parvus* could be the main source of dinosterol and 24-methylcholesterol. The abundance of methanogenic archaea and the cellular membrane lipid content (GDGTs) could be estimated.

Although microbial biomass reconstruction based on lipid biomarkers is often limited due to the non-specificity of lipids and their lability with respect to degradation, the use of high resolution multi-proxy records can improve the distinction of biomarker sources. Biomarker analysis can trace short term, and eutrophication related ecosystem and microbial community changes.

2.5 Acknowledgements

The project was funded by the European Union project “Hypox – In situ monitoring of oxygen depletion in hypoxic ecosystems of coastal and open seas and land-locked water bodies” (EC grant 226213).

The authors wish to express their thanks to P. Schaeffer and P. Adam (University of Strasbourg, France) for helpful discussions and support in interpreting biomarker data. We would also like to express gratitude to H. Niemann (University of Basel, Switzerland) for help with ether cleavage. A. Zwyssig (Eawag) is thanked for field support and G. Nobbe (Eawag) for help in the laboratory. We thank I. Brunner (Eawag) for measuring TIC using a Coulomat for comparison with our method. R. Kipfer, B. Wehrli, North and D. Carstens (all Eawag) are acknowledged for helpful suggestions and discussions. We thank P.A. Meyers and an anonymous reviewer for comments and critical review of the paper.

Chapter 3: Maleimides in recent sediments – Using chlorophyll degradation products for palaeoenvironmental reconstructions

Sebastian Naeher, Philippe Schaeffer, Pierre Adam, Carsten J. Schubert

In Review for Geochimica et Cosmochimica Acta

Abstract

Maleimides (transformation products of chlorophylls and bacteriochlorophylls) were studied in recent sediments from the Swiss lake Rotsee and the Romanian Black Sea Shelf to investigate chlorophyll degradation, the role of oxygen in maleimide formation, and to identify their sources. Naturally occurring maleimides (i.e., “free” maleimides) and maleimides obtained after chromic acid oxidation of sediment extracts (i.e., “bound” maleimides) were analysed. 2-Methyl-maleimide (Me,H maleimide), 2,3-dimethyl-maleimide (Me,Me maleimide), 2-methyl-3-vinyl-maleimide (Me,vinyl maleimide), 2-methyl-3-ethyl-maleimide (Me,Et maleimide) and traces of 2-methyl-3-*iso*-butyl-maleimide (Me,*i*-Bu maleimide) occurred naturally in the sediment with a large predominance of the Me,Et homologue. Tetrapyrrolic pigments related to chlorophylls were the main source of maleimides, although a small contribution of other sources such as cytochromes and/or phycobilins cannot be completely ruled out. The predominant Me,Et maleimide and Me,vinyl

maleimide most likely originate from chlorophyll *a* related pigments. The same holds for Me,H maleimide, which might be formed following degradation of ring E from the tetrapyrrolic nucleus, whereas the source of Me,Me maleimide remains unknown. 2-Methyl-3-*n*-propyl-maleimide (Me,*n*-Pr maleimide) and Me,*i*-Bu maleimide arising from bacteriochlorophyll related pigments traced the presence of phototrophic sulfur bacteria (Chlorobiaceae), which indicates photic zone euxinic and anoxic conditions in Rotsee during the last 150 years and throughout the Black Sea history, including the limnic phase of the Black Sea (Unit 3). Some other minor maleimides with specific alkylation pattern also originate from bacteriochlorophylls, while the source of others could not be identified. Free maleimides were mainly formed in the absence of oxygen in the sediment. Novel maleimide degradation indices are proposed to estimate the degree of OM degradation (OM freshness/degradability). These proxies are applicable on longer timescales than e.g. the chlorin index.

3.1 Introduction

Chlorophylls and bacteriochlorophylls (the structures of chlorophylls and bacteriochlorophylls can be found in the Appendix) are the most abundant and most important pigments on Earth (Scheer, 2006). These structurally diverse compounds are required for light absorption and are key compounds for photosynthesis (Scheer, 2006). Apart from their physiological importance, they and/or their transformation products (chlorins, porphyrins, maleimides) can be preserved in limnic and marine sediments as well as in crude oils (e.g. Hodgson et al., 1968; Quirke et al., 1980; Grice et al., 1996, 1997, 2005; Louda et al., 1998; Naylor and Keely, 1998; Wilson et al., 2004).

These compounds can serve as important indicators for palaeoenvironmental reconstructions, such as e.g. palaeoproductivity estimates (Summerhayes et al., 1995; Harris et al., 1996; Schubert et al., 1998) and OM freshness (Shankle et al., 2002; Schubert et al., 2010). Within the water column and in the sediment, chlorophylls undergo minor to major transformations, which continue during diagenesis and lead to the formation of porphyrins and maleimides

(Grice et al., 1996; 1997; Airs et al., 2000; Villanueva and Hastings, 2000; Pancost et al., 2002). Porphyrins, diagenetic transformation products of chlorophylls, have been intensely studied since the 1930s (e.g. Treibs, 1936; Hodgson et al., 1968; Casagrande and Hodgson, 1976; Barwise and Roberts, 1984; Baker and Louda, 1986; Keely et al., 1994; Ohkouchi et al., 2008). In contrast, maleimides (1*H*-pyrrole-2,5-diones; the structures of the different maleimides mentioned in the text can be found in the Appendix), the oxidation products of the tetrapyrrole nuclei from pigments - but also potentially from other sources such as cytochromes (e.g. Paoli et al., 2002; Munro et al., 2009) and phycobilins (e.g. Glazer et al., 1976; Brown et al., 1990) - have been hardly examined so far in recent sedimentary settings (the structures of cytochromes and phycobilins are presented in the Appendix). Most studies focused on the degradation of porphyrins in crude oils and ancient deposits, for instance Permian Kupferschiefer and Mid-Triassic shales (Grice et al., 1996, 1997), petroleum source rocks in Australia, which comprise the Permian-Triassic boundary (Grice et al., 2005), Cretaceous Boscan crude oil (Quirke et al., 1980), Cretaceous/Tertiary boundary formations (Shimoyama et al., 2001) and Neogene sediments (Kozono et al., 2001). Free Me₂Et maleimide in recent sediments was first reported from Tokyo Bay, Japan (Kozono et al., 2002). The authors explained this observation by chlorophyll oxidation in the photic zone under the presence of light and oxygen.

However, there is still a need for the detection and characterisation of maleimides in recent sediments in order to determine their partly unknown precursors, their formation processes and their significance in terms of environmental conditions.

Me₂Et and Me₂Me maleimides from porphyrins were assigned to phytoplanktonic chlorophylls based on structural grounds (Grice et al., 1996). The chlorophyll precursor compounds of Me₂*n*-Pr and Me₂*i*-Bu maleimides are bacteriochlorophylls *c*, *d* and *e* from phototropic sulfur bacteria of the family Chlorobiaceae (Grice et al., 1996). Together with the diagenetic derivatives of the carotenoids isorenieratene and chlorobactene, these maleimides were used to reconstruct photic zone euxinia (Grice et al., 1996, 1997, 2005; Pancost et al., 2002).

Furthermore, it has been noted previously that maleimides are oxidation products, which were also found in anoxic and euxinic settings (Grice et al., 1996, 1997; Magness, 2001; Pancost et

al., 2002). This observation indicated that maleimides might also be formed by other electron acceptors independent of the presence of oxygen in the water column and/or the sediment of aquatic ecosystems (Magness, 2001; Pancost et al., 2002). There is a need to determine the implications of the presence or absence of oxygen on chlorophyll transformation into maleimides. More insight into the preservation and decomposition of chlorophylls might also help to reconstruct water column properties, depositional conditions during sedimentation and diagenesis with valuable information regarding the degree of oxygen depletion in the studied system.

The aim of this paper was to study the distributions of naturally occurring maleimides (i.e. “free maleimides”) in recent sediments of the Swiss lake Rotsee and the Black Sea and to compare them with those released after chromic acid oxidation of their parent tetrapyrrolic precursors, in order to investigate chlorophyll and chlorin degradation and to identify the maleimide sources. The role of oxygen in maleimide formation and the usefulness of maleimides as degradation indices were evaluated.

3.2 Methods

3.2.1 Study sites and sample collection

Rotsee is a small (0.46 km²), prealpine, monomictic and eutrophic Swiss lake. It has a stratified water column with a chemocline between about 6 and 10 m depth and an anoxic hypolimnion during most of the year (Schubert et al., 2010). At the maximum lake depth of 16 m, two sediment cores (54 and 58 cm long) were recovered with a gravity corer in August 2010 (GPS position N47°4.251 E8°18.955, WGS84; Naeher et al., 2012). The sedimentation rate is about 0.38 cm yr⁻¹ (Naeher et al., 2012). The cores were sliced in 2 cm intervals and frozen at -20 °C shortly after recovery.

The Black Sea (0.46 million km², max. depth of 2220 m) is a semi-enclosed brackish sea and the largest modern anoxic basin in the world (Ozsoy and Unluata, 1997). It is connected to the Marmara Sea and the Mediterranean Sea through the Bosphorus and Dardanelles straits. Since

9.3 ka, inflow of more saline water through the Bosphorus strait into the deep water of the Black Sea has led to a permanent stratification with the pycnocline located in 50-150 m water depth (Ozsoy and Unluata, 1997; Piper and Calvert, 2011). The Black Sea evolved from an isolated limnic-brackish lake to a restricted intermediate-salinity sea (Ross and Degens, 1974; Piper and Calvert, 2011). Permanent stratification led to bottom water anoxia since approximately 8.4 ka (Piper and Calvert, 2011).

A 242 cm long sediment core was recovered with a gravity corer at the sampling site 10MA10 (N 43° 43.905 E 30° 11.962, WGS84) at a water depth of 220 m during a RV *Mare Nigrum* cruise on the Romanian Black Sea Shelf in May 2010. It showed the typical Black Sea sediment sequence (Ross and Degens, 1974; Piper and Calvert, 2011). The transition of Unit 3 to Unit 2 was at 109 cm, with a clear colour contrast and a sandy base of Unit 2. This transition could not have occurred earlier than about 6 ka BP in this shallow water depth based on estimates by Ross and Degens (1974). Unconformities at 86 cm and 97 cm indicated an incomplete sedimentation record. Based on estimates of Ross and Degens (1974), the core comprises ca. 9-10 ka.

3.2.2 Sample preparation

3.2.2.1 Lipid biomarkers and pigments

The detailed procedure used for lipid biomarker and pigment analysis procedure is reported in Naeher et al. (2012). In short, the sediment was extracted by ultrasonication with mixtures of methanol (MeOH) and dichloromethane (DCM). Internal standards were added for quantification (α -Cholestane, C₁₉ *n*-fatty acid, C₁₉ *n*-alcohol). After saponification, neutrals were further separated into apolar and polar fractions over NH₂ columns (Hinrichs et al., 2003). The polar fraction was derivatised with BSTFA for 1h at 80 °C and the FA fraction with 14% BF₃/MeOH. FA double bond positions were determined according to (Spitzer, 1997). In case of Black Sea sediment extracts, an aliquot of the polar fraction was desulfurised with Raney-Nickel catalyst (Sinninghe Damsté et al., 1988), followed by hydrogenation for 2 h with PtO₂ as catalyst in a solution of acetic acid and ethyl acetate (1:1, v:v). Instrumentation and measurement conditions are described in Naeher et al. (2012).

3.2.2.2 Free and oxidised maleimide analysis

For maleimide analysis, the method of Grice et al. (1996) was used with slight modifications, whereas the same maleimide nomenclature for that study and Grice et al. (1996) was used. Freeze-dried and ground sediment samples from Rotsee (13-28 g) and the Black Sea (58-296 g) were extracted with 150-500 ml dichloromethane (DCM)/acetone (1:1, v:v; 3 x), first by stirring for 1 h (1 x), and by 20 min ultrasonication (2 x). After each extraction step, the mixture was centrifuged (2800 rpm, 4 min), the supernatant recovered and combined, the solvent being removed by rotary evaporation.

While one half of the total lipid extract remained untreated (comprising naturally occurring maleimides; free fraction), the other half was oxidised using chromic acid (comprising both naturally occurring maleimides and those formed by oxidation of chlorophylls and related tetrapyrrole pigments in the sediment; oxidised fraction) using modifications of existing protocols (Quirke et al., 1980; Folly and Engel, 1999). For the oxidation procedure, the lipidic extract was dissolved in 1 ml trifluoroacetic acid (TFA). 50 ml of 1.7% chromic acid was added dropwise under continuous stirring for 1 h at room temperature. The solution was transferred in a separation funnel and the organic extract was recovered using ethyl acetate (EtOAc, 3 x) and DCM (1 x).

The free and oxidised fractions were separated on a silica column into three fractions, eluting with DCM (F1), 20% EtOAc in DCM (F2) and DCM/MeOH (1:1, v:v, F3). A known aliquot of F2 was further purified by preparative thin layer chromatography (TLC), eluting with 20% EtOAc in DCM on Merck silica gel plates (20 x 20 cm², 0.5 mm thickness, preeluted with EtOAc and activated at 120 °C). During these chromatographic separations only alkylated maleimides are obtained and the more polar maleimides bearing acidic functional groups are not recovered. H₂H maleimide was used as a retention standard (retention factor R_f 0.5), eluted in parallel with the sample on the margins of the TLC plate. Maleimides were visualised with UV light at 254 nm and the fluorescent band between ca. R_f 0.5 and 0.8 was scraped and recovered by elution on a short silica column using EtOAc. After removal of the solvent under reduced pressure, the recovered fraction was dissolved in 150 µl pyridine and derivatised overnight using 100 µl MTBSTFA (N-(*tert*-butyldimethylsilyl)-N-methyl trifluoroacetamide, Pierce) to obtain TBDMS (*tert*-butyldimethylsilyl) derivatives (Grice et

al., 1996). The solvent and excess reagent were removed under a stream of N₂ at room temperature, and the resulting crude mixture was further purified on a silica gel column eluting with DCM. The purified fraction was measured on a gas chromatograph equipped with a flame ionisation detector (GC-FID) and on a gas chromatograph coupled to a mass spectrometer (GC-MS).

Maleimides (as TBDMS derivatives) were identified based on their relative GC retention times and comparison with published mass spectra (Grice, 1995; Grice et al., 1996). Me,H, Me,Me and Me,Et maleimides were quantified by coinjection with the TBDMS derivative of H,H maleimide used as a reference (ca. 12 ng/injection). The other maleimides were quantified by GC-MS based on the Me,Me maleimide concentration using the area of their respective peaks on the *m/z* 75 mass chromatogram. For the Black Sea samples, Me,*n*-Bu maleimide was quantified using the *m/z* 224 (base peak) mass chromatogram of Me,*i*-Bu maleimide due to low concentrations. Similarly, the *m/z* 238 (base peak) mass chromatogram was used to quantify Me,*neo*-Pentyl and Me,*n*-Pentyl maleimides. However, no response factors have been determined for the quantification of the different maleimides and the standard, so only relative concentrations are given in this study. Maleimides with additional carboxylic groups (e.g. hematinic acid and related compounds) were not investigated in this study.

3.2.2.3 Chromic acid oxidation of methyl pyropheophorbide *a*

Methyl pyropheophorbide *a* (29 mg) was dissolved in trifluoroacetic acid (2 ml) and a 1.7% chromic acid solution (28 ml) was added under stirring at room temperature. After 90 min, water (15 ml) was added and the crude mixture was extracted with EtOAc (2 x 50 ml). The combined organic fractions were washed with water (3 x 50 ml) and the solvent evaporated under reduced pressure, yielding 7 mg of crude degradation products. An aliquot of the organic extract (4 mg) was further filtered over a small silica gel column. The fraction recovered by eluting with a mixture of DCM/MeOH (1:1, v:v) and containing the maleimides (3.5 mg) was derivatised using N-(*tert*-butyldimethylsilyl)-N-methyl trifluoroacetamide (MTBSTFA; 400 µl) in pyridine (400 µl). The solvent and the excess of reagents were removed under a stream of N₂ and the fraction was further analysed by GC-MS. To compare

the relative concentrations of Me,Et and Me,vinyl maleimides, the obtained fraction was measured by GC-FID and GC-MS using in the latter case the m/z 75 mass fragmentogram. Since the response factor of Me,Et- and Me,vinyl maleimides are different on the m/z 75 mass chromatogram, a correction factor was determined using the response of both maleimides on the FID signal, allowing determination of their real proportion based on the following equation: $[Me,vinyl]/([Me,vinyl]+[Me,Et]) = 0.72 (A_{Me,vinyl})/(A_{(Me,vinyl+Me,Et)})$, with A corresponding to the areas measured on the m/z 75 mass fragmentogram.

3.2.2.4 Instruments

GC analysis was carried out on an Agilent Hewlett-Packard HP6890 GC equipped with an Agilent HP-5 column [30 m x 0.32 mm inner diameter (ID) x 0.25 μ m film thickness (FT)], an on-column injector and a flame ionisation detector (FID). The GC oven temperature program as follows: 40 °C to 100 °C at 10 °C min⁻¹, 100 °C to 300 °C at 4 °C min⁻¹, 30 min isothermal at 300 °C. Hydrogen was used as the carrier gas with a constant flow rate of 2.5 ml min⁻¹.

GC-MS analysis was performed with a Thermo TSQ Quantum mass spectrometer equipped with a HP-5 MS column (30 m x 0.25 mm ID x 0.25 μ m FT) and a programmed temperature vaporising (PTV) injector and was operated at an electron ionisation of 70 eV and a source temperature set at 210 °C. Helium was used as carrier gas (1 ml min⁻¹), and the m/z scan range was set between 50 and 700 Da. The oven was programmed as follows: 40 °C (10 min isothermal), 40 °C to 100 °C at 10 °C min⁻¹, 100 °C to 300 °C at 4 °C min⁻¹, isothermal at 300 °C. Single ion monitoring (SIM) analyses were performed using the ions m/z 75.0, 168.1, 182.1, 196.2, 210.2, 224.2 and 238.2.

3.2.3 Definition of Me,Me and Me,Et indices

Novel maleimide-based degradation indices were defined as follows:

Me,Me index = ([Me,Me] in the free fraction) / ([Me,Me] in the oxidised fraction*)

Me,Et index = ([Me,Et] in the free fraction) / ([Me,Et] in the oxidised fraction*)

Where:

[Me,Me] = concentration of 2,3-dimethyl-maleimide ($\mu\text{g g}^{-1}$ TOC)

[Me,Et] = concentration of 2-methyl-3-ethyl-maleimide ($\mu\text{g g}^{-1}$ TOC)

*: Note that the oxidised fraction contains both the free maleimides and those formed upon oxidation of chlorophyll derivatives.

3.3 Results and discussion

3.3.1 Me,vinyl and Me,Et maleimides in the free and oxidised fraction from Rotsee samples

Me,Et maleimide was the dominant maleimide from Rotsee samples (> 96% of all maleimides) in both the “free” fractions and those obtained upon chromic acid oxidation (Figs. 3.1A , 3.1C, 3.2). Such a large predominance in all sediment extracts is to be expected since this compound can be formed from most of the tetrapyrrole pigments, including notably chlorophyll *a* derivatives from primary producers living in the oxic part of the water column, as well as from bacteriochlorophylls thriving in the anoxic photic zone of the water column (Grice et al., 1996).

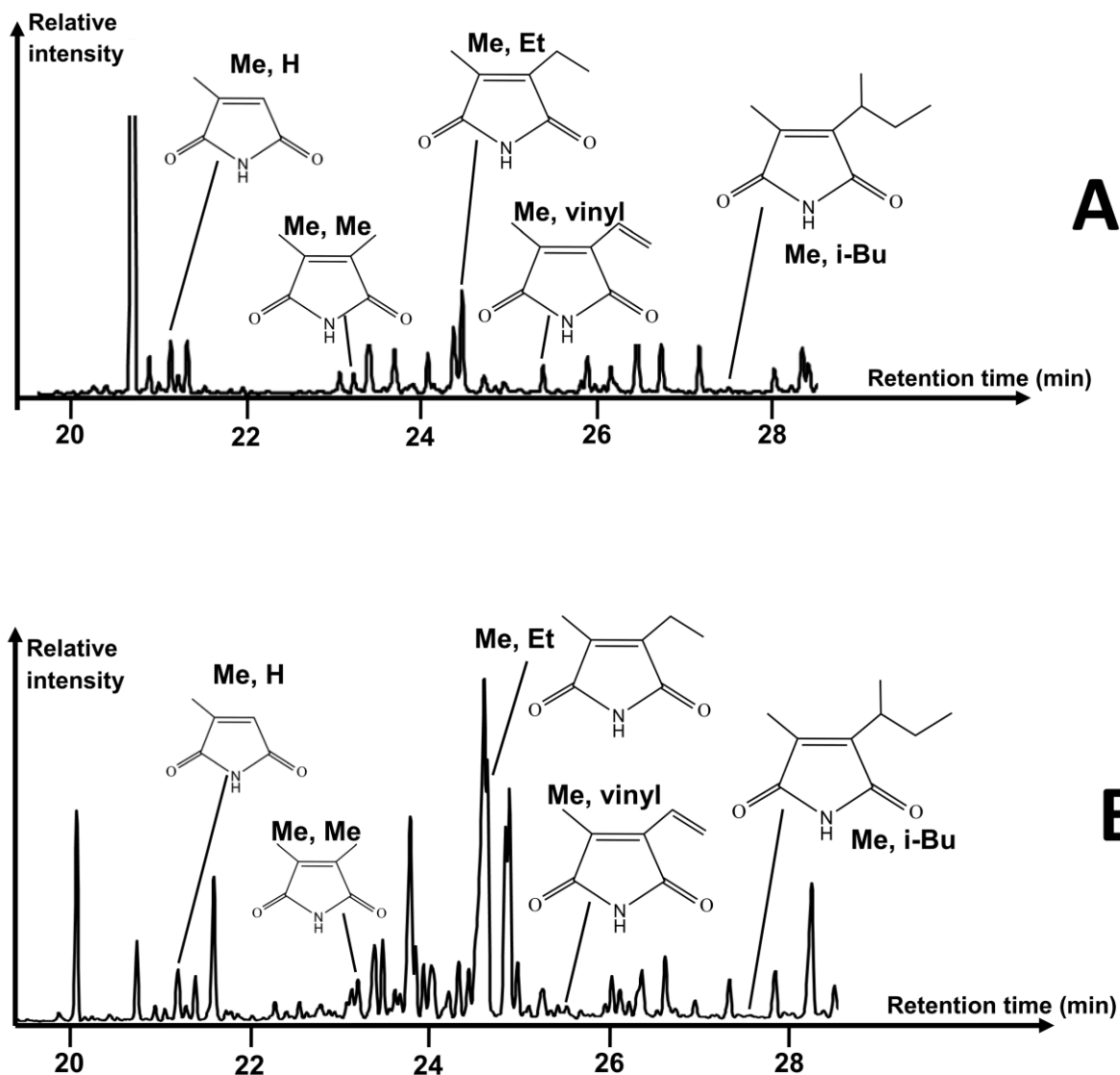
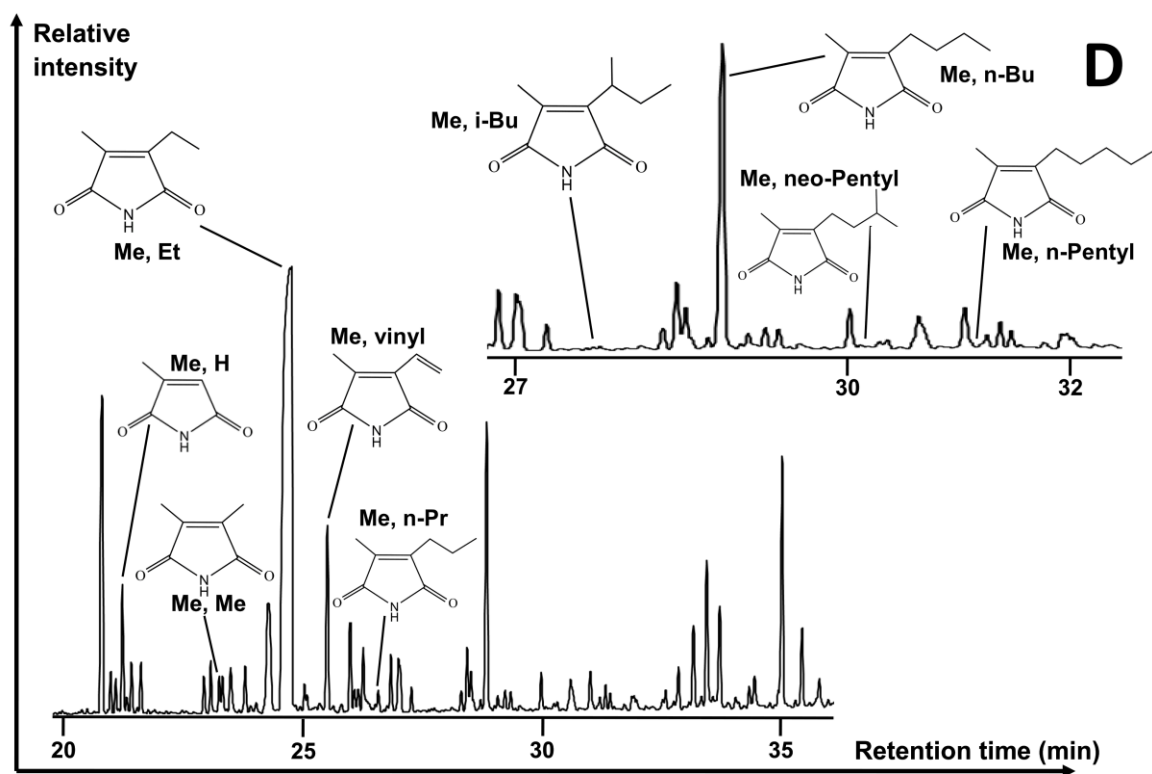
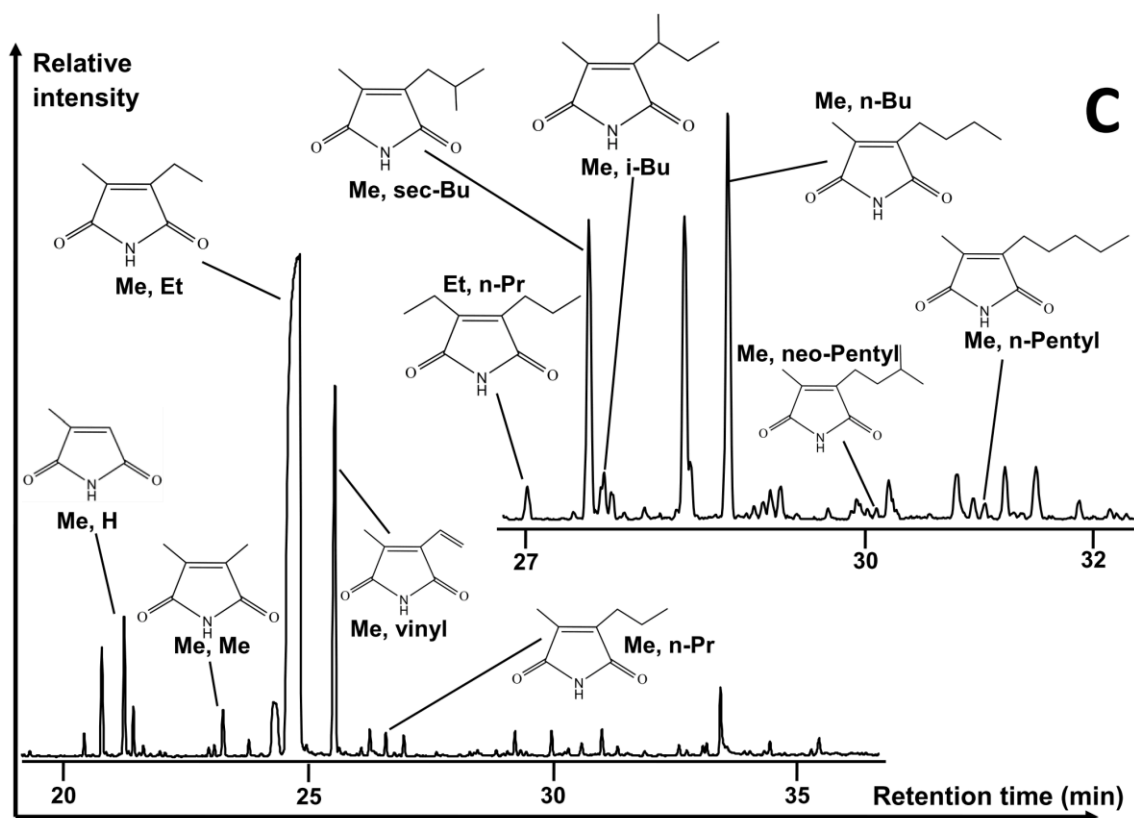


Fig. 3.1. Gas chromatogram (reconstructed ion chromatogram, RIC) showing the maleimides in the free fraction of Rotsee (A) and the Romanian Black Sea Shelf (B) surface sediment and (continued on the next page) the corresponding oxidised fractions of Rotsee (C) and Romanian Black Sea Shelf (D) surface sediment. Insert chromatograms in (C) and (D) represent enlargements of the chromatogram at retention times between 27 and 32 min. The maleimides are analysed as TBDMS derivatives.

(figure 3.1 continued)



Additional (indirect) sources, comprising hemes and/or phycobilins (e.g. Glazer et al., 1976; Brown et al., 1990; Paoli et al., 2002; Munro et al., 2009), might also be considered in the case of recent sediments, but the formation of Me₂Et-maleimide from such molecule precursors would require in most cases a first diagenetic step involving reduction of the vinylic double bond or C-S bond present on these precursor molecules. Such a reduction reaction might be operative in strong anoxic, sulfur-rich environments as those investigated here. Indeed, Pickering and Keely (2011) have shown by means of laboratory experiments that during early diagenesis, the double bond of the C₃ vinyl substituent of chlorophyll *a* and related derivatives can be reduced in the presence of H₂S, albeit this reaction occurs in rather low yields. Therefore, although the predominant contributions by far for Me₂Et-maleimide are most likely chlorophyll-related pigments, one cannot exclude other minor sources, as proposed based on stable carbon isotopic grounds in the case of a C₃₂ etioporphyrin from Cretaceous and Tertiary sediments (Boreham et al., 1989).

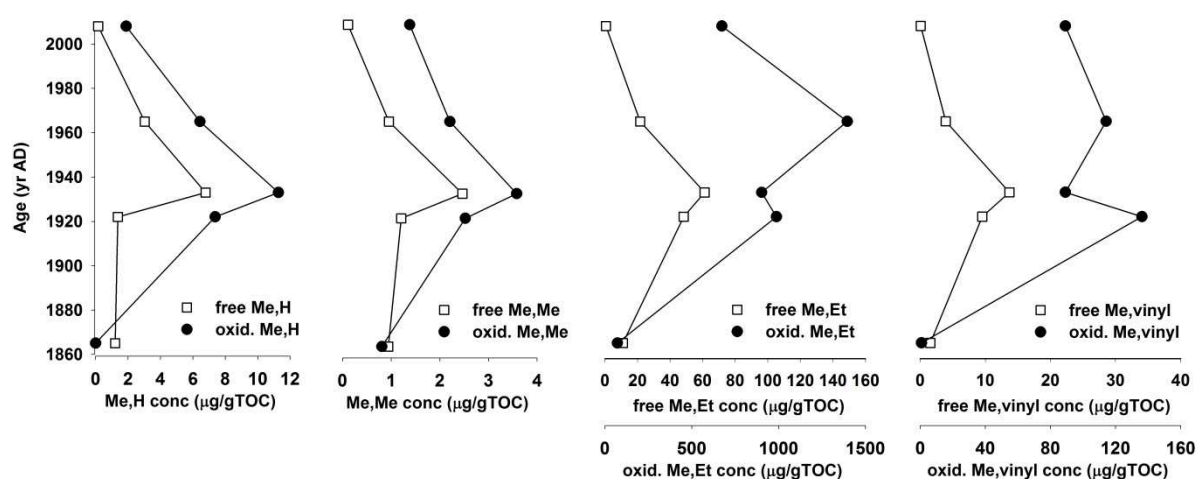


Fig. 3.2. Concentrations (“conc”) of Me₂H, Me₂Me, Me₂Et and Me₂vinyl maleimides in the free and oxidised (“oxid.”) fractions in Rotsee sediment vs. age (AD).

Free Me₂Et maleimide peaked at around 1933, whereas in the oxidised fraction, this compound was most abundant in the beginning of the 1920s and during the 1960s (Fig. 3.2). Naeher et al. (2012) showed that bacterial biomass was higher in the beginning 1930s, based on higher concentrations of C₃₀ and C₃₁ hopanes, 21 β (H)-bishomohopan-32-ol and straight and branched acyclic alkanes. The more abundant bacteria at that time might be the result of

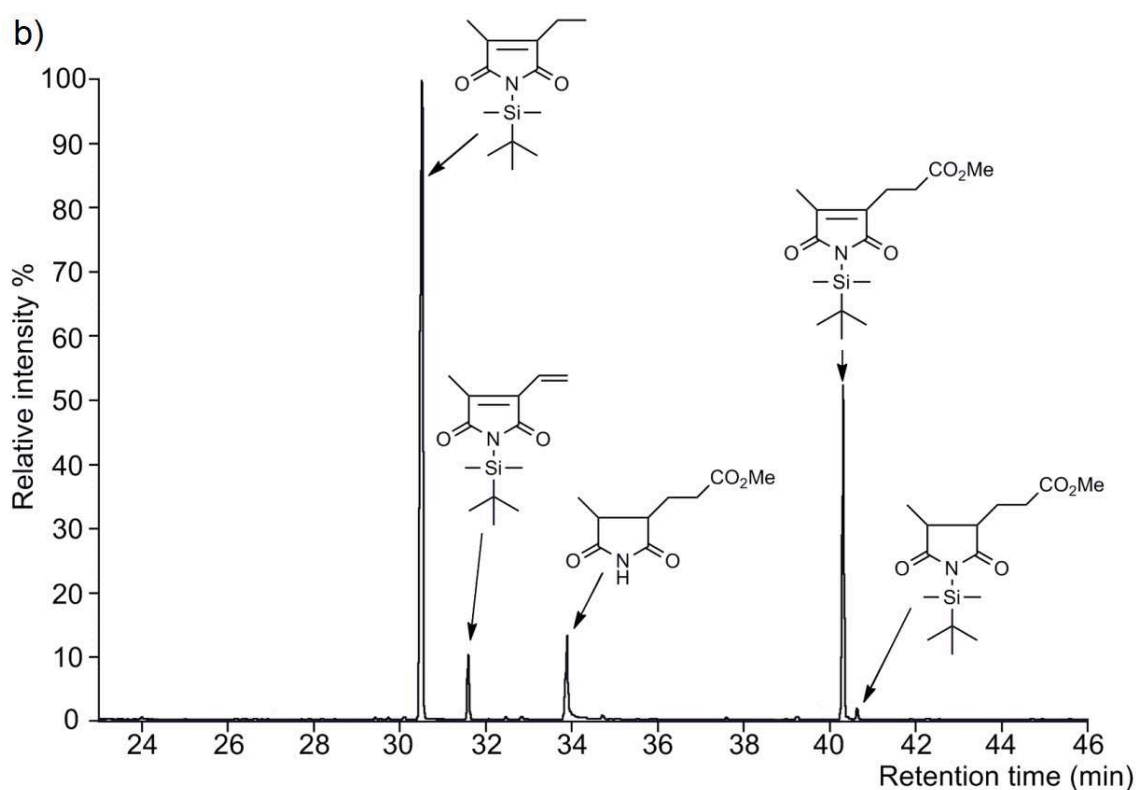
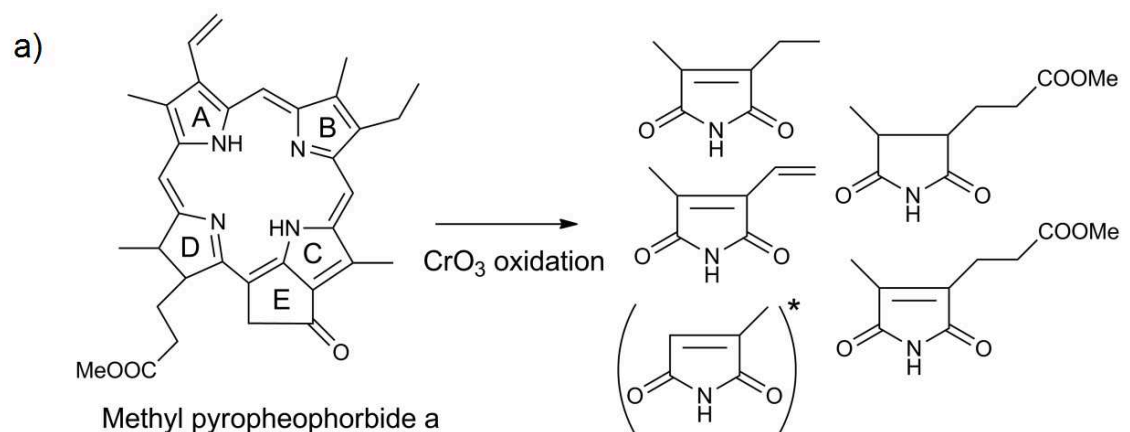


Fig. 3.3.a) Maleimides recovered upon chromic acid oxidation of methyl pyropheophorbide *a*.

*: Me,H maleimide was obtained in very low amounts, and probably arises from chromic acid oxidation of a minor impurity (i.e., an oxidised derivative of the starting product formed during storage)

b) Gas chromatogram (RIC) showing the maleimides obtained after chromic acid oxidation of methyl pyropheophorbide *a*. Note that the concentration of Me,H maleimide is too low to be detected directly on the RIC trace.

higher mineralisation rates, which could have also affected the decomposition of chlorophylls and the related increase of maleimides in the free fraction at this depth.

Another explanation could be the formation of maleimides by higher concentrations of dissolved oxygen in the water column, at a time with maybe higher oxygen levels in the water column due to a lower productivity. In contrast, the peaks of Me,Et maleimide after oxidation matched well with productivity peaks during the 1920s and 1960s, indicated by higher TOC accumulation and higher concentrations of algal biomarkers in these time intervals (Naeher et al., 2012), which could indicate that Me,Et maleimide mainly originates from chlorophyll *a*.

Me,vinyl maleimide was also detected in both fractions in all Rotsee samples (Fig. 3.2). The profile shapes of Me,vinyl and Me,Et maleimides were very similar (Fig. 3.2), which indicate a common source. Based on structural grounds, oxidative cleavage of chlorophyll *a* and related derivatives bearing a vinylic group on ring A is expected to lead to a 1:1 ratio of Me,vinyl and Me,Et maleimides. Me,vinyl maleimide is formed from chlorophyll *a*, *b* or *c1* (or eventually other sources like hemes or phycobilins; see above), whereas Me,Et maleimide can also originate from most of the chlorophyll nuclei, including bacteriochlorophylls (Grice et al., 1996). Me,vinyl maleimide is formed from chlorophyll *a*, whereas Me,Et maleimide can also originate from most of the chlorophyll nuclei, including bacteriochlorophylls (Grice et al., 1996). This would explain the observed discrepancy in the concentrations of both maleimides in the free fractions in the Rotsee samples (Fig. 3.2). Alternatively, as pointed out previously, the C₃ vinylic substituent from tetrapyrrole pigments can be reduced, during early diagenesis under anoxic conditions following the process described by Pickering and Keely (2011).

Regarding “bound” maleimides, the vinylic double bond is prone to oxidation upon chromic acid treatment. In order to determine the effect of chromic acid on the vinylic functionality, we carried out chromic acid oxidation of methyl pyropheophorbide *a* (a chlorophyll *a* derivative) under experimental conditions similar to those used for treatment of Rotsee and Black Sea samples. This experiment did not yield Me,Et and Me,vinyl maleimides in similar quantities, the vinyl group being almost completely oxidised upon treatment, and yielding less than 5% of Me,vinyl maleimide (compared to Me,Et maleimide). This indicates that chromic acid oxidation leads to the almost complete removal of this double bond by oxidation.

Therefore, Me,vinyl maleimide in the oxidised fraction, whatever its precursor molecules (i.e., chlorophyll-related pigments, phycobilins or hemes) and biological sources, cannot be used for palaeoenvironmental reconstructions. The natural conditions that yielded free maleimides are much less drastic than those used during chromic acid oxidation as indicated by the higher relative amounts of Me,vinyl maleimide on Me,Et maleimide in the free fraction compared to the oxidised one.

In addition, the oxidation of methyl pyropheophorbide *a* yielded hematinic and dihydrohematinic acid (Ellsworth, 1970), which are maleimides bearing a carboxylic acid functionality (Figs. 3.3a, b). Although similar compounds are also likely to be present among the free and bound maleimides from our samples, they were not investigated in the present study (Section 3.2.2.2) and will not be further discussed.

3.3.2 Me,H and Me,Me maleimides in the free and oxidised fraction from Rotsee samples

In the Rotsee samples, Me,H and Me,Me maleimides were much less abundant than their Me,Et homologue (Fig. 3.2). Their concentrations were highest in ca. 1929-1934 both in the free and oxidised fraction (Fig. 3.2). Based on a constant ratio of Me,Me maleimide to Me,Et maleimide, a common primary production source was proposed for ancient deposits (Grice et al., 1996). However, this ratio was not constant in Rotsee and ranged between 0.17 and 0.34 and between 0.14 and 0.64 in the free and oxidised fraction, respectively. Hence, Me,Me and Me,Et maleimides must originate from different sources or must be formed by different degradation processes in recent sediments. Other studies suggested that the degradation of Me,Et maleimide to Me,Me maleimide depends on maturity (Kozono et al., 2001; Shimoyama et al., 2001), but Rotsee sediments are low maturity deposits, so a relationship with maturity can be excluded. Furthermore, the interpretations made for ancient deposits cannot be used to explain observations in recent sediments, since maleimides in old sediments and crude oils likely arise from (petro)porphyrins with structural features inherited during early to late diagenesis, which do not resemble these in chlorophylls and related derivatives occurring in recent sediments.

Trace amounts of Me,H maleimide were also obtained from methyl pyropheophorbide *a* oxidation (Fig. 3.3a), which indicated that this compound can be formed by chlorophyll *a* oxidation. The relatively high concentrations of these maleimides in the Rotsee samples compared to the amounts obtained by oxidation of methyl pyropheophorbide *a* suggest that contributions from other chlorophyll derivatives need to be considered.

Me,H maleimide was found at both sites to be the second most abundant maleimide in the oxidised fraction (Fig. 3.2). In contrast, at least in petroleum and ancient sediments, Me,Me maleimide was the second most common maleimide (Shimoyama et al., 2001). Similarly to Me,Et maleimide in the free fraction and Me,Me maleimide in both free and oxidised fractions, Me,H maleimide concentrations peaked in the 1930s (Fig. 3.2), which coincides with a higher bacterial biomass at that time (Naeher et al., 2012). Similar to free Me,Et maleimide, the peak of Me,H and Me,Me maleimides in the free fraction during the 1930s might be the result of higher mineralisation rates of OM, which led to increased chlorophyll decomposition. Alternatively, higher concentrations of dissolved oxygen in the water column might have led to higher concentrations of these maleimides in the free fraction.

At least Me,H maleimide might result from the oxidation of chlorophyll transformation products, likely to occur in recent sediments and having pyrrole rings with adequate substituents. In this respect, tetrapyrroles in which ring E has been degraded would be ideal candidates (Fig. 3.4). Holt et al. (1966) have indeed shown that acidic treatment of pheophorbide *a* such as **3** (Fig. 3.4) and bearing two carboxylic acid groups leads to the loss of these two acid groups, replaced by two hydrogen atoms (compound **4** in Fig. 3.4). Such a process might also be envisaged either under natural conditions or upon chromic acid treatment and might operate on chlorophyll degradation products like purpurin **2** and chlorin **3**. The latter compounds are transformation products of chlorophyll *a* formed during senescence of algal cells or by oxidative processes at the earliest stages of diagenesis (Louda et al., 1998; Bale et al., 2011) and have been detected in various recent sediments (Ocampo and Repeta, 1999; Airs et al., 2000; Naylor and Keely, 1998). Their formation from chlorophylls (and/or bacteriochlorophylls) involves chlorin intermediates bearing oxygenated functionalities on ring E, which result from the oxidation of ring E (Fig. 3.4). Further alteration of such compounds (**2**, **3**) might lead 1) to chlorins like **4** by a natural process, although such compounds have not been detected yet in sediments, which would then lead to

the formation of maleimides, including Me,H-maleimide, or 2) by chemical treatment (chromic acid oxidation) directly to the maleimides shown in Figure 3.4, and including notably Me,H-maleimides.

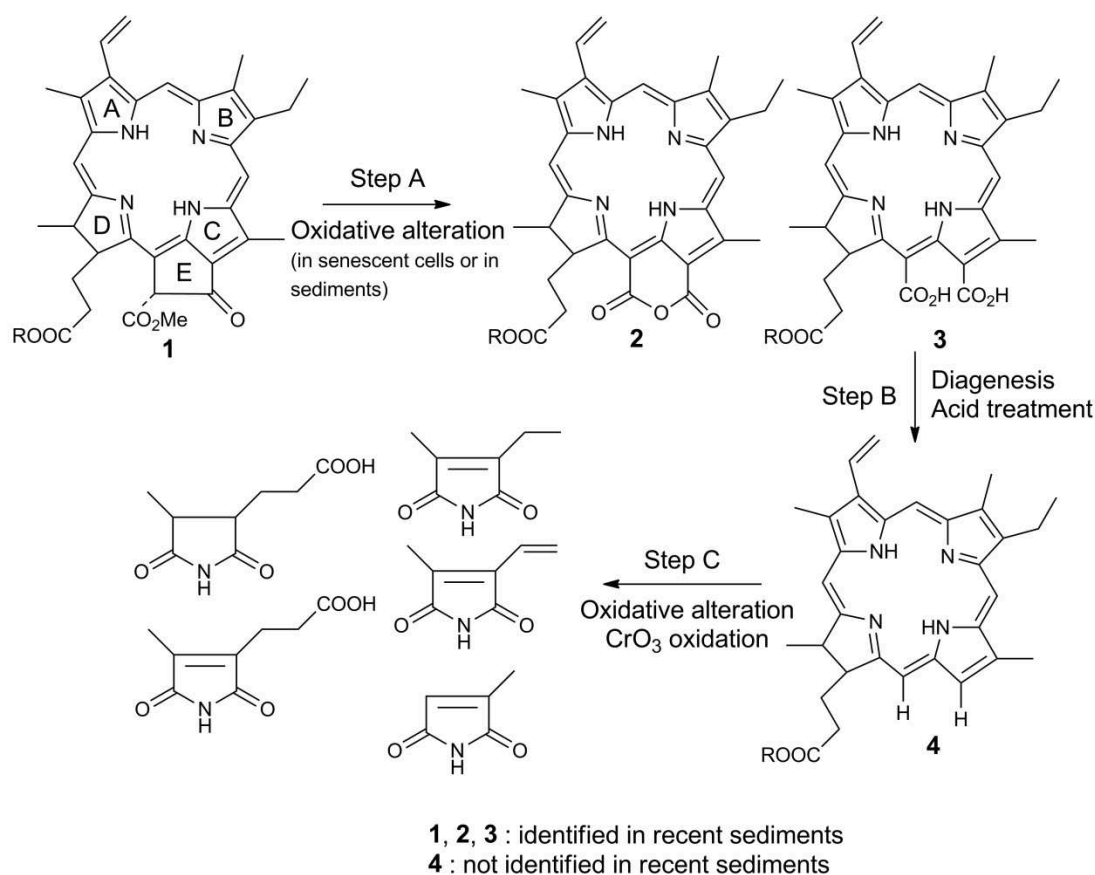


Fig. 3.4. Proposed formation pathway for maleimides from chlorophyll related derivatives in recent sediments.

3.3.3 Maleimides and photic zone euxinia in Rotsee

Trace amounts of Me,*i*-Bu maleimide were found in the free and oxidised fractions in Rotsee, whereas Me,*n*-Pr maleimide was only detected in the oxidised fractions (Figs. 3.5, 3.6). Me,*i*-Bu and Me,*n*-Pr maleimide concentrations were highest in 1918-1924 (Fig. 3.5). Based on structural grounds, Me,*i*-Bu and Me,*n*-Pr maleimides likely originate from bacteriochlorophylls *c* and *d* biosynthesised by green, shallower dwelling Chlorobiaceae

(Pfennig, 1978). Alternatively, and/or concomitantly, it can be envisaged that Me,*i*-Bu and Me,*n*-Pr maleimides arise from bacteriochlorophyll *e* from green-brown, deeper dwelling Chlorobiaceae (Pfennig, 1978), but in this case, an additional step involving the reduction of the aldehyde group on ring B of bacteriochlorophyll *e* has to be considered. Such a reduction process may indeed occur in anoxic, sulfur-rich settings, and would involve a mechanism similar to that described by Hebling et al. (2006) regarding the reduction of carbonyl groups. It is worth noting that Grice et al. (1996) report the presence of Me,*n*-Pr maleimide formed upon oxidation of porphyrins from Permian sediments, and suggest that the *n*-propyl group could arise from reduction of the C₃ acid substituent of the ring D from chlorophyll derivatives after ester hydrolysis. If such a mechanism can be considered in the case of porphyrins (diagenetic products of chlorophylls which have undergone thermal alteration/reduction), this possibility is highly unlikely in the case of recent sediments since it would involve the complete reduction of a carboxylic acid functionality under mild and anoxic conditions.

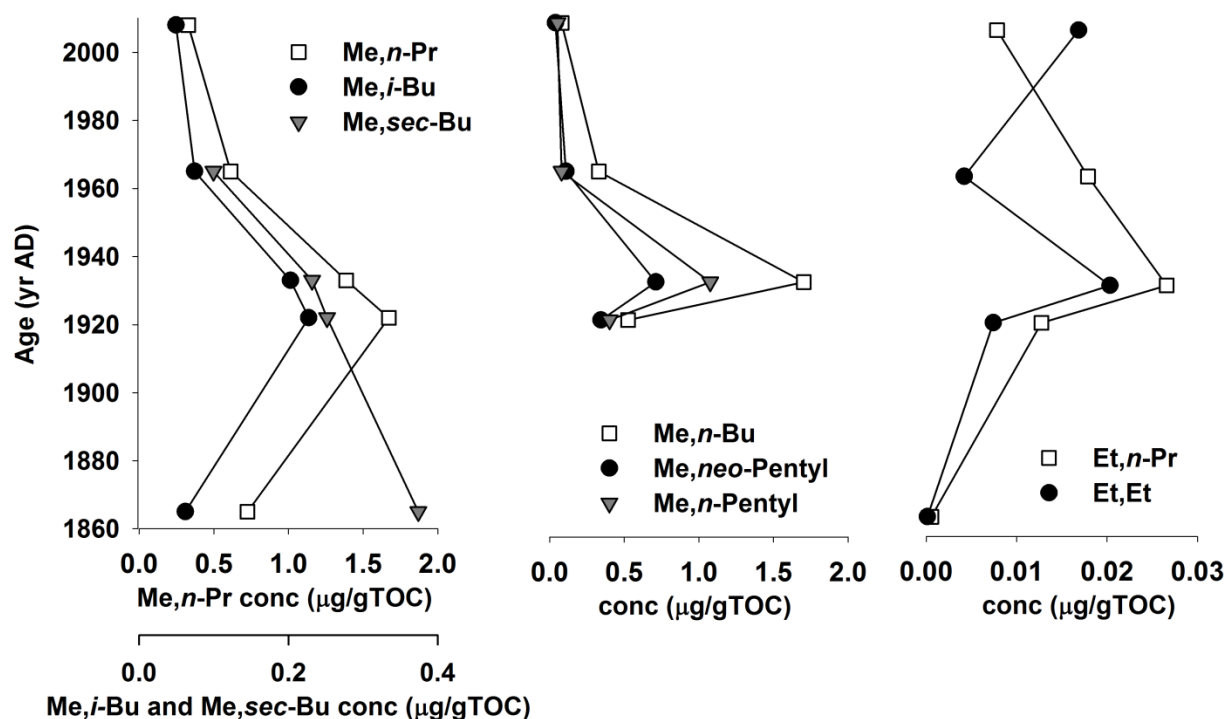


Fig. 3.5. Concentrations (“conc”) of Me,*n*-Pr, Me,*i*-Bu, Me,*sec*-Bu, Me,*n*-Bu, Me,*neo*-Pentyl, Me,*n*-Pentyl, Et,*n*-Pr, Et,Et maleimides in the oxidised fraction in Rotsee sediment vs. age (AD).

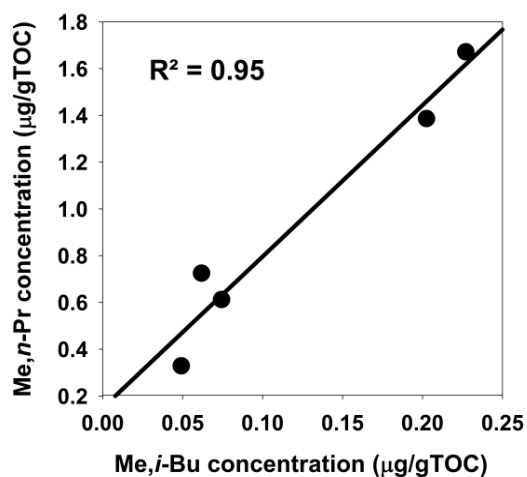


Fig. 3.6. Correlation between concentrations of Me,*i*-Bu and Me,*n*-Pr maleimides in Rotsee sediment with correlation coefficient (R^2) value.

source bacteria thrive under similar environmental conditions (Wilson et al., 2004).

In contrast to Chlorobiaceae, the principal tetrapyrrolic pigments from Chromatiaceae (purple sulfur bacteria) are bacteriochlorophylls *a* and *b*, whereas bacteriochlorophyll *a* is also present as an accessory pigment in Chlorobiaceae (Pfennig, 1978). Given their structures, chromic acid oxidation of bacteriochlorophylls *a* and *b* does not yield maleimides having a specific alkylation pattern and hence, the occurrence of such bacteriochlorophylls cannot be traced based on maleimide distributions. However, the presence of the pigment okenone in Rotsee sediment (this study) indicated the presence of Chromatiaceae in the water column of the lake, in agreement with the findings reported by Züllig (1985b).

The higher concentrations of okenone in Rotsee compared to isorenieratene (Züllig, 1985b) may be an indication for a higher abundance of Chromatiaceae compared to Chlorobiaceae, which is supported by results from microbial data (Kohler et al., 1984). The presence of okenone and isorenieratene together with Me,*i*-Bu and Me,*n*-Pr maleimides indicate photic zone euxinic and anoxic conditions in Rotsee. In our study, isorenieratene could not be quantified with the used method due to low concentrations, but the decrease of Me,*i*-Bu and Me,*n*-Pr maleimide concentrations since the 1920s together with continuously increasing

Grice et al. (1996) used Me,*n*-Pr and Me,*i*-Bu maleimides and the Me,*i*-Bu/Me,*Et* ratio as indicators for Chlorobiaceae and hence, for the occurrence of photic zone anoxia in the Zechstein Sea, supported by carbon isotopic data and correlation with the presence of diagenetic derivatives from the aromatic carotenoids chlorobactene and isorenieratene from Chlorobiaceae. The high correlation between Me,*n*-Pr and Me,*i*-Bu maleimides in the Rotsee samples ($R^2=0.95$; Fig. 3.6) suggests that these two compounds either share the same origin or populations of the

okenone concentrations (Züllig, 1985b) indicate a community shift towards Chromatiaceae. Although Smittenberg et al. (2004) interpreted the relative increase in isorenieratene vs. okenone concentrations in terms of increasing eutrophication in an euxinic Norwegian fjord, the opposite trend is observed in Rotsee (Züllig, 1985b). In the latter case, the increased okenone concentrations and higher abundance of Chromatiaceae can be explained by a rising oxycline into shallower waters as a result of eutrophication (Züllig, 1985b). The development of dense bacterial biomass (including Chromatiaceae) during eutrophication might have led to a reduction of the light penetration depth, resulting in a relative reduction of Chlorobiaceae although they proliferate at lower light irradiance in deeper waters than Chromatiaceae (Ormerod, 1983).

The bacteriochlorophyll *e* maximum below the peak of bacteriochlorophyll *a* (Kohler et al., 1984) agrees with the typical vertical segregation of deeper dwelling brown Chlorobiaceae below shallower Chromatiaceae (Ormerod, 1983) in the chemocline of Rotsee. Chromatiaceae in Rotsee are *Chromatium okenii*, *Pelochromatium roseum*, *Lamprocystis roseopersicina* and *Thiopedia rosea*, whereas Chlorobiaceae mainly consist of *Chloronema giganteum* (Kohler et al., 1984; Züllig, 1984), which might respectively be the sources of okenone and isorenieratane in this lake. However, except *Thiopedia rosea*, cell numbers were too low for reliable cell counting (Kohler et al., 1984), which can explain the low concentrations of these pigments in the sediment. Züllig (1985b) mentioned that okenone must originate at least from *Chromatium okenii* and the genus *Thiopedia*.

3.3.4 Sources of other maleimides in the oxidised fraction from Rotsee samples

In addition to the maleimides described above, chromic acid oxidation of the solvent extracts from the Rotsee samples also yielded other maleimides, comprising 2-methyl-3-*sec*-butyl-maleimide (Me,*sec*-Bu maleimide), 2-methyl-3-*n*-butyl-maleimide (Me,*n*-Bu maleimide), 2-methyl-3-*neo*-pentyl-maleimide (Me,*neo*-Pentyl maleimide), 2-methyl-3-*n*-pentyl-maleimide (Me,*n*-Pentyl maleimide), 2,3-diethyl-maleimide (Et,Et maleimide) and 2-ethyl-3-*n*-propyl-maleimide (Et,*n*-Pr maleimide). The structures of these maleimides were proposed in Grice (1995) and Grice et al. (1996) based on available standards, relative retention times and/or

mass spectra. They occurred in low abundance, with concentrations $< 2 \mu\text{g g}^{-1}$ TOC for most of the compounds (Fig. 3.5). Some of them (Me,*n*-Bu, Me,*neo*-Pentyl, Me,*n*-Pentyl maleimides) were under detection limits in the lowermost sample (Fig. 3.5).

Me,*neo*-Pentyl maleimide (Fig. 3.5) can be derived from bacteriochlorophylls with *neo*-pentyl substituents (Smith et al., 1980, 1983; Otte et al., 1993), which have also been reported from recent lake and pond sediments (Squier et al., 2002; Wilson et al., 2005). Et,*n*-Pr maleimide and other higher alkylated homologues might derive from bacteriochlorophyll derivatives with extended alkylations with up to seven additional carbon atoms on ring B, which have been detected in recent sediments from lakes and ponds (Squier et al., 2002; Wilson et al., 2005; Baltenweck-Guyot and Ocampo, 2007).

Although the precursors of Me,*sec*-Bu, Me,*n*-Bu, Me,*n*-Pentyl and Et,Et maleimides are unknown, these observations suggest that such alkylated maleimides originate from unknown bacteriochlorophylls or their derivatives. This would be in line with coinciding concentration peaks of Me,*n*-Bu and Et,Et maleimides with Me,*neo*-Pentyl and Et,*n*-Pr maleimides in 1929-1934 (Fig. 3.5). The similarity between Me,*sec*-Bu, Me,*n*-Pr and Me,*i*-Bu maleimide concentration profiles (Fig. 3.5) indicate a common biological source or similar living conditions for the (micro)organisms producing the molecule precursors of maleimides (Wilson et al., 2004).

3.3.5 Maleimides in samples from the Romanian Black Sea Shelf

Similar to Rotsee, Me,Et maleimide was the predominant maleimide ($> 96\%$) in both free and oxidised fractions of the Black Sea sediment extracts (Figs. 3.1B, 3.1D Table 3.1). The same maleimide homologues and distributions were found in the free and oxidised fraction in samples from the Romanian Shelf, except Me,*sec*-Bu and Et,*n*-Pr maleimides which could not be detected in the Black Sea samples. Me,vinyl maleimide was only found in traces in the sample from Unit 1, which indicated that it is less well preserved compared to Me,Et maleimide and other alkylated maleimides.

Previous studies showed that the productivity was higher during deposition of Unit 1 and 2 compared to Unit 3, based for instance on the higher OM accumulation, the presence and/or predominance of coccolithophores, the formation of sapropels and the establishment of anoxic conditions in the upper units compared to Unit 3 (Ross and Degens, 1974; Repeta, 1993; Arthur and Dean, 1998). These interpretations are in agreement with higher concentrations of dinosterol, C_{22:6}, C_{25:5} and C_{25:4} FA, 24-methyl-cholesterol, C₃₀-C₃₂ alkyl diols, C₃₀ keto-ol and C₃₀ highly branched isoprenoid alkenes in Unit 1 and 2 (unpublished data), which indicated more abundant organic matter inputs from dinoflagellates, diatoms and other microalgae (Volkman et al., 1992; Shanchun et al., 1994; Massé et al., 2004a, 2004b). These higher inputs from primary producers would also explain the higher Me,Et maleimide concentrations in the oxidised fraction in Unit 1 and 2. The presence of diatoms and dinoflagellates in our samples also suggest that chlorophylls *c*, main chlorophylls of chromophyte algae (diatoms, dinoflagellates, some prymnesiophytes, cryptophytes) (Zapata et al., 2006), might contribute significantly to the Me,Et maleimide pool in the Black Sea.

Table 3.1: Concentrations ($\mu\text{g g}^{-1}$ TOC) of Me,H, Me,Me and Me,Et maleimides in the free and oxidised fractions in Black Sea sediment units on the Romanian Shelf.

Sediment unit	Free Me,H	Free Me,Me	Free Me,Et	Oxidised Me,H	Oxidised Me,Me	Oxidised Me,Et
1	0.8	0.2	6.5	1.8	2.7	344.4
2	1.1	0.2	5.5	2.8	1.2	243.5
3	0.9	1.9	16.6	4.9	2.5	115.8

In contrast to Unit 1 and 2, the concentration of Me,Et maleimide was higher in the free fraction in Unit 3. This could either mean that more free Me,Et maleimide was formed due to higher oxygen levels in the past water column or this could be due to the longer time since deposition, which might have resulted in more intense degradation of chlorophyll *a* and related derivatives compared to the Units 1 and 2.

However, the predominance of *des*-A-arbora-5(10),9(11)-diene (Hauke et al., 1992; Jaffé and Hausmann, 1995) and the detection of lupeol, β -amyirin and its degradation products in Unit 1 may suggest that Me₂Et maleimide partly originates from terrestrial derived chlorophylls supplied by the Danube delta to the shelf. The Danube River is the largest source of freshwater and terrigenous material (including OM), which is transported to the Black Sea (Shimkus and Trimonis, 1974; Saliot et al., 2002). Me₂Et maleimide might have partly been derived from chlorophylls during transport of the OM to the Black Sea, but also after deposition on the shelf.

As outlined in section 3.3.1, it cannot be excluded that part of Me₂Et maleimide might also have sources from hemes and phycobilins in addition to chlorophyll/chlorin sources on the Romanian Black Sea Shelf.

In contrast to Rotsee, the concentration profiles of Me₂*n*-Pr and Me₂*i*-Bu maleimides were not correlated in the Black Sea (data not shown), which suggests changing environmental conditions and structural differences in the bacterial communities such as for instance increased competition for light or nutrients (Wilson et al., 2004). Throughout the core, Me₂*n*-Pr maleimide concentrations were 3 to 6 times higher than those of Me₂*i*-Bu maleimide.

The presence of Me₂*i*-Bu maleimide and most likely also Me₂*n*-Pr maleimide in all Black Sea units trace the occurrence of Chlorobiaceae in the chemocline of the Romanian Black Sea Shelf. Their detection in Unit 3 suggests that photic zone anoxia occurred before the Bosphorus connection, at least temporary. In contrast, isorenieratene was only found in Units 1 and 2 (Repeta, 1993; Sinninghe Damsté et al., 1993). Repeta and Simpson (1991) showed that Chromatiaceae and green strains of Chlorobiaceae were not present in the central Black Sea, because okenone, bacteriochlorophylls *a* and *b* and chlorobactene were absent. The predominance of the deeper dwelling brown strains of Chlorobiaceae (bacteriochlorophyll *e*, isorenieratene) in the Black Sea chemocline at 80-100 m depth was attributed to light and sulfide limitation (Repeta et al., 1989; Repeta and Simpson, 1991; Sinninghe Damsté et al., 1993).

The chemocline of the Romanian Shelf during sampling was located at ca. 50-70 m. The presence of chlorobactane and isorenieratane obtained after hydrogenation of an aliquot of the polar fraction and the detection of Me₂*n*-Pr and Me₂*i*-Bu maleimides together with the

shallower chemocline might indicate that also the shallower dwelling green strains of Chlorobiaceae were present in the chemocline on the shelf.

3.3.6 Factors responsible for chlorophyll degradation and maleimide formation

Maleimide formation and its timing could not be satisfactorily answered so far. Possible processes include photo-oxidative or enzymatically induced transformation of chlorophyll derivatives in the oxic part of the water column (Brown et al., 1980; Rontani et al., 1991). In fact, maleimides can be formed by chlorophyll degradation in the photic zone under the presence of oxygen (Kozono et al., 2002). Bacteriochlorophylls in the chemocline are likely preserved due to the lack of oxygen, which might explain the occurrence of some maleimides (from bacteriochlorophylls) exclusively in the oxidised fraction. However, detection of traces of free Me,*i*-Bu maleimide obtained from samples in both settings indicate that maleimide formation is not limited to the oxygenated part of the photic zone. This means that natural maleimide formation does not occur exclusively within the oxygenated water column.

It was also proposed that maleimides can be produced by sunlight irradiation of chlorophyll *a* under the presence of oxygen (Jen and MacKinney, 1970) or UV light irradiation of porphyrins (Grice, unpublished results). Since we have not worked under dark and oxygen-free conditions, our results might be biased, as suggested by previous authors (Grice et al., 1996; Kozono et al., 2002). However, the observation of some maleimides in the free fraction while others are only detected in the oxidised fraction in Rotsee and Black Sea samples (Figs. 3.2, 3.5, Table 3.1) indicate that light and oxygen during sample preparation cannot account (or, at least, not significantly) for the presence of free maleimides. Furthermore, in the free fraction of the Rotsee surface sediment, maleimides were almost absent and their concentrations increased with depth (Figs. 3.2, 3.5). This indicates that maleimides are to a large extent formed within the sediment. It was previously proposed that maleimides can be generated during early diagenesis (Magness, 2001), also in lakes with overlying euxinic water columns, which could explain the occurrence of free maleimides in ancient deposits formed under oxygen limited conditions (Grice et al., 1997; Magness, 2001). Therefore, also other oxides (e.g. nitrate, iron and manganese oxides, sulfate) might support chlorophyll

destruction. This would explain why the abundance of naturally occurring maleimides in the free fraction increased within the sediment of both Rotsee and Black Sea (Fig. 3.2, Table 3.1). The coincidence of higher concentrations of free Me,H, Me,Me, Me,Et, Me,vinyl maleimides in the free fraction of Rotsee with a higher bacterial biomass at the beginning 1930s (Naeher et al., 2012) likely indicate that higher OM mineralisation rates at that time were responsible for more intense (bacterio)chlorophyll decomposition (Fig. 3.2). However, the natural processes involved in the formation of maleimides are not yet understood.

3.3.7 Maleimide degradation indices

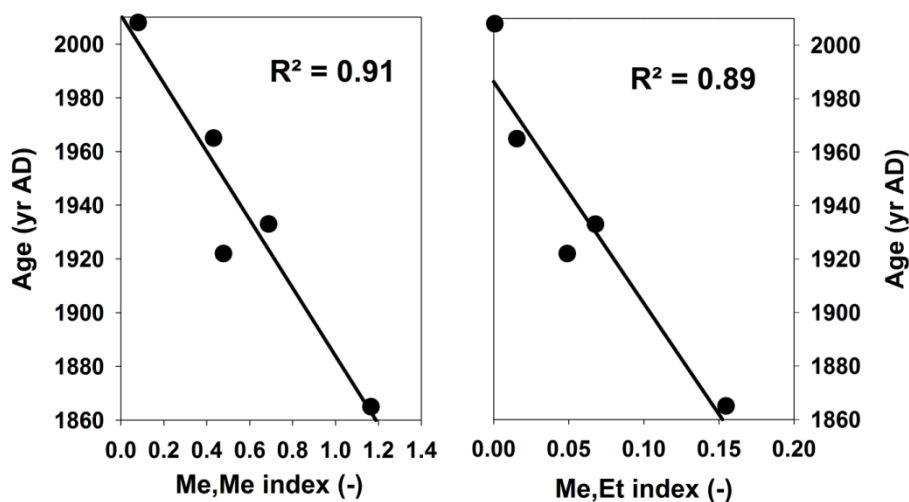


Fig. 3.7. Maleimide degradation indices (Me,Me index and Me,Et index) vs. age (AD) in Rotsee sediment with correlation coefficient (R^2) values.

The chlorin index (CI) is a pigment based proxy (Schubert et al., 2005), which has also been used to estimate the degree of OM degradation in Rotsee (Naeher et al., 2012). The CI is defined as the ratio between fluorescence activity of an acetone extract of a sediment sample and the same extract treated with hydrochloric acid (Schubert et al., 2005). Therefore, this index represents the ratio between chlorophyll and related degradation products. With increasing time, this ratio increases from 0.2 for freshly deposited chlorophylls to 1.0 for chemically inert material (Schubert et al., 2005). CI values were > 0.71 for sediment older

than about 45 years in Rotsee and were especially high in the lowermost part of the core (Naeher et al., 2012). This indicated that the proxy is better for applications in recent parts of the sediment. However, for pigment-based reconstructions of the degree of OM degradation in older deposits, other proxies are needed.

To estimate the degree of OM degradation for longer timescales, novel maleimide degradation indices (Me,Me index; Me,Et index) similar to the CI were defined (Section 3.2.3). The Me,Me index in Rotsee increased constantly from the surface sediment with a

value of 0.08 to 1.17 in 1865-1870, whereas the Me,Et index increased from 0.001 to 0.16 (Fig. 3.7). The Me,Me index value above 1.0 in the deepest sample might be the result of measurement uncertainties (Fig. 3.2 and 3.7). While the Me,Me index increased at a rate of $8.1 \times 10^{-3} \text{ yr}^{-1}$ with depth ($R^2=0.91$), the Me,Et index rose at a rate of $1.2 \times 10^{-3} \text{ yr}^{-1}$ ($R^2=0.89$) (Fig. 3.7). These rates indicated that the application limit of the Me,Me index with values of 1.0 was reached after more than ca. 100 yr, whereas extrapolation of the Me,Et index would reach unity after less than about 1000 yr in Rotsee sediment.

In the Black Sea sediments, both indices were almost constant within Units 1 and 2 (Me,Me: < 0.1 , Me,Et: ca. 0.02; Fig. 3.8). In contrast, values were much higher in Unit 3 (Me,Me: 0.8, Me,Et: 0.14; Fig. 3.8), which consists of reworked material (Ross and Degens, 1974). Despite the fact that the sediment of this core is older than in the Rotsee core, the values of the Me,Me and Me,Et indices were in the same order of magnitude, which suggests that the decomposition of tetrapyrrole pigments proceeded at lower rates than in Rotsee. If it is assumed that the transition of Unit 2 and 3 occurred at 6000 yr BP based on estimates for the shelf from Ross and Degens (1974) and that the maleimide sample from Unit 3 would have this age, the applicability of the Me,Me index can be extrapolated to at least 7700 yr BP, whereas the Me,Et index could be used for up to at least 42 ka BP old sediment.

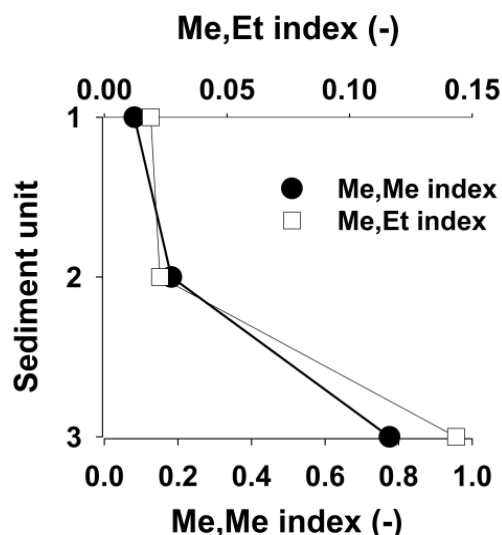


Fig. 3.8. Maleimide degradation indices (Me,Me index and Me,Et index) vs. sedimentary unit in Romanian Black Sea Shelf sediment.

The longer applicability of the maleimide indices compared to the CI can be explained by the higher degradation progress of chlorophylls considered in this method. Maleimides are oxidation products, which are formed by the destruction of tetrapyrrole rings, either by natural processes or chromic acid oxidation. In contrast, the use of hydrochloric acid in CI analysis (Schubert et al., 2005) is not sufficient to decompose tetrapyrrole rings, so a lower degradation progress is considered compared to the more severe chromic acid oxidation (Ellsworth, 1970; Grice et al., 1996). Therefore, the new indices are applicable to longer timescales than the CI. They can be used for estimates regarding the quality, freshness and degradability of OM based on the decomposition of tetrapyrrole pigments in older sediments, in which the CI reached unity and can therefore not be applied.

3.4 Conclusions

Maleimides were studied in recent sediments from the Swiss lake Rotsee and the Romanian Black Sea Shelf. Me,H, Me,Me, Me,vinyl, Me,Et maleimides and traces of Me,*i*-Bu maleimide occurred naturally in most samples. Me,Et maleimide was the predominant maleimide in all sediment extracts. Me,Et and Me,vinyl maleimides mainly originated from chlorophyll *a*, but sources other than chlorophyll derivatives, such as hemes and phycobilins, cannot be completely excluded. Additionally, chromic acid oxidation of sediment extracts yielded Me,*n*-Pr, Me,*n*-Bu, Me,*neo*-Pentyl, Me,*n*-Pentyl and Et,Et maleimides in both settings, whereas Me,*sec*-Bu and Et,*n*-Pr were only present in Rotsee. Me,Et maleimide mainly originates from chlorophyll *a* in Rotsee, whereas terrestrial derived chlorophylls supplied by the Danube could represent additional sources of Me,Et maleimide in the Black Sea. The correlation between Me,*n*-Pr and Me,*i*-Bu maleimides suggested a common Chlorobiaceae origin or similar environmental conditions under which the source organisms thrive. Based on maleimides and carotenoid pigments, both Chromatiaceae and Chlorobiaceae were observed in Rotsee, whereas only Chlorobiaceae could be traced on the Romanian Black Sea Shelf. The presence of Chromatiaceae and/or Chlorobiaceae indicated photic zone euxinic conditions in both settings, including the freshwater phase of Black Sea (Unit 3). In Rotsee, a community shift from Chlorobiaceae to Chromatiaceae was observed by a relative increase of

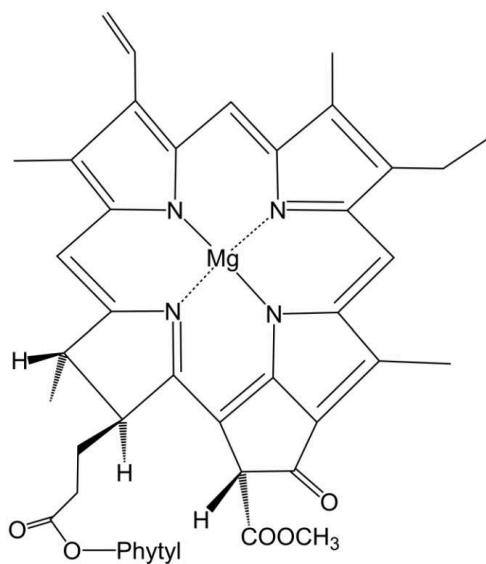
okenone concentration together with decreasing Me,*n*-Pr and Me,*i*-Bu maleimide concentrations since the 1920s due to eutrophication and a shallowing of the oxycline. Other maleimides obtained in this study either originated from bacteriochlorophylls with appropriate alkylation patterns in ring B or were of unknown origin. Maleimide formation in Rotsee mainly occurred within the lake sediment. Me,Me and Me,Et indices are proposed as novel proxies for estimating the degree of OM degradation, which are applicable for longer timescales than e.g. the chlorin index.

3.5 Acknowledgements

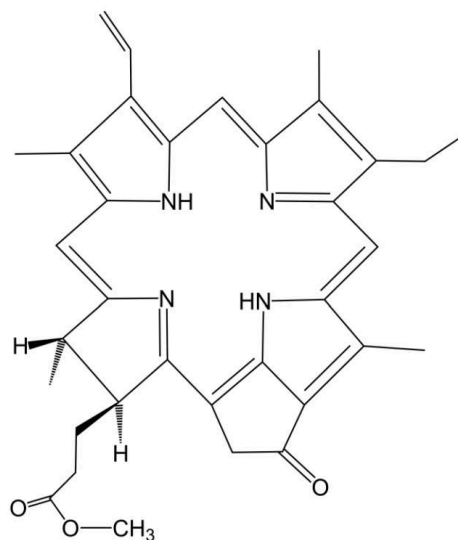
We would like to express our gratitude to Gaby Schmitt and Céline Munsch (University of Strasbourg, France) for their work on pigment analysis and help in the laboratory. We thank the whole team of the R/V Mare Nigrum cruise and the staff of GeoEcoMar on board (Romania) with special thanks to Jana Friedrich (AWI, Bremerhaven, Germany), Marian-Trajan Gomoiu, Dan Secieru, Sorin Balan and Remzi Bectas (all GeoEcoMar, Constanta, Romania). Christophe Jeandon (University of Strasbourg, France) is thanked for providing a standard of methyl pyropheophorbide *a*. Alois Zwyssig (Eawag) is thanked for field support on Rotsee. This research project was funded by the European Union project “Hypox – In situ monitoring of oxygen depletion in hypoxic ecosystems of coastal and open seas and land-locked water bodies“ (EC grant 226213). The network REALISE (“Alsace Region Research Network in Environmental Sciences and Engineering”) and the Alsace Region are also acknowledged for financial support (PA, PS). Additional funds came from the Eawag PhD mobility support grant (SN).

3.6 Appendix

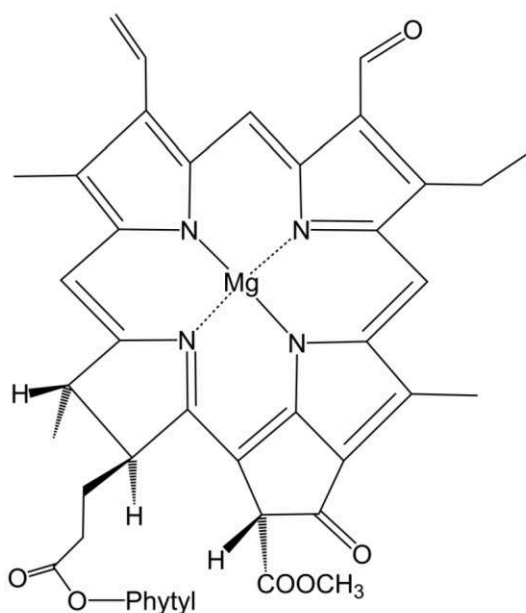
Structures of chlorophylls, bacteriochlorophylls, related derivatives, hemes (cytochromes), phycobilins and maleimides discussed in this study.



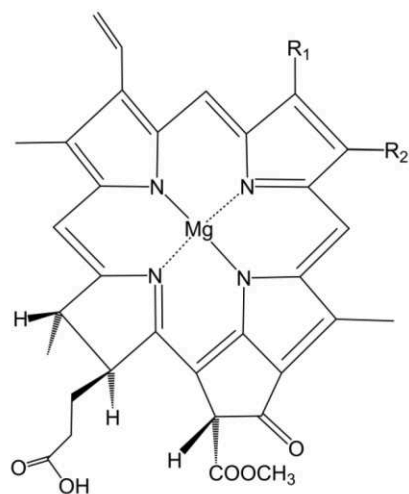
Chlorophyll a



Methyl pyropheophorbide a

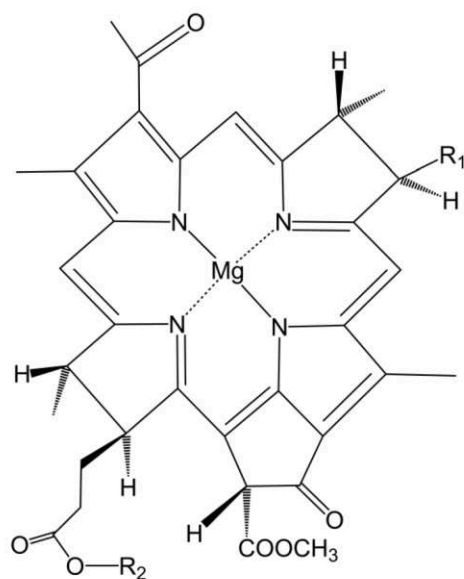


Chlorophyll b



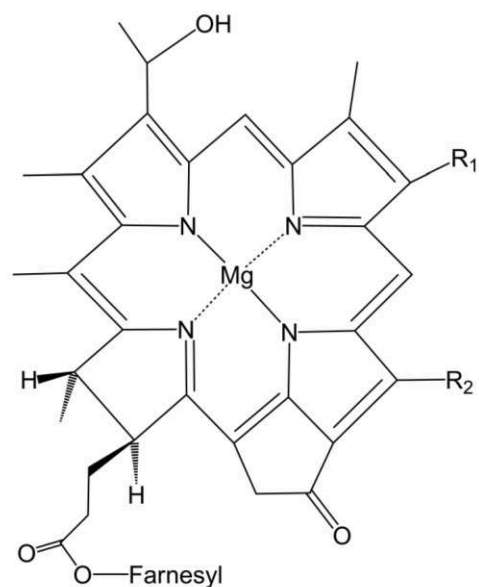
- c1** R₁ = Me, R₂ = Et
c2 R₁ = Me, R₂ = Vinyl
c3 R₁ = CO₂ Me, R₂ = Vinyl

Chlorophylls c



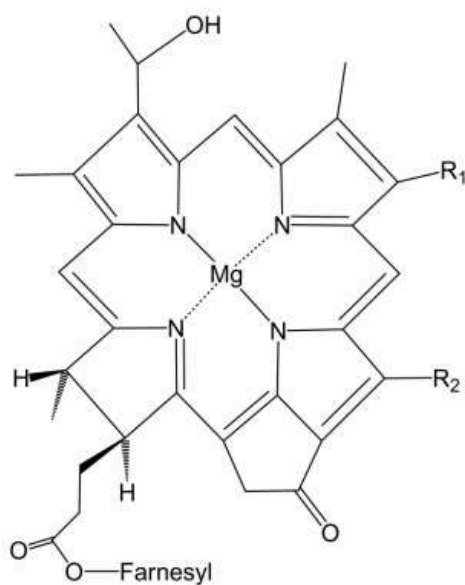
a $R_1 = \text{Et}$, $R_2 = \text{Phytyl, Geranylgeranyl}$
b $R_1 = \text{Ethylidiene}$, $R_2 = \text{Phytyl}$

Bacteriochlorophylls *a* and *b*



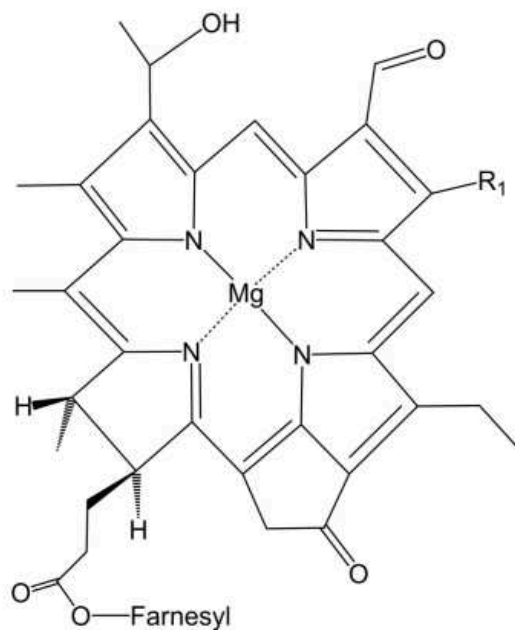
$R_1 = \text{Et, } n\text{-Pr, } i\text{-Bu, } neo\text{-pentyl}$
 $R_2 = \text{Me, Et}$

Bacteriochlorophylls *c*



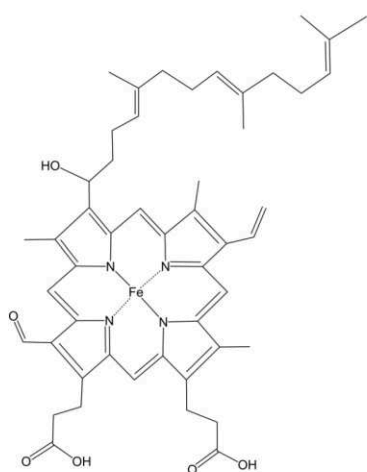
$R_1 = \text{Et, } n\text{-Pr, } i\text{-Bu, } neo\text{-pentyl}$
 $R_2 = \text{Me, Et}$

Bacteriochlorophylls *d*

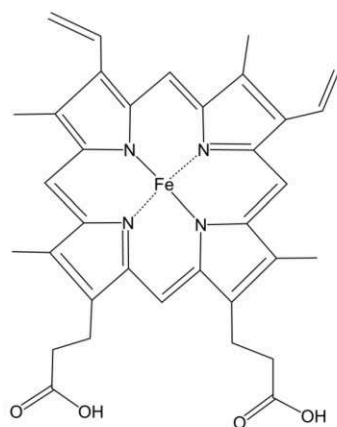


$R_1 = \text{Et, } n\text{-Pr, } i\text{-Bu, } neo\text{-pentyl}$

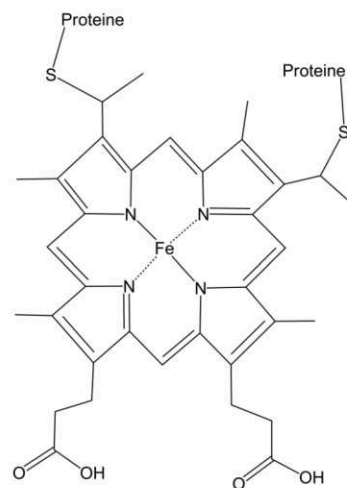
Bacteriochlorophylls *e*



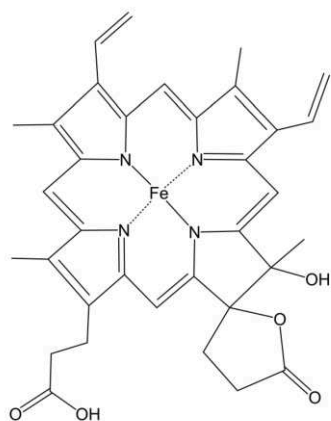
Heme a



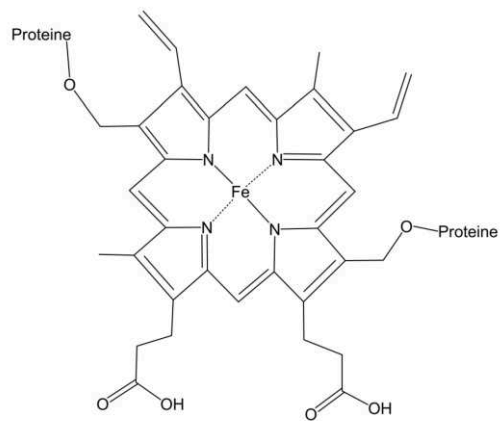
Heme b



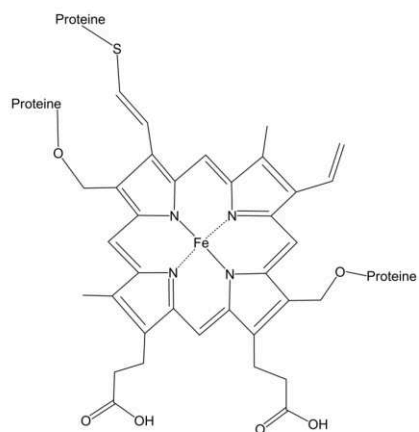
Heme c



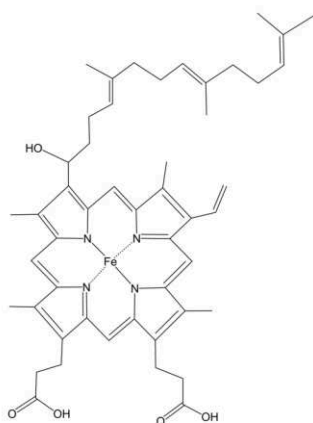
Heme d



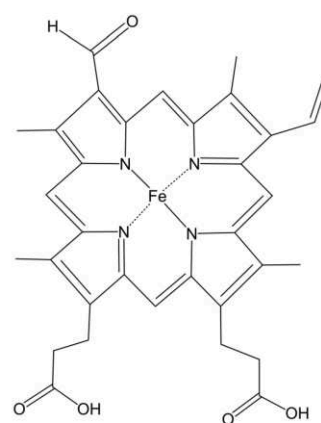
Heme l



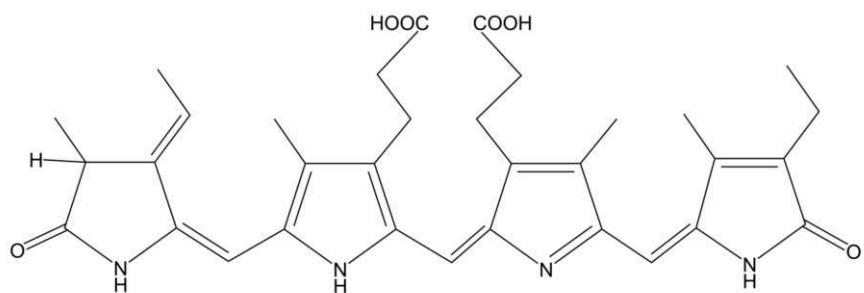
Heme m



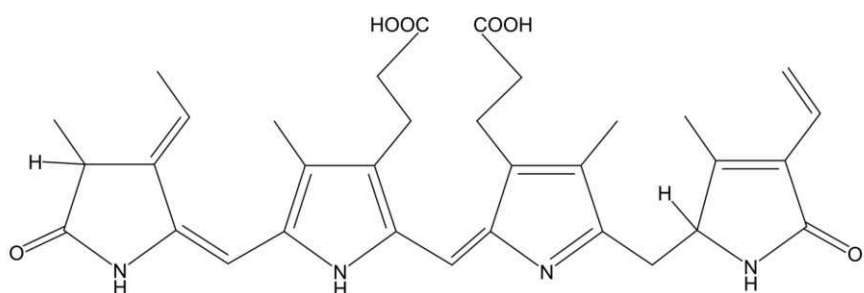
Heme o



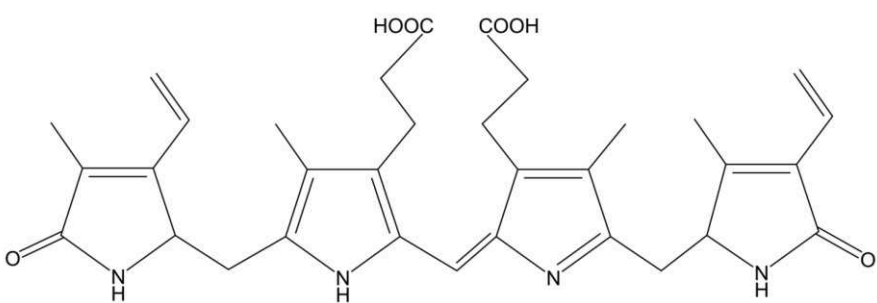
Heme s



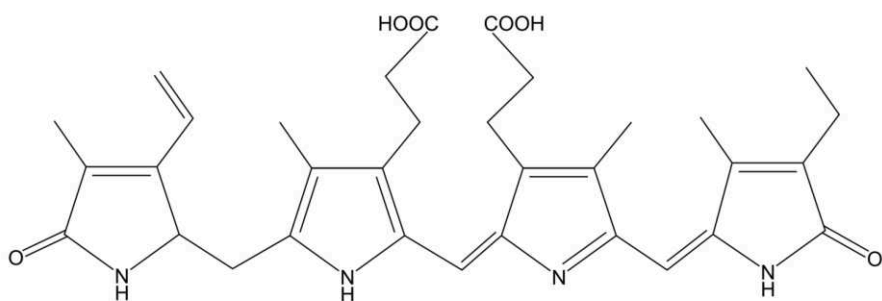
Phycocyanobilin



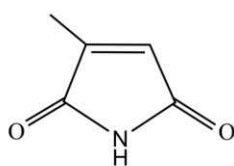
Phycoerythrobilin



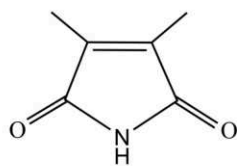
Phycocourobilin



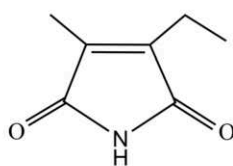
Phycobiliviolin



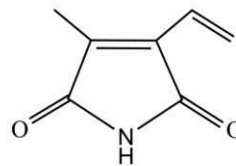
Me,H



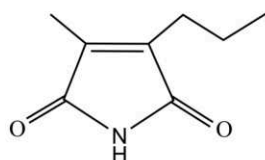
Me,Me



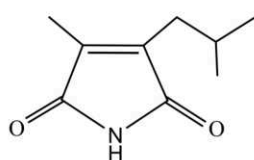
Me,Et



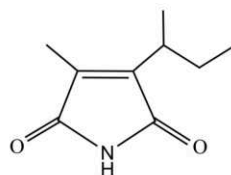
Me,vinyl



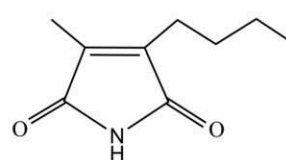
Me,*n*-Pr



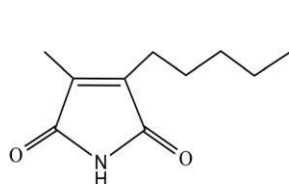
Me,*sec*-Bu



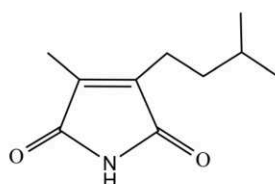
Me,*i*-Bu



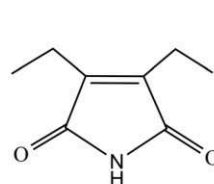
Me,*n*-Bu



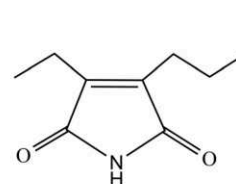
Me,*n*-Pentyl



Me,*neo*-Pentyl



Et,Et



Et,*n*-Pr

Chapter 4: Tracing bottom water oxygenation with sedimentary Mn/Fe ratios in Lake Zurich, Switzerland

Sebastian Naeher, Adrian Gilli, Ryan North, Yvonne Hamann, Carsten J. Schubert

In Review for Chemical Geology

Abstract

Redox dynamics of manganese (Mn) were studied in the sediment of Lake Zurich using precise sediment core age models, monthly long-term oxygen (O₂) monitoring data (1936-2010) and high-resolution XRF core scanning. The age models were based on bi-annual lamination and calcite precipitation cycles. If present, Mn exhibits distinct maxima, which coincide with annual maximum deep-water O₂ concentrations in spring according to the monitoring data. In contrast, the iron (Fe) signal is mainly the result of calcite dilution, as indicated by a good negative correlation between Fe and calcium (Ca) XRF data. The Mn/Fe ratio in the core from the maximum lake depth (ZH10-15, 137 m) revealed a good correlation with O₂ measurements in the lake bottom water confirming the successful application of the Mn/Fe ratio to semi-quantitatively reconstruct bottom water oxygenation in the lake. Mostly low ratios were observed between 1895 and the mid-1960s as a result of eutrophication. However, geochemical and sediment focusing and sedimentological factors can reduce the

applicability of the Mn/Fe ratio for reconstructions of annual O₂ concentrations in the bottom water of lakes.

4.1 Introduction

Trace metals, such as Fe and Mn, have received much attention in the last decades due to their redox-sensitive behaviour in aquatic environments. This behaviour is strongly dependent on processes of oxidation and reduction of the coupled pairs Fe(II)/Fe(III) and Mn(II)/Mn(IV), which result either in precipitation or (re)dissolution (Calvert and Pedersen, 2007; Davison, 1993). Especially in lakes, seasonal redox changes in the hypolimnion result in the cycling of Fe and Mn (Davison, 1993; Sigg et al., 1987). Reducing conditions are the result of O₂ consumption during organic matter (OM) remineralisation, which lead to a release of Fe and Mn (Nealson and Saffarini, 1994; O'Sullivan and Reynolds, 2005). After oxygenation at the chemocline due to partial or total mixing of the water column, Fe and Mn precipitates are deposited and potentially preserved in the sediment (Engstrom and Wright, 1984; Schaller and Wehrli, 1996). Mn precipitation is furthermore catalysed by Mn oxidising bacteria (Diem and Stumm, 1984). In fact, Mn-enrichments surrounding “*Metallogenium*” / *Leptothrix echinata* were found in Lake Zurich (Diem, 1983; Giovanoli et al., 1980).

The oxidation of Fe(II) proceeds more rapidly than Mn(II) (Engstrom and Wright, 1984) and the involvement of numerous interdependent reactions, transformation processes and mineral phases lead to a complex pattern of redox-sensitive trace metals (Davison, 1993). However, Fe is not necessarily remobilised by redox changes and can also be a tracer for terrigenous sources, such as in the eutrophic Lake Rotsee (Switzerland), where Fe together with potassium (K) and titanium (Ti) represent detrital sources (Naeher et al., 2012). In Lake Zurich, particulate Fe is supplied by sewage treatment plant effluents, soil particles and sediment resuspension (Sigg et al., 1987; Wieland et al., 2001). There are two sedimentation maxima during the year, one in winter and another in summer, as shown by sediment trap data (Sigg et al., 1987; Wieland et al., 2001). A major part of the Fe in the sediment is finely

dispersed as amorphous iron-oxy-hydroxide phases (only partly as goethite) or mineral phase coatings (Giovanoli et al., 1980; Sigg et al., 1987; Wieland et al., 2001).

Mn precipitates in the sediment of Lake Zurich are Mn oxides/hydroxides (MnO_2 , Mn_3O_4 , MnOOH), partly with needle habitus (Diem, 1983; Giovanoli et al., 1980). Manganite (γ - MnOOH) is the predominant mineral phase in the sediments of this lake (Diem, 1983; Giovanoli et al., 1980). However, extended x-ray absorption fine structure spectroscopy (EXAFS) analysis in the eutrophic Lake Sempach (Switzerland) showed that Mn precipitates, which are formed in the water column, are of poorly crystallized H^+ -birnessite (Friedl et al., 1997). They further showed that Mn was associated with authigenic particles in the sediment, consisting of $(\text{Ca,Mn})\text{CO}_3$ and $(\text{Fe,Mn})_3(\text{PO}_4)_2 \cdot 8\text{H}_2\text{O}$. About 55-60% of Mn was incorporated into carbonate, whereas 40-45% entered phosphate particles.

The cycling of redox-sensitive trace metals by reductive dissolution and (re)oxidation progressively leads to geochemical focusing, which is a process that transfers and enriches these elements in deeper waters (Schaller and Wehrli, 1996). Geochemical focusing was previously described at a lower temporal resolution in similar lake systems, such as Lake Baldegg in Switzerland (Schaller and Wehrli, 1996). In a lake, geochemical focusing only occurs if at some point in the year the oxygenated water column is stratified and the sediment becomes anoxic, which leads to redissolution of Mn precipitates. Even without a large source of Mn from the inflow, distinct horizontal patterns of Mn in the sediment may result. The focusing seems to be controlled by different horizontal and vertical mass transport processes that result from turbulent mixing and changes in deep-water O_2 concentrations (Schaller and Wehrli, 1996).

Although the redox-sensitive behaviour of Fe and Mn is quite well understood, the effect of short-term changes in bottom water O_2 concentrations on the sediment pattern of redox-sensitive trace metals still needs to be shown. Fe and Mn are oxidised at different rates, which was used to reconstruct O_2 dynamics (Davison, 1993; Engstrom and Wright, 1984). Mn/Fe ratios have been used repeatedly to reconstruct changing redox conditions in lakes (e.g. Dean and Doner, 2012; Koinig et al., 2003; Loizeau et al., 2001; Melles et al., 2012). In all of these studies, higher Mn/Fe ratios indicated higher O_2 concentrations in the water column, whereas lower ratios suggested lower O_2 levels. This is explained by a more rapid oxidation of Mn in

oxic conditions and under reducing conditions Mn release precedes that of Fe (e.g. Davison, 1993; Dean and Doner, 2012). Therefore, Mn is considered to be more sensitive than Fe to changes in O₂ concentrations (Dean and Doner, 2012).

High-resolution measurements of Mn and Fe may also improve the understanding of short-term impacts on dissolution and precipitation of these elements and their transport within lakes, potentially revealing the detailed processes behind geochemical focusing. The development of X-ray fluorescence (XRF) core scanners has enabled rapid high-resolution, semi-quantitative and non-destructive measurements of trace metals in sediment cores (Richter et al., 2006). This technology could allow the reconstruction of O₂ concentrations from inorganic proxies, which was not possible previously.

The aim of this paper is to study the relationship between short-term (i.e. annual) bottom water O₂ concentrations and the content of Fe and Mn in the sediment of Lake Zurich (Switzerland) in order to better understand the redox dynamics at the sediment-water interface. This lake was chosen because it is a well-studied system for trace metals (Diem, 1983; Diem and Stumm, 1984; Giovanoli et al., 1980; Sigg et al., 1987; Wieland et al., 2001), has a seasonally hypoxic hypolimnion and it is very sensitive to temperature changes that can induce water column mixing (Livingstone, 1997; Livingstone, 2003). But most importantly, monthly O₂ monitoring data for the full water column are available from 1936 until the present. This long time-series of monitoring data makes Lake Zurich an ideal site to study and calibrate recent limnological and limnogeological processes (e.g. Posch et al., 2012).

The majority of the sediment in Lake Zurich is well laminated and these bi-annual layers could be precisely counted, which resulted in a very accurate age model. We show that hypolimnetic oxygenation events can be traced with Mn and that the Mn/Fe ratio in the core taken at the lake's deepest point is a useful indicator to semi-quantitatively reconstruct bottom water O₂ concentrations.

4.2 Materials and methods

4.2.1 Study site

The mesotrophic Lake Zurich (Lower Lake, 406 m.a.s.l; Fig. 4.1) has a surface area of 67.3 km² and a volume of 3.3 km³ with a maximum water depth of 137 m (Wieland et al., 2001). The lake is of glacial origin (Kelts, 1978) and its basin is orientated from the southeast to the northwest (Fig. 4.1). The lake is divided into two basins by a three-meter deep moraine sill, forming the Upper and Lower Lake Zurich (Livingstone, 2003). The main allochthonous riverine supply from the Linth River is effectively entrapped in the Upper Lake, which acts as a settling basin (Wieland et al., 2001). The majority of the water flow (84%) into the Lower Lake is over the sill (Omlin et al., 2001). The water residence time is about 1.5 yr (Wieland et al., 2001). The lake can behave as monomictic or dimictic depending on prevailing winter conditions (Livingstone, 2003).

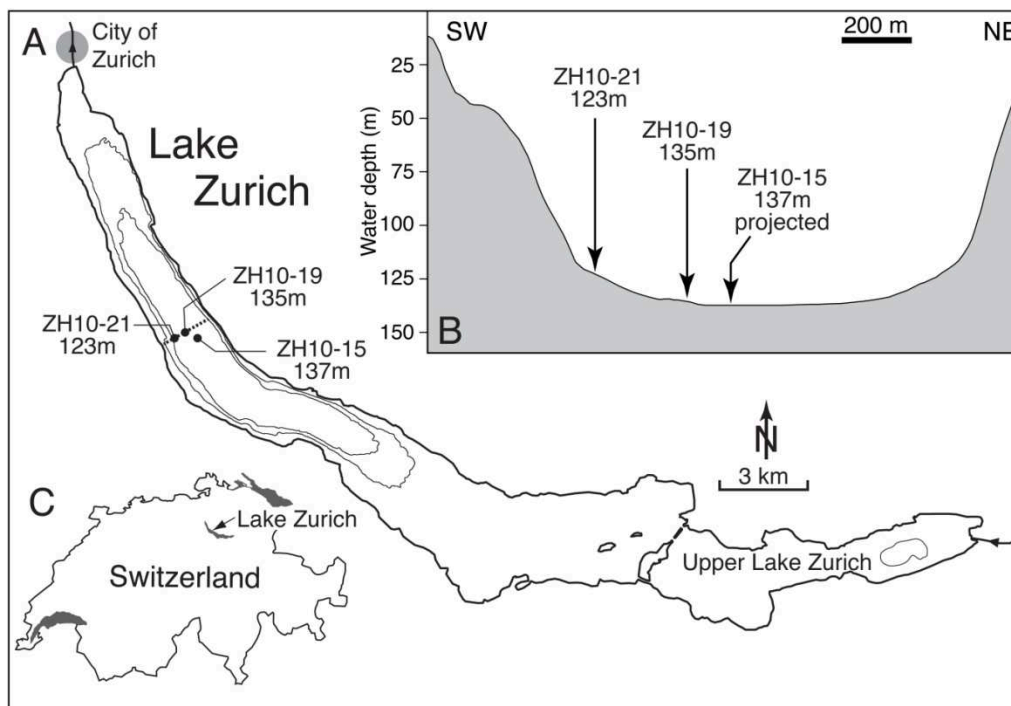


Fig. 4.1. (A) Map of Lake Zurich with the coring locations and the position of the cross-section profile (dashed line). The contour interval is 50 m. (B) The cross-section profile shows the lake morphology near the coring locations and is based on previous seismic investigations (Strasser et al., 2008). (C) Map of Switzerland with Lake Zurich (arrow).

4.2.2 Developments of bottom water oxygenation in Lake Zurich

Long-term monitoring of Lake Zurich began in 1936 and includes O₂ concentration data at 19 different water depths (typically 0.3, 1, 2.5, 5, 7.5, 10, 12.5, 15, 20, 30, 40, 60, 80, 90, 100, 110, 120, 130 and 135 m). The monitoring data indicate that before 1955 bottom water O₂ concentrations (at 135 m) in the lake were generally low. This is likely a result of eutrophication, which was first identified from massive blooms of *Tabellaria fenestrata* in 1896 and *Oscillatoria rubescens* in 1898 (Hasler, 1947; Minder, 1938). Wastewater treatment plants were first constructed in 1955, but it was not until the 1970s when improvements in phosphorus removal and a phosphate ban in detergents led to a continuous decline in lake phosphorus concentrations. The drop in phosphorus initiated a change from a eutrophic to a mesotrophic state (Bossard et al., 2001). Over this period, bottom water oxygen concentrations increased in the late 1950s and at the end of the 1960s. The variability in O₂ concentrations since 1955 shows that other forcing factors, such as climate, also influence O₂ replenishment of deeper waters. The decline in annual O₂ concentration maxima observed since 2000 could be related to increasing air temperatures related to climate change, resulting in reduced mixing intensities, and bottom water oxygen renewal (Livingstone, 1997; Livingstone, 2003).

4.2.3 Core retrieval and age model

In November 2010, short sediment cores were obtained at depths of 137 m (maximum lake depth, ZH10-15, 110 cm long), 135 m (ZH10-19, 111 cm long), and 123 m (ZH10-21, 116 cm long) (Fig. 4.1). The GPS positions (WGS84) of the recovered cores were N 47° 16.995 E 8° 35.624 (ZH10-15), N 47° 17.130 E 8° 35.371 (ZH10-19), and N 47° 17.062 E 8° 35.166 (ZH10-21). The upper part of all three cores is varved (i.e. annually laminated) for more than 100 years as a result of eutrophication, whereas the lower part is bioturbated (Fig. 4.2). The laminations alternate between a light, brownish, carbonate-rich layer and a dark, brown-black OM-rich layer, representing spring/summer and fall/winter, respectively (Fig. 4.2). The age model was based on varve counting and was crosschecked with previously published age

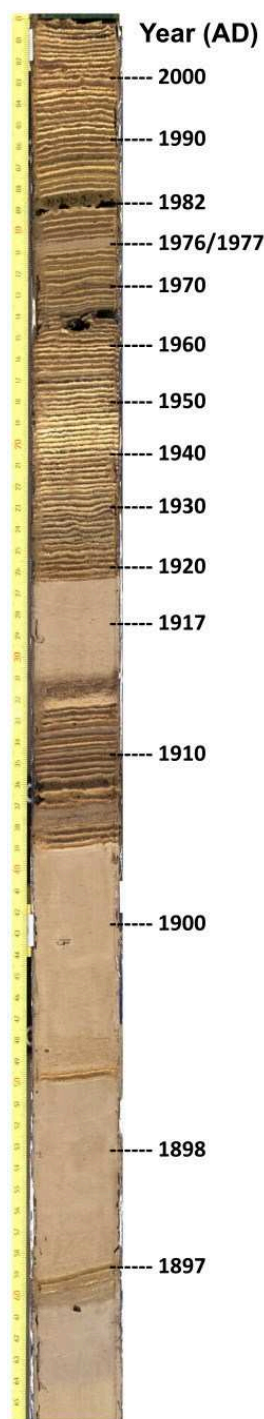


Fig. 4.2. Picture of the short core ZH10-15 taken at the deepest point of Lake Zurich (137m) including the age model. The lighter intervals in the years 1898, 1900, 1918 and 1976/77 are turbidite deposits.

models (Kelts, 1978; Nipkow, 1927). As the seasonal variations are clearest in the Ca XRF data, the Ca minima were attributed to the beginning of a year. The measurements between the Ca minima were then linearly interpolated. The seasonally resolved age model for core ZH10-15 (Fig. 4.2) reaches back until 1895, for ZH10-19 until 1897 and for ZH10-21 until 1901. The average sedimentation rate in the varved sections of all three cores is approximately 0.28 cm yr^{-1} .

4.2.4 XRF core scanning

XRF core scanning provides rapid, non-destructive and high-resolution determinations of elements in the atomic mass range of aluminium (Al) to uranium (U) (Richter et al., 2006). However, XRF core scanning provides only relative results, as XRF counts instead of absolute concentrations. In addition, profiles of trace metals in a core can be biased by the water content (Tjallingii et al., 2007), OM content changes (Löwemark et al., 2011) and grain size variability (Cuven et al., 2010). Before measurement, the core halves were dried for 24 hours at room temperature due to the high water content of the Lake Zurich cores. The core surface was then carefully cleaned and covered with an ultra-thin ($4\mu\text{m}$) SPEXCerti Prep Ultralene foil. The core halves were scanned with the energy dispersive XRF core scanner (AVAATECH) at ETH Zurich, Switzerland. A Rhodium target X-ray tube was operated at excitation energies of 10 and 30 kV for 30 seconds with a spatial resolution of 0.3 mm. With this analytical resolution between 8 and 10 measurements covered one annual cycle in the Lake Zurich sediment cores. In ZH10-15 no XRF data were available between 1963 and 1966 due to a small sediment collapse

in the core. Data between 1983 and 1988 were missing in ZH10-21 because of a turbidite that caused a deformation in this core interval, while a continuous record was established for ZH10-19.

4.3 Results

4.3.1 Ca, Mn and Fe seasonality

The sediment core taken at the deepest point of the lake (core ZH10-15, 137 m) showed a pronounced seasonal pattern in the Ca, Mn and Fe signals (Fig. 4.3). Maxima in Ca are observed in the light layers, which represent the deposition of autochthonous bio-induced precipitated carbonate during summer. Previous studies showed that calcite precipitation in Lake Zurich occurs in pulses during phases of high primary production between May and October (Sigg et al, 1987, Kelts, 1978).

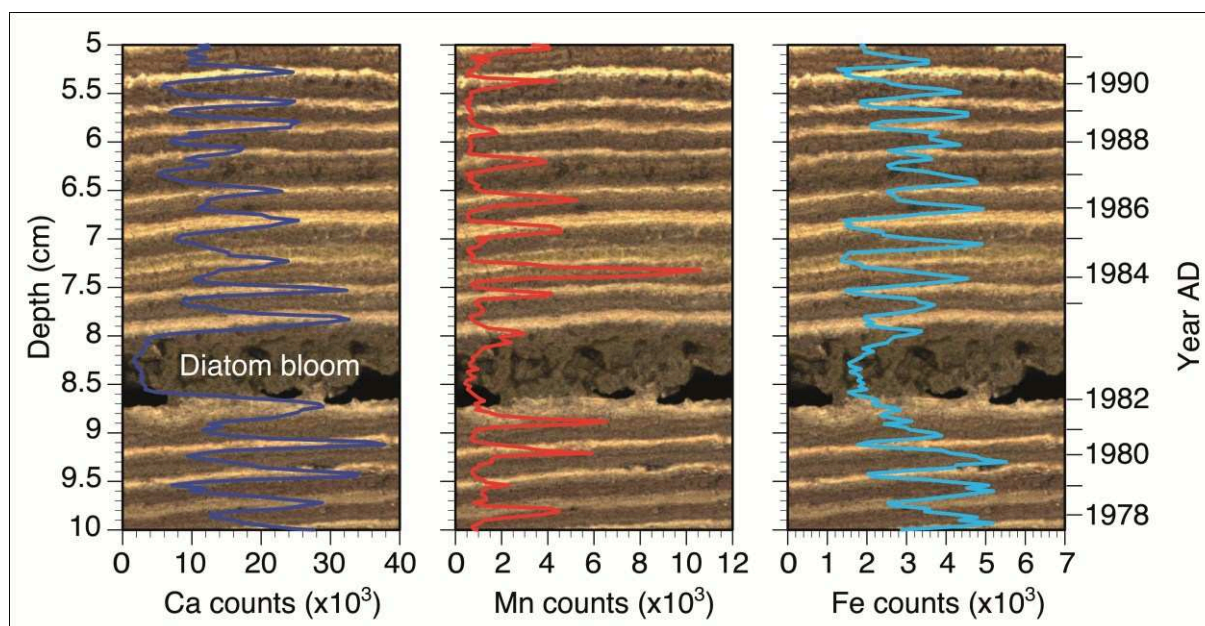


Fig. 4.3. Ca, Fe and Mn XRF signals (x 1000) in core ZH10-15 overlying the corresponding core photograph (note the different scales) showing their seasonal behaviour. The beginning of each year is aligned with the Ca minima and occurs in the dark lamina. Only the central 12 mm are scanned and represented in the XRF data.

If present in the record, Mn exhibits clear maxima in the upper part of the dark layer (Fig. 4.3) coinciding with observed annual maximum deep-water O₂ concentrations, which occur in spring.

Fe shows the opposite behaviour to Ca with peaks in the darker layers (Fig. 4.3) deposited during winter. Fe in lake sediments could have multiple sources, as it can be sedimented in the particulate form or precipitated through redox processes. The particle flux in Lake Zurich

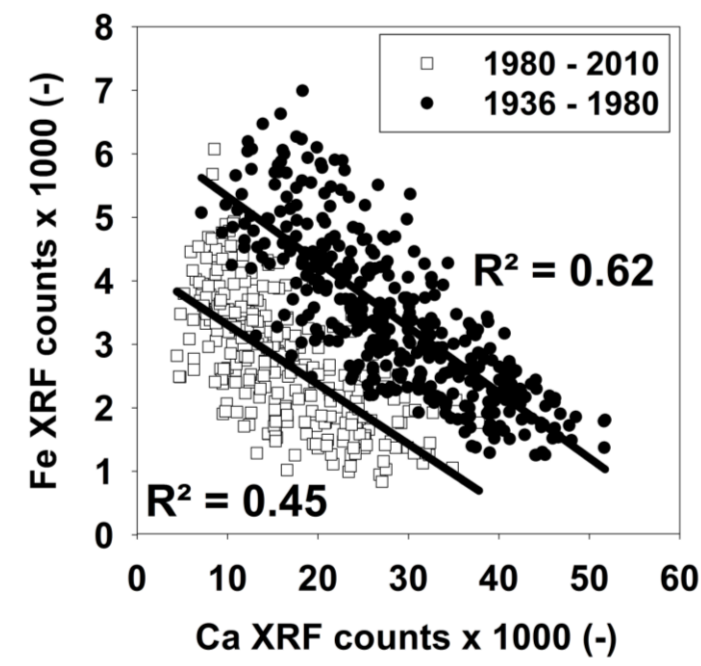


Fig. 4.4. Correlation between XRF counts of Ca and Fe (x 1000) in core ZH10-15 with correlation coefficients for the time intervals 1936-1980 and 1980-2010. The R^2 values comprise all data in the corresponding time intervals, except the missing values between 1963 and 1966.

was studied with sediment traps in 1983 and 1984, during which two Fe maxima were recorded, one in winter (December-February) and one in summer (July-September) (Sigg et al., 1987; Wieland et al., 2001). These results disagree with the XRF data, which only shows one Fe peak in each year. Fe precipitation rates from redox processes reach a maximum during periods of O₂ replenishment to the bottom water. Lake Zurich normally does not freeze over in winter, and is considered to be facultatively

dimictic. During very cold winters it may overturn twice, but generally only overturns once during normal winters, or not at all during milder winters (Peeters et al., 2002). Therefore, the deep-water is generally replenished only once a year, as seen in the monitoring data, which shows that O₂ resupply to the bottom water only occurs sometime between January and April.

Another reason for the missing Fe peak in summer may be diagenetic alterations. Fe can be remobilised after dissolution of iron-oxy-hydroxide precipitates under anoxia and resulting in its loss from the sedimentary archive (Granina et al., 2004; Thamdrup et al., 1994). However, previous studies showed that Fe is not necessarily remobilised and/or fixed by changing redox

conditions (Davison, 1993; Engstrom and Wright, 1984; Glasby and Schulz, 1999). This was also concluded from results of sediment trap data (Sigg et al., 1987), which indicated only minor Fe remobilisation from the traps and therefore also from the sediment. A third possible explanation of the missing Fe maxima in late summer might be dilution effects by other elements, because XRF core scanning is a relative determination of the element concentrations (Richter et al., 2006). Based on sediment trap data, CaCO_3 alone already represents about 20-80% (dry weight) of settling particles in Lake Zurich (Sigg et al., 1987). Therefore, the dominance of Ca in the varve couplet may introduce artefacts by decreasing the concentration of the other elements during the deposition of the light lamina. A negative correlation between Fe and Ca XRF data points towards a possible dilution by calcite in core ZH10-15 (Fig. 4.4). In contrast, Mn could have been less affected by dilution effects as showing a distinct peak in most cases before the onset of the light, calcium-rich lamina and the Mn signal stays low during the light lamina (Fig. 4.3). These dilution artefacts can be circumvented by calculating elemental intensity ratios to minimize variations in the physical sediment properties and any interactions between different elements within the cores (Weltje and Tjallingii, 2008). Especially in the upper part of sediment cores, where porosity increases, XRF ratios could also account for reduced intensities of XRF signals due to higher water contents (Tjallingii et al., 2007; Löwemark et al., 2011). The effect of differences in water content are indicated by the same slope but different intercept of the regression functions of the correlations between Fe and Ca XRF counts considering different time intervals (Fig. 4.4). As a consequence, the ratio of Mn to Fe was defined, in order to explore bottom water oxygenation in Lake Zurich.

4.3.2 Mn/Fe ratios along a core transect

Mn/Fe ratios were determined in the three Lake Zurich cores taken at different water depths (Fig. 4.5): ZH10-15 (137m), ZH10-19 (135 m) and ZH-21 (123 m). The seasonal character of the Mn signal (Fig. 4.3) is observed in all three cores, but its amplitude varies strongly with water depth in which the core was taken and the respective time interval considered within the cores. Core ZH10-15 shows a prominent increase in the amplitude of the Mn/Fe ratio after

1967, characterised by strong inter-annual variability with Mn/Fe ratios up to 3.7 (Fig. 4.5). Before this year the Mn/Fe ratios are low with values below 1, except in the years 1906, 1954, 1955 and 1956. Despite a water depth difference of only 2 m between ZH10-15 (137m) and ZH10-19 (135m), the latter core exhibits considerably less variability in the Mn/Fe ratio. The ratio remained below 1 in every year except 1954, 1967 and 1971 (Fig. 4.5). These three elevated Mn/Fe ratios coincide with elevated ratios in core ZH10-15. Mn/Fe ratios in ZH10-19 were on average about 26% lower than in core ZH10-15, whereas in core ZH10-21 (123m) the values were on average 45% lower. The latter core was taken 15 m above the section of relatively flat lake bottom (Fig. 4.1B). No distinct Mn peaks are present and only during the years 1944 and 2009 slightly higher Mn/Fe ratios are observed (Fig. 4.5).

4.3.3 Mn/Fe ratios as a proxy for bottom water oxygenation

The relationship between Mn/Fe ratios measured in core ZH10-15 (137 m, maximum lake depth) and O₂ concentrations measured at the lake bottom, was investigated using annual maxima and minima (Fig. 4.6, 4.7). Restricting the comparison to maxima and minima avoids inconsistencies resulting from the linearly interpolated age model, which cannot account for sedimentation rate variations over the course of the year (Bloesch, 2007). Furthermore, the minimum and maximum O₂ concentrations were based on three-month running mean levels, which generally occurred during fall (minimum) and spring (maximum). In contrast, values of Mn/Fe data were not smoothed due to the low number of values obtained in each year.

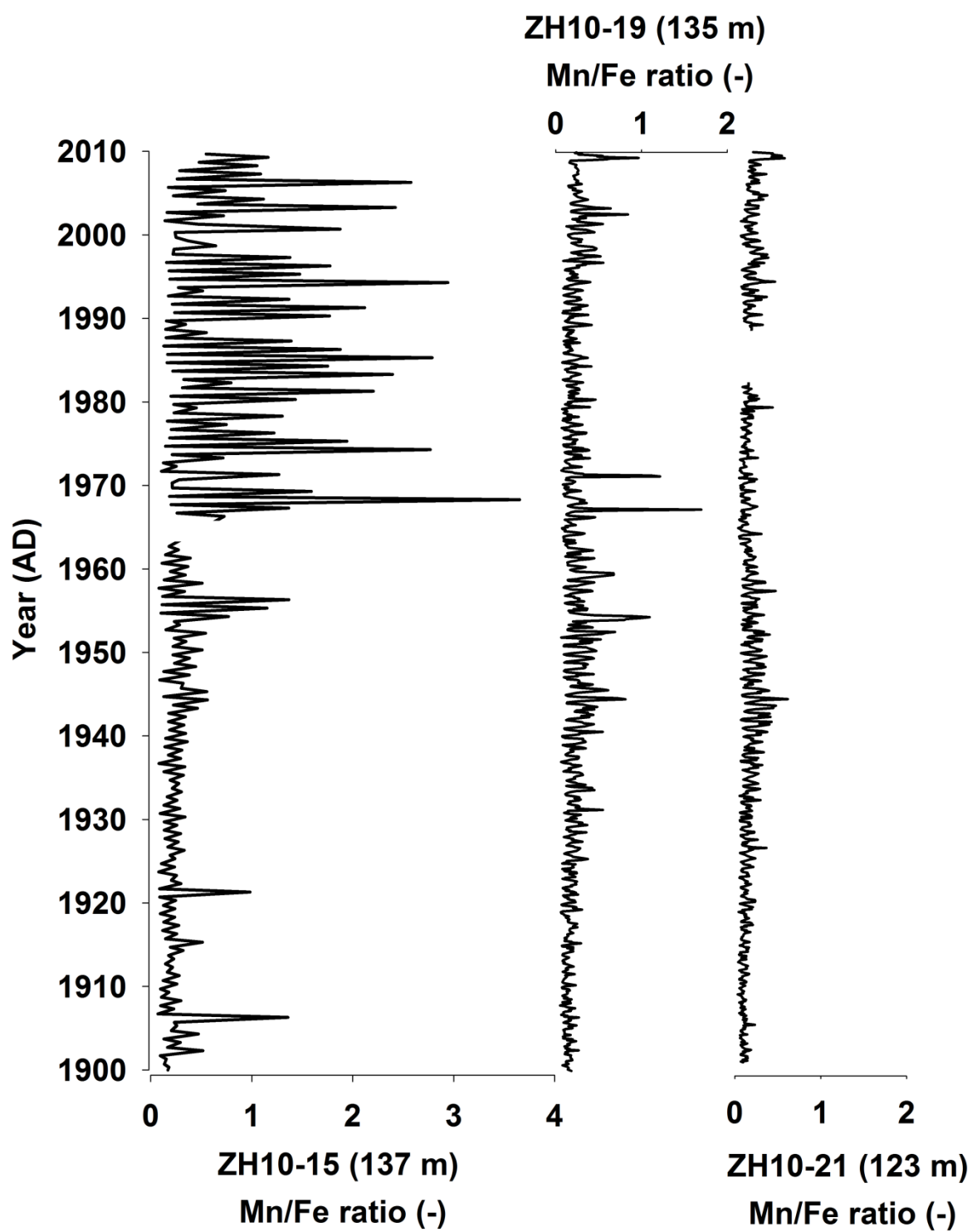


Fig. 4.5. Profiles of the Mn/Fe ratio (complete dataset) in cores ZH10-15, ZH10-19 and ZH10-21 between 1900 and 2010.

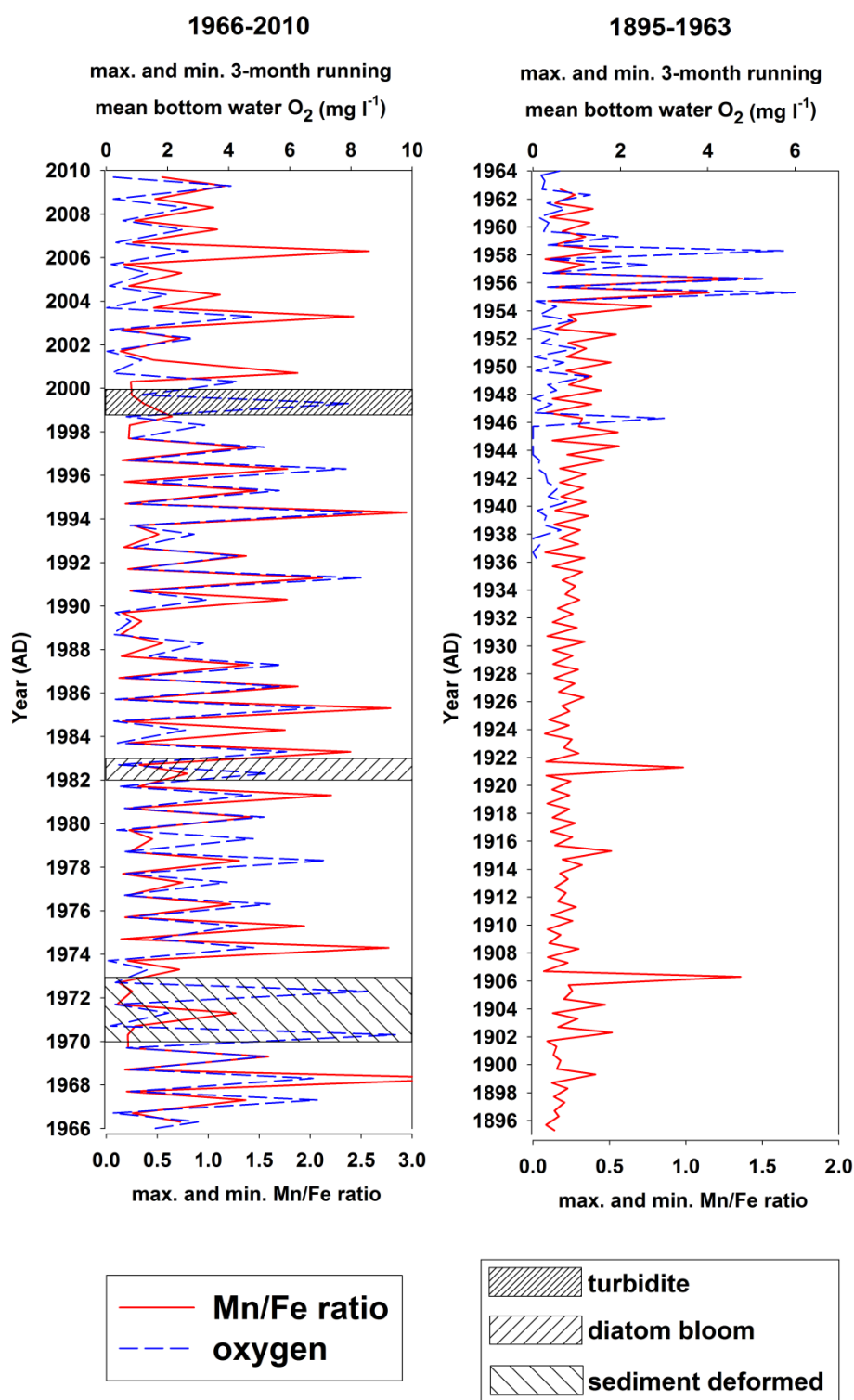


Fig. 4.6. Profiles of maximum (winter/spring) and minimum (summer/fall) Mn/Fe ratios in core ZH10-15 and the corresponding maximum and minimum three-month running mean bottom water oxygen concentrations (in mg l⁻¹) at 135 m (monitored since 1936) vs. time (yr AD). No XRF data were available between 1963 and 1966. Shaded areas show parts of the core influenced by a turbidite (1999), a diatom bloom (dominated by *Melosira*, 1982) and small-scale deformation of the sediment (1970-1972).

max. 3-month running mean bottom water O₂ (mg l⁻¹)

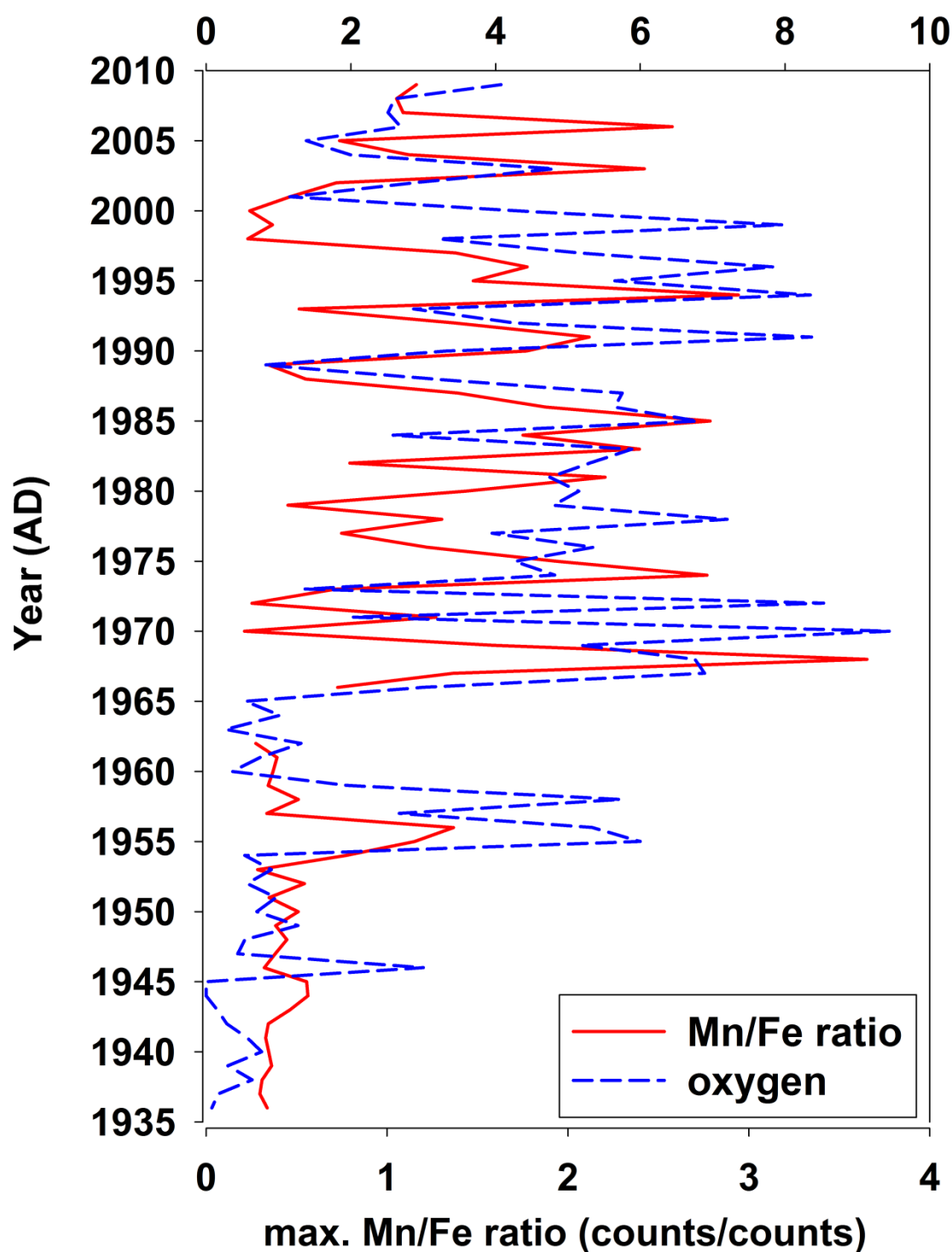


Fig. 4.7. Profiles of maximum (winter/spring) Mn/Fe ratios in core ZH10-15 and corresponding maximum three-month running mean bottom water oxygen concentrations in mg l⁻¹ (135 m, monitoring data) vs. time (yr AD). No XRF data were available in ZH10-15 between 1963 and 1966.

The Mn/Fe ratios and bottom water O₂ concentrations exhibited a clear seasonal pattern (Fig. 4.6). Prior to 1967 the annual maxima of both the Mn/Fe ratios and the O₂ concentrations were consistently low with a small variance (Mn/Fe ratios <0.6 and [O₂] <2 mg O₂ l⁻¹), except between 1955 and 1958 with up to 6 mg O₂ l⁻¹ and a Mn/Fe ratio of up to 1.4, and in 1946 with 3 mg O₂ l⁻¹ (Fig. 4.6, 4.7). After 1967, the variance increased and amplitudes were consistently larger (Mn/Fe ratios up to 3.7 in 1968 and up to 9.4 mg O₂ l⁻¹ in 1970; Fig. 4.6, 4.7). However, between 2000 and 2010, annual maximum bottom water O₂ concentrations at 135 m were consistently below 5 mg O₂ l⁻¹ (Fig. 4.6, 4.7). This observation is in line with lower Mn/Fe ratios over the same period (Fig. 4.6, 4.7).

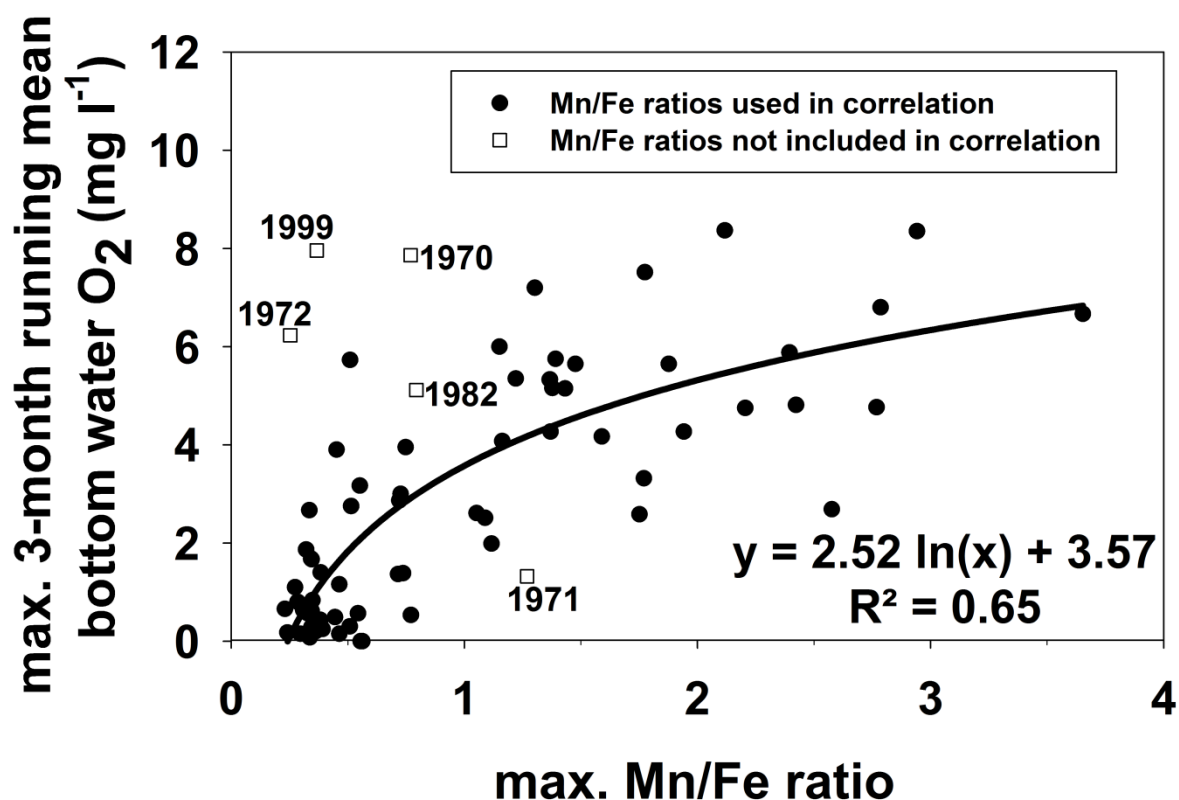


Fig. 4.8. Correlation between maxima of the Mn/Fe ratio in core ZH10-15 and maximum (winter/spring) three-month running mean bottom water oxygen concentrations in mg l⁻¹ (135 m, monitoring data). Square symbols (with years) represent values that have been excluded from the correlation (see text for details).

Maxima of the Mn/Fe ratio in core ZH10-15 (137 m) were well correlated with maxima of the three-month running mean bottom water O₂ concentration data ($R^2=0.65$, $n=66$; $p<0.01$; 1936-2010, XRF data missing: 1963-1966; Fig. 4.8). In general, the Mn/Fe ratio is increasing with higher bottom water O₂ concentrations and the relationship is best approximated by a logarithmic function (Fig. 4.8). However, there is considerable variability in this relationship, but by a careful sedimentological analysis some outliers can be explained. The layers of the years 1970-1972 are slightly deformed as a result of core disturbance (Fig. 4.6). A dominant diatom layer (dominated by *Melosira*) occurred in spring 1982 (Fig. 4.3) and a turbidite deposit in spring 1999 likely blurred the Mn/Fe ratio (Fig. 4.6). Therefore, these 5 years were excluded from the correlation (Fig. 4.8).

4.4 Discussion

4.4.1 Bottom water oxygen reconstructions based on Mn/Fe ratios

The good correlation of the Mn/Fe ratio with the O₂ concentration data (Fig. 4.8) indicated that this ratio could be used as a high-resolution proxy to semi-quantitatively reconstruct bottom water oxygenation in annually laminated sediments. However, there is still considerable variability in this relationship, reflecting the complexity of the redox processes that are involved.

The Mn/Fe ratio decrease systematically from the maximum lake depth towards shallower water depths (Fig. 4.5). This is likely due to geochemical focusing, a process in which redox-sensitive trace metals are transferred and enriched at higher lake water depths (Schaller and Wehrli, 1996). Geochemical focusing can explain major deviations between the Mn/Fe ratio and the O₂ monitoring data as well as the subsequent decrease of the Mn XRF signal up to peak disappearance in the shallower cores.

Sediment focusing could support redox-driven transfer to deeper waters (Garrett, 1990; Wieland et al., 2001). It causes higher sedimentation rates with increasing water depth. Probably, sediment focusing can also increase Mn transfer towards deeper sediment, therefore

enhancing geochemical focusing. Because of the low densities and fine textures of Mn and Fe precipitates, water turbulence and mixing tend to preferentially move these particles to deeper regions of the lake, also affecting Mn and Fe (Engstrom and Wright, 1984).

The difference between O₂ monitoring data and Mn/Fe ratios increased progressively between 1955 and 1958, and also in 1994, 1996 and 1999 at times of generally high O₂ levels (Fig. 4.7). Therefore, persistently higher maximum O₂ concentrations in successive years seemed to result in lower maximum Mn/Fe ratios in the following years (Fig. 4.7). Oxidation of Mn in shallow waters may have effectively trapped Mn, which reduced the supply of Mn to deeper water depths.

Also heterogeneities of Mn and Fe in the sediment might influence Mn/Fe ratios, which especially arise at high spatial resolution measurements (Cuven et al., 2010; Löwemark et al., 2011). Very subtle changes in the internal structure of the annual lamination may lead to variations in the maximum Mn/Fe ratio, which would lead to inaccurate bottom water O₂ reconstructions from Mn/Fe ratios. Applying Micro-XRF technique with repetitive measurements might overcome limitations associated with heterogeneities and sampling resolution.

4.4.2 Indication of diagenetic alteration of the Mn/Fe ratio

The errors between reconstructed and observed bottom water O₂ show only a slight trend throughout core ZH10-15 (Fig. 4.9 a), which indicates that the errors in the reconstructed O₂ did not change significantly with time. Therefore, the Mn/Fe signal in the lake sediment is largely preserved in the sediment after deposition. This suggests that despite the anoxic conditions in the sediment, there is not a substantial loss of Mn from the sediment due to reductive dissolution. The trendline mainly results from the relatively low O₂ concentrations during deposition of the lower part of the core, in which the estimates of past bottom water O₂ concentrations are too high compared to the upper part of the core with relatively lower reconstructed O₂ levels (Fig. 4.9 a, b).

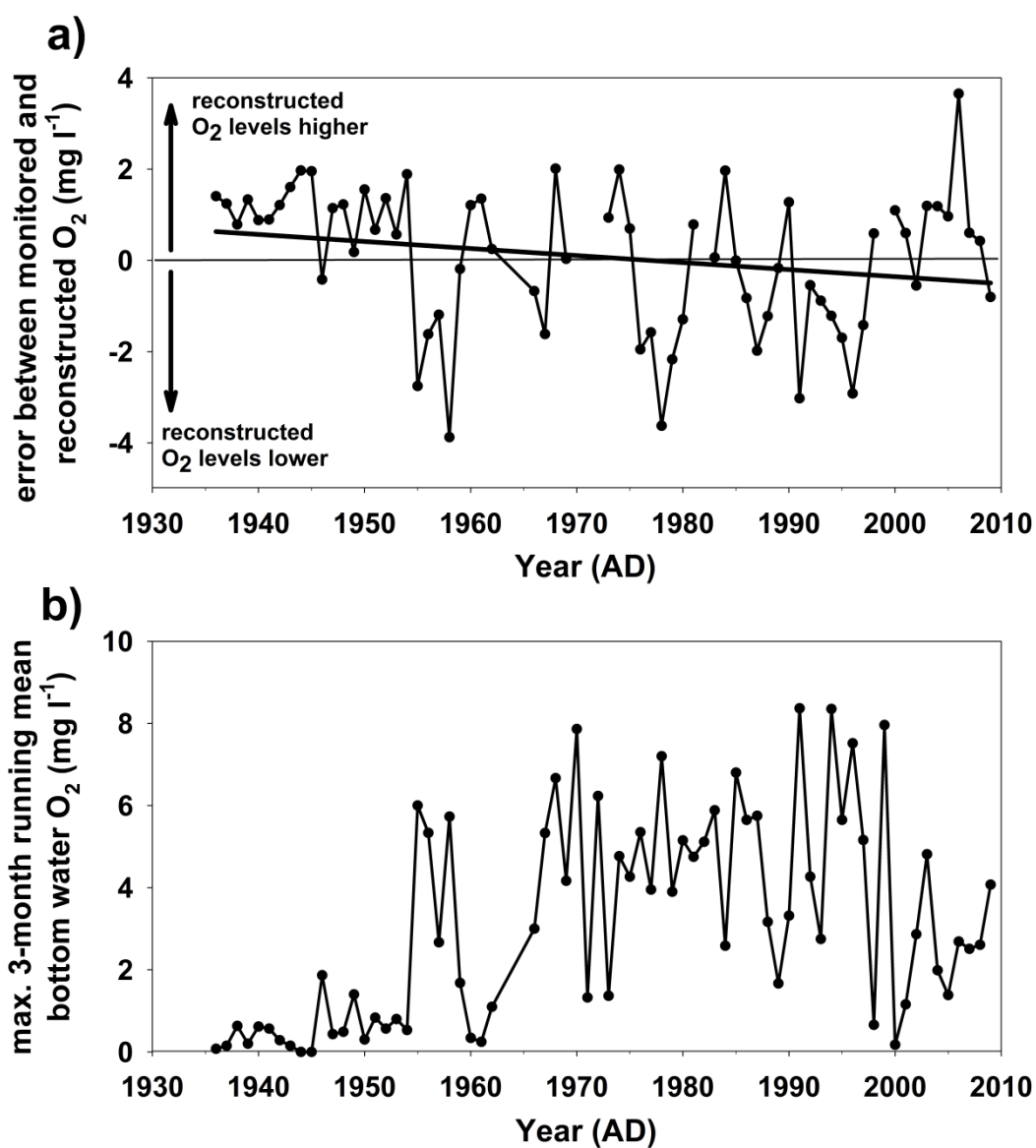


Fig. 4.9. a) Plot of errors (in mg l^{-1}) between the three-month running mean bottom water O_2 monitoring data (135 m) and the reconstructed O_2 concentrations based on the Mn/Fe ratios. Positive values indicate that the Mn/Fe ratios based estimates of bottom water O_2 levels are higher than the monitoring data, whereas negative values represent lower values. The trendline of the data is shown as a thick solid line. The values for 1970-1972, 1982 and 1999 were removed from the dataset (see text for details).

b) Maxima of three-month running mean bottom water O_2 concentrations from the monitoring data at 135 m. No values were removed from the dataset.

The application of the Mn/Fe proxy might be limited to special cases, in which oxygenated systems show pronounced seasonal redox changes throughout the year. If the whole water body is oxygenated throughout the year, Mn is trapped completely as soon as it enters the lake and remains immobilised. In contrast, in a consistently anoxic water body Mn remains in solution under reducing conditions and/or precipitates are dissolved (Davison, 1993; Friedl et al., 1997). This means that if the impact of alteration processes can be assessed, the Mn/Fe ratio might be an accurate indicator for bottom water O₂ reconstructions in similar lake settings.

4.4.3 Oxygen concentrations in the early 20th century in Lake Zurich

The correlation between the annual maxima of Mn/Fe ratios and three-month running mean bottom water O₂ concentrations (Fig. 4.8) can be used to semi-quantitatively reconstruct bottom water O₂ levels for the unmonitored period of the laminated part of core ZH10-15 (1895 to 1936). The Mn/Fe ratios are varying around 0.3 throughout this section of the core and only exceed 1 in 1906 (1.4) and 1921 (1.0) (Figs. 4.5 and 4.6). Based on the correlation shown in Figure 4.8, these ratios would indicate an O₂ concentration below 1 mg O₂ l⁻¹. Only in the years 1906 and 1921 higher O₂ concentration of 4.4 and 3.6 mg O₂ l⁻¹ were reached. Despite the errors and uncertainty of the correlation, the low Mn/Fe ratios and reconstructed O₂ concentrations suggest that Lake Zurich bottom water O₂ levels were generally very low between 1895 and 1936.

4.5 Conclusions

Due to precise sediment age models, monthly long-term O₂ monitoring data and high-resolution XRF core scanning, Mn redox dynamics could be studied on a seasonal resolution in the sediment of Lake Zurich, Switzerland. The age models were based on bi-annual lamination in sediment cores and yearly calcite precipitation cycles. Ca, Fe and Mn showed pronounced seasonal behaviour. Ca was governed by higher calcite precipitation during

summer, whereas Fe showed peaks in winter and Mn in spring. The strong negative correlation between Ca and Fe suggested that the Fe XRF signal was governed by calcite dilution. Mn traced bottom water oxygenation due to its redox-sensitive behaviour. The Mn/Fe ratio was correlated with three-month running mean bottom water O₂ concentrations. Therefore, the Mn/Fe ratio from core ZH10-15 (137 m, maximum lake depth) was used as a proxy for bottom water oxygenation. Oxygenation has been consistently high since the mid-1960s, and relatively lower prior to this time because of eutrophication. However, it was shown that geochemical and sediment focusing, and also sedimentological factors can bias or even prevent the utilisation of the Mn/Fe ratio for O₂ reconstructions in the bottom water of lakes.

4.6 Acknowledgements

This research project was funded by the European Union project “Hypox – In situ monitoring of oxygen depletion in hypoxic ecosystems of coastal and open seas and land-locked water bodies” (EC grant 226213). Oxygen data from Lake Zurich were kindly provided by the City of Zurich Water Supply and the Zurich Cantonal Laboratory. Ulrike van Raden and Stefanie Wirth (both ETH) are thanked for field support. David Livingstone, Bernhard Wehrli and Beat Müller (all Eawag) are acknowledged for helpful discussions and suggestions.

Chapter 5: Environmental variations in a semi-enclosed embayment (Amvrakikos Gulf, Greece) – reconstructions based on benthic foraminifera abundance and lipid biomarker pattern

Sebastian Naeher, Maria Geraga, George Papatheodorou, George Ferentinos, Heleni Kaberi, Carsten J. Schubert

Published in Biogeosciences, Volume 9, 2012, Pages 5081-5094

<http://dx.doi.org/10.5194/bg-9-5081-2012>

Abstract

The evolution of environmental changes during the last decades and the impact on the living biomass in the western part of Amvrakikos Gulf was investigated using abundances and species distributions of benthic foraminifera and lipid biomarker concentrations. These proxies indicated that the gulf has markedly changed due to eutrophication. Eutrophication has led to a higher productivity, a higher bacterial biomass, shifts towards opportunistic and tolerant benthic foraminifera species (e.g. *Bulimina elongata*, *Nonionella turgida*, *Textularia agglutinans*, *Ammonia tepida*) and a lower benthic species density. Close to the Preveza Strait (connection between the gulf and the Ionian Sea), the benthic assemblages were more diversified under more oxygenated conditions. Sea grass meadows largely contributed to the organic matter at this sampling site. The occurrence of isorenieratane, chlorobactane and

lycopane supported by oxygen monitoring data indicated that anoxic (and partly euxinic) conditions prevailed seasonally throughout the western part of the gulf with more severe oxygen depletion towards the east. Increased surface water temperatures have led to a higher stratification, which reduced oxygen resupply to bottom waters. Altogether, these developments led to mass mortality events and ecosystem decline in Amvrakikos Gulf.

5.1 Introduction

Coastal development, pollution and a range of anthropogenic activities including extensive agriculture, aquaculture, urban and industrial wastes are main causes of decline and loss of coastal habitats observed over the last decades (Airoldi and Beck, 2007; Diaz and Rosenberg, 2008).

Amvrakikos Gulf, located in northwestern Greece, is a semi-enclosed embayment characterized by a complex lagoonal system and an extensive delta (Kapsimalis et al., 2005). It has a fjord-like oceanographic regime because of a shallow sill, which reduces deep-water exchange with the ocean (Ferentinos et al., 2010). The gulf is protected under the international Ramsar Convention as Wetlands of International Importance. In addition it is designated as a Special Protection Area (SPA), according to the European Union Directive 79/409/EU, and it is included in the Natura 2000 Network. Despite the efforts, which have been made for the protection and conservation of this unique area, the western part of the gulf is suffering from seasonal hypoxia (oxygen concentrations $<2 \text{ mg l}^{-1}$), whereas the eastern part is also affected by seasonally anoxic conditions (oxygen concentrations $<0.5 \text{ mg l}^{-1}$) (Kountoura and Zacharias, 2011). This was caused by the excessive use of fertilizers, the increase in animal stocks, intensive fish farming and domestic effluents for the last 20 to 30 years (Ferentinos et al., 2010; Kountoura and Zacharias, 2011). Recently, in February 2008 the environmental stress in the gulf resulted in a sudden massive mortality of fish in aquaculture rafts in the northeastern part of the gulf (Ferentinos et al., 2010).

The purpose of the present paper is to illustrate the evolution of the environmental conditions in the Amvrakikos Gulf over the last 50 years by means of sedimentary proxies. Benthic

foraminifera have been proven useful in the reconstruction of palaeoenvironmental conditions since changes in abiotic and biotic parameters such as salinity, nutrient content, oxygen concentration, substrate, water depth and pollution do modify benthic assemblages (Scott et al., 1979; Jorissen, 1987; Debenay et al., 2005; Murray, 2006). Due to their short reproductive life cycles, benthic foraminifera can be used as proxies to reconstruct short-term environmental changes in oxygen conditions, organic matter (OM) supply and lithology at the sea bottom (Murray, 2001).

More specific in environments where oxygen depletion in the bottom water occurs, benthic foraminifera populations and their diversity are usually reduced and the assemblages are dominated by relatively tolerant species (Sen Gupta and Machain-Castillo, 1993). The changes in benthic assemblage characteristics have been used to evaluate the past evolution of oxygen depletion in a wide spectrum of coastal environments (Filipsson and Nordberg, 2004; Platon et al., 2005).

Lipid biomarkers have been used as tracers for human alteration and eutrophication of water bodies (e.g. Smittenberg et al., 2004; Naeher et al., 2012). Specific indicators of severe oxygen depletion are the pigments isorenieratene, chlorobactene and okenone (or related derivatives), which have been used to trace photic zone euxinic conditions (e.g. Brocks and Summons, 2003). Apart from oxygen depletion, water column properties such as stability of stratification and salinity can be traced by tetrahymanol and gammacerane (Sinninghe Damsté et al., 1995; Thiel et al., 1997; Bechtel and Schubert, 2009), whereas long-chain alkenones have been proven useful in reconstructing surface water temperatures (Prah and Wakeham, 1987; Müller et al., 1998).

In this study, the combined approach of benthic foraminifera and sedimentary lipid biomarker proxies in two sediment cores was used to characterise environmental changes and the implications for living biomass during the recent history in Amvrakikos Gulf. Changes in eutrophication within the last decades and the role of the ocean regarding water exchange and oxygen supply to the gulf was studied. The effects of low oxygen concentrations (traced by lipid biomarkers) on foraminifera assemblages (adaptation, community shifts, species extinction) were determined. Furthermore, the applicability and robustness of biotic and geochemical proxies for reconstructions of such environmental alterations was tested.

5.2 Regional setting

Amvrakikos Gulf was formed during the mid-Quaternary period (ca. 50-11 ka BP) (Kapsimalis et al., 2005; Anastasakis et al., 2007) and is approximately 35 km long and 6-15 km wide (Fig. 5.1). It is separated from the open Ionian Sea by a beach-barrier complex and is connected to the open sea through a narrow, elongated channel, the Preveza Strait, which is approximately 6 km long, 0.8 to 2.5 km wide and 20 m deep. The delta of the Arachthos and Louros Rivers and associated lagoons are located at the northern border of the gulf.

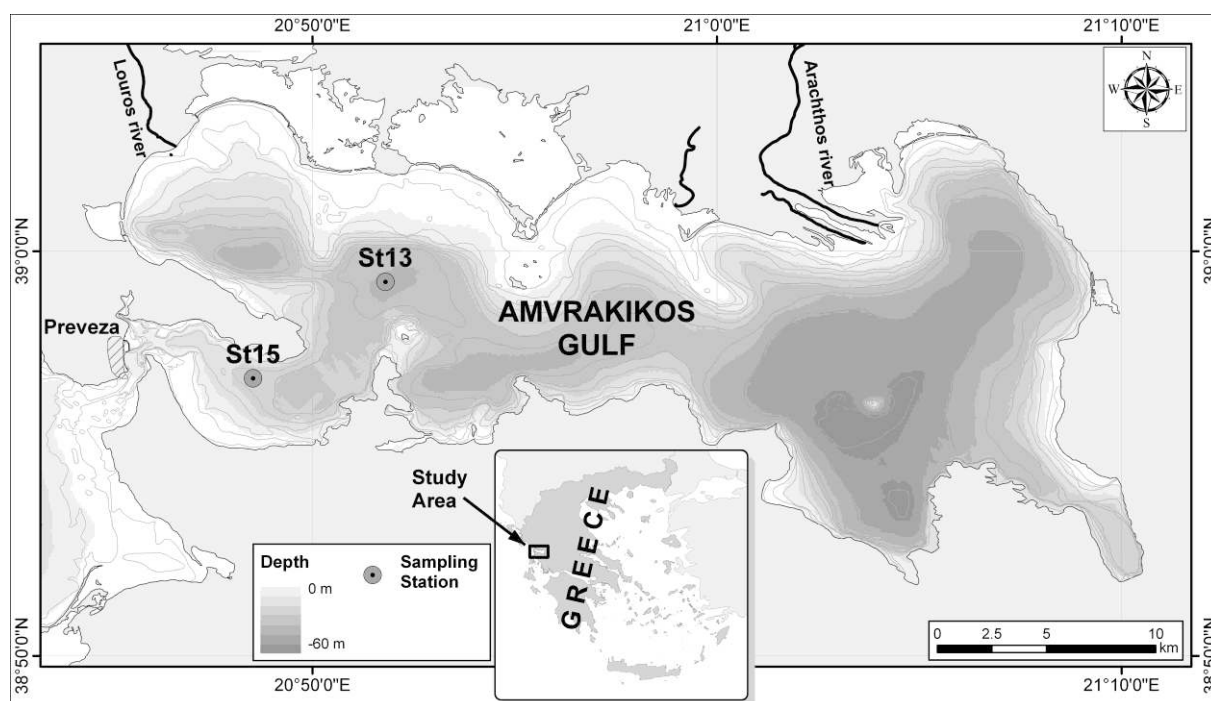


Fig. 5.1. Map of Amvrakikos Gulf, Greece. The major rivers (Louros and Arachthos Rivers), the Preveza Strait (connection with the Ionian Sea) and the sampling stations of cores Amvr13 and Amvr15 are illustrated.

The water column is stratified during most time of the year with a brackish surface layer and a saline bottom layer, which are separated by a sharp halocline between 8 and 12 m (Ferentinos et al., 2010). The surface layer is well oxygenated with concentrations ranging from 7.5 to 9 mg l⁻¹, but the dissolved oxygen content in the bottom water layer only reaches 0-2 mg l⁻¹

during the summer months in the western part and year-round in the eastern part of the gulf (Ferentinos et al., 2010 and unpublished data). Brackish surface water flows out of the gulf, whereas saline water enters into the bottom water. Summer months temperatures and salinity in the surface water ranged between 28.3 and 29.3°C and between 32.9 and 33.7, respectively. Temperatures in the bottom water ranged between 15.8 and 16.0°C, whereas the salinity was around 37.7. These values were recorded seasonally for two years (2009-2010; Ferentinos et al., 2010). Similar ranges were also reported by Kountoura and Zacharias (2011) and in 1987 by the Hellenic Centre for Marine Research (unpublished data). Seasonal hypoxia has been documented at the sampling sites since the last 2-3 decades (Kountoura and Zacharias, 2011).

Since the 1970s the gulf has been altered, mostly due to extensive agriculture, aquaculture and urban development, and the establishment of oil stations along the southern border of the gulf. Furthermore, since the construction of two dams the run-off of the Arachthos River has been controlled. Now also the surface water layer suffers occasionally from oxygen depletion (Ferentinos et al., 2010). In 2008, water with a higher density filled the deeper parts of the basin and lifted the anoxic layer, which led to a massive fish mortality event (Ferentinos et al., 2010). Fish mortality events in aquaculture rafts have also been observed in the past (1988, 1992 and 1998), although less intense than in 2008 (Ferentinos et al., 2010).

5.3 Methods

Two short sediment cores were retrieved in October 2010 from Amvrakikos Gulf by a KC Kajak sediment core sampler. Core Amvr15 (42 cm long) was collected from an area close to the entrance of the gulf (38° 56' 53''N, 20° 48' 31''E) at a water depth of 32 m (Fig. 5.1). The 30 cm long core Amvr13 was retrieved from the inner part of the gulf (38° 59' 15''N, 20° 51' 48''E) at a water depth of 40 m (Fig. 5.1).

The actual sediment accumulation rates at the sampling sites were calculated from the vertical distribution of ^{210}Pb in the cores, following the constant rate of supply (CRS) model of Appleby and Oldfield (1978). The downcore ^{210}Pb activity was determined through the activity of its α -emitting granddaughter ^{210}Po , assuming secular equilibrium with ^{210}Pb . The

supported ^{210}Pb activities, which correspond to sediment layers deposited earlier than the last 100-120 years, were calculated from the vertical profiles of ^{226}Ra published by Tsabaris et al. (2011) in the same area.

Benthic foraminifera were studied on 29 samples from core Amvr15 and 20 samples from core Amvr13. The sampling interval for faunal analyses ranged between 0.5 and 2 cm in each core. The samples were washed over a 63 μm sieve and dried in an oven. At least 200 specimens of benthic foraminifera were picked and identified from each sample; a microsplitter device was used in cases where foraminifera were very abundant. Each taxon was expressed as a percentage of the total benthic assemblage. An estimation of the species diversity was performed using the $H(s)$ index following the Shannon-Wiener equation (Shannon, 1948; Buzas and Gibson, 1969). The ratio of the number of benthic foraminifera per weight of dry sediment ($>63 \mu\text{m}$) was used as an index of benthic foraminifera productivity (Blackwelder et al., 1996). Hierarchical cluster analysis (R-mode) was performed on 18 benthic foraminifera species and genera, which were sufficiently abundant in both cores. The tree diagram was constructed using the Ward's method based on Euclidian distance on SPSS software.

Bulk parameters were analysed and measured as described previously (Naeher et al., 2012): in short, total carbon (TC), total nitrogen (TN) and total organic carbon (TOC) were determined on untreated and decalcified sediment samples, respectively, with errors of up to $\pm 0.2 \text{ wt}\%$ by means of an elemental analyser (Carlo Erba 2500). The total inorganic carbon (TIC) was calculated from the difference between TC and TOC. The isotopic composition of OM ($\delta^{13}\text{C}_{\text{TOC}}$ and $\delta^{15}\text{N}$) was analysed by an Isoprime mass spectrometer connected to an elemental analyser (Carlo Erba 2500). The error was $\pm 0.3\text{‰}$ and values are reported against the international standards Vienna Pee Dee Belemnite (VPDB, carbon) and air (nitrogen). The chlorin index (CI) and total chlorin concentrations were determined according to Schubert et al. (2005). For biomarker analysis, the same extraction and treatment was used as described in Naeher et al. (2012). An internal standard was added for quantification (α -Cholestane, C_{19} *n*-fatty acid, C_{19} *n*-alcohol) before extraction with MeOH/DCM. After saponification and separation of fatty acids (FA) and neutrals, the latter were further separated into apolar and polar fractions over NH_2 columns (Hinrichs et al., 2003). The polar fraction was derivatised with BSTFA for 1h at 80°C . FA were converted into methyl esters with 14% BF_3/MeOH . FA

double bond positions were determined according to Spitzer (1997). A sample aliquot of the polar fraction was desulfurized with Raney-Nickel catalyst (Sinninghe Damsté et al., 1988), followed by hydrogenation for 2h with PtO₂ as catalyst in a solution of concentrated acetic acid and ethyl acetate (1:1, v:v). Instruments and measurement conditions are described in Naeher et al. (2012). Alkenones were quantified on an Agilent 7890A GC system, equipped with an Agilent column (30 m long x 320 µm inner diameter x 0.32 µm film thickness) and a flame ionization detector (FID). The GC oven temperature program was 70 °C to 180 °C at 40 °C min⁻¹, then to 320 °C at 2 °C min⁻¹ and held for 10 min.

5.4 Results

5.4.1 Sediment cores and age model

The sediment in cores Amvr15 and Amvr13 consisted of grey mud. The colour of the sediments in the top 5 cm in each core appeared darker in relation to the rest of the core. At the sampling site of core Amvr15, seagrass meadows were present on the sediment surface.

According to the CRS model, the estimated average sediment accumulation rates in core Amvr15 were 0.6 cm yr⁻¹ and 0.8 cm yr⁻¹ in core Amvr13 (Fig. 5.2). Regarding core Amvr15, the estimated rate was in agreement with the one calculated by Tsabaris et al. (2011) from the same area. From the vertical profiles of ²¹⁰Pb, no significant bioturbation was observed. Based on the age models (Fig. 5.2), the cores comprised sediments deposited since 1940 (Amvr15) and 1975 (Amvr13).

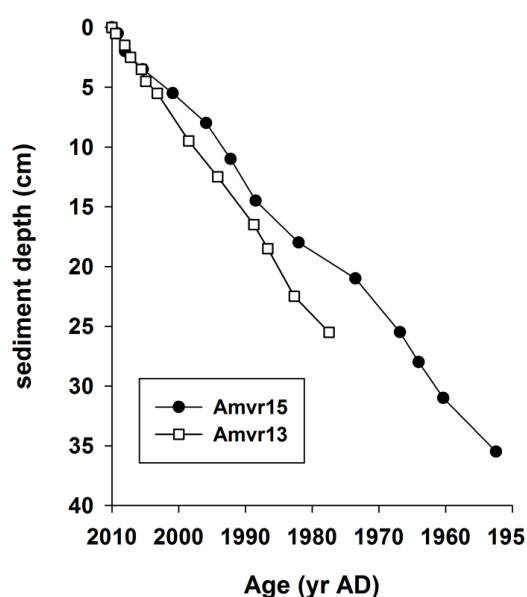


Fig. 5.2. Age models of cores Amvr15 and Amvr13 based on the specific activity of ²¹⁰Pb in the sediment.

5.4.2 Benthic foraminifera

Benthic foraminifera were present throughout both cores. A total of 127 foraminiferal species were recognized in samples from core Amvr15. The number of benthic foraminifera specimen per g of sediment was high, except in the intervals 25-30 cm (1960-1968), 10-15 cm (1985-1993), 6-7 cm (1998-2000) and 1-2 cm (2007-2008) (Fig. 5.3). The H(s) diversity index ranged between 2.6 and 3.6 and exhibited lower values from around 18 cm (since ca. 1980) to the top of the core. Within the upper 3 cm of the core (since ca. 2005), the H(s) index represented small-scale oscillation with low values in the dark colour laminae. Furthermore, at around 1 cm (ca. 2009) the reduction of the H(s) index was accompanied by a reduction of the benthic foraminifera population. A shift of both indices to higher values occurred in the light-coloured muddy sediments at the top of the core. The downcore variation of the abundances of selected taxa is shown in Fig. 5.3.

Benthic foraminifera assemblages consisted of miliolids (*Quinqueloculina seminulum*, *Quinqueloculina oblonga*, *Quinqueloculina laevigata*, *Quinqueloculina stelligera*, *Quinqueloculina lata*, *Quinqueloculina subpoezana*, *Miliolinella subrotunda*, *Triloculina* spp), epifaunal (*Rosalina globularis*, *Discorbis* spp., *Planorbulina mediterranensis*, *Cibicides* spp) and infaunal taxa (*Bulimina aculeata*, *Bolivina dilatata*, *Bolivina spathulata*, *Ammonia beccarii*, *Ammonia tepida*, *Nonion depressum*, *Nonionella turgida* and *Nonionella bradii*).

A total of 77 foraminiferal species were recognized in samples from core Amvr13 (Fig. 5.4). The H(s) diversity index ranged between 1.8 and 2.7 and exhibited lower values at around 20 cm (ca. 1985) and 1 cm depth (ca. 2009). Shallow and deep infaunal species dominated the benthic assemblages almost throughout the core, including high abundances of *Bulimina elongata*, *Bulimina aculeata*, *Bolivina dilatata*, *Bolivina spathulata*, *Hopkinsina pacifica*, *Ammonia tepida*, *Nonionella turgida* and *Nonionella bradii*. The agglutinated species included mostly *Textularia conica* and *Textularia agglutinans* and the porcelaneous included Miliolids. *Quinqueloculina* spp and *Miliolinella* spp showed similar fluctuations and higher abundances at around 25 cm (ca. 1978), 15 cm (ca. 1992) and 8 cm (ca. 2000) (Fig. 5.4).

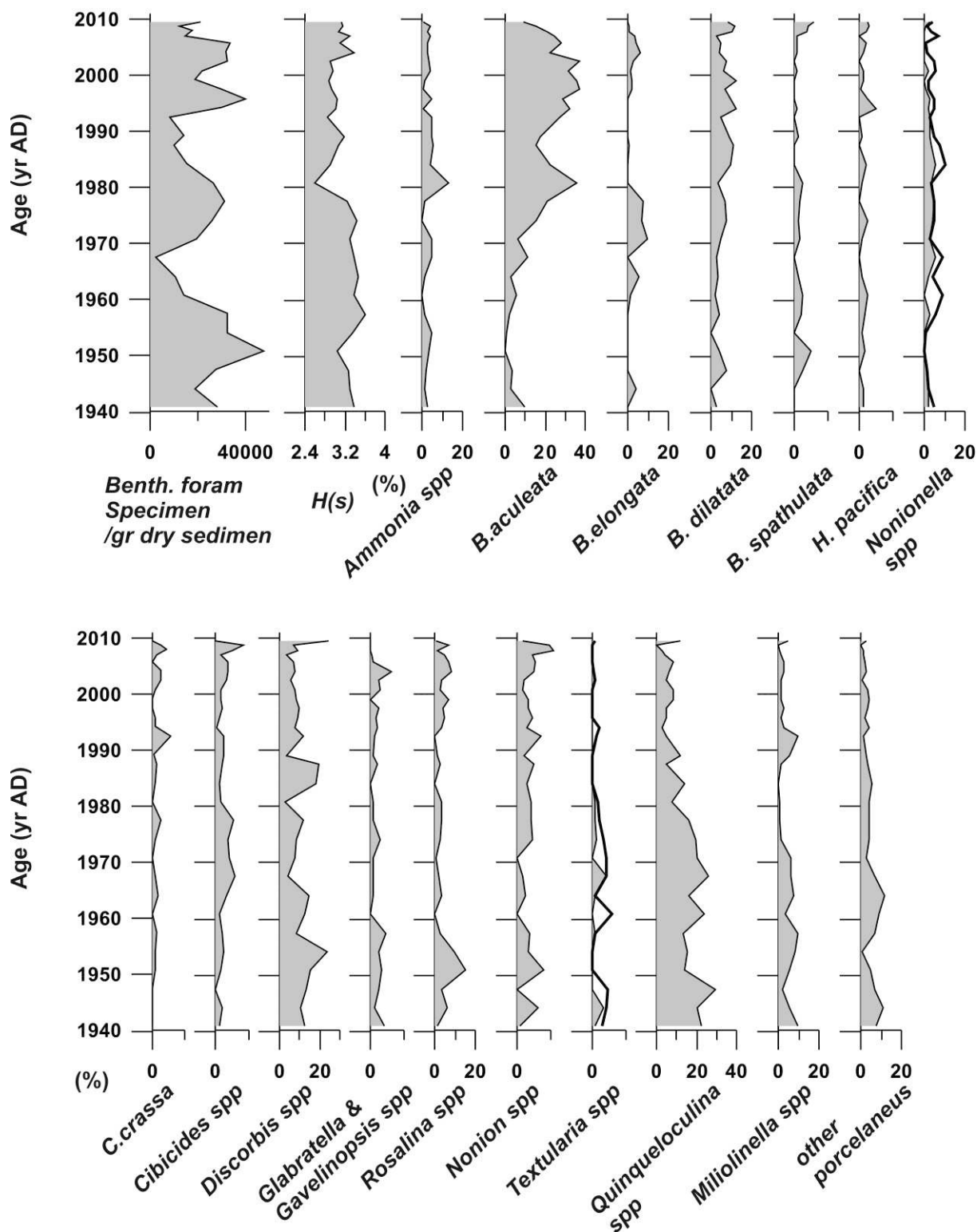


Fig. 5.3. Downcore changes of benthic foraminifera in per cent (%) of the total benthic foraminifera assemblages in core Amvr15 versus sediment depth together with the indices of benthic productivity (benthic foraminifera specimen/ g of dry sediment) and diversity ($H(s)$). Grey bands in the diagrams of *Textularia spp* and *Nonionella spp* indicate the relative amounts of *T. agglutinans* and *N. turgida*, respectively.

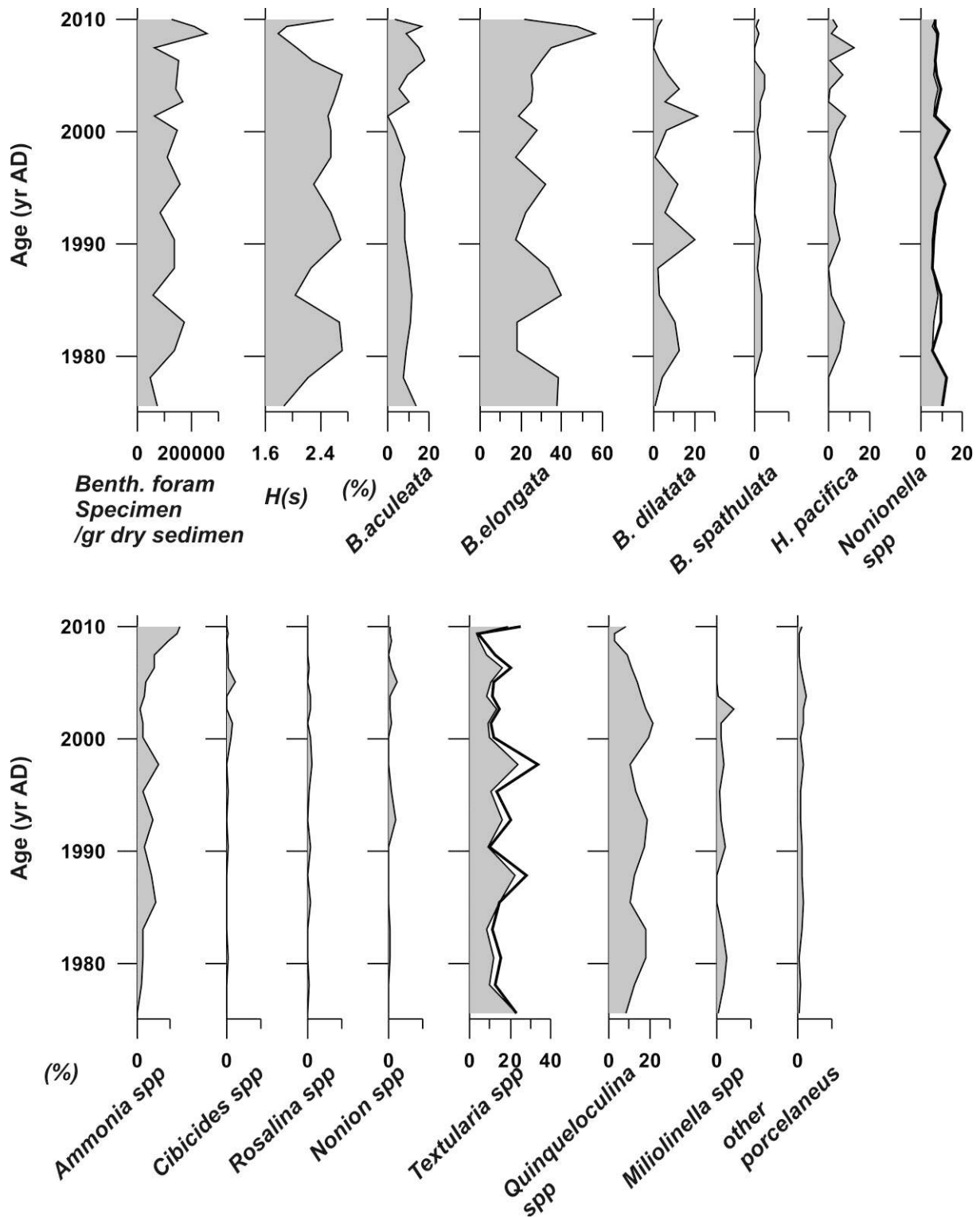


Fig. 5.4. Downcore changes of benthic foraminifera in per cent (%) of the total benthic foraminifera assemblages in core Amvr13 versus sediment depth, together with the indices of benthic productivity (benthic foraminifera specimen/ g of dry sediment) and diversity (H(s)). Grey bands in the diagrams of *Textularia spp* and *Nonionella spp* indicate the relative amounts of *T. agglutinans* and *N. turgida*, respectively.

5.4.3 Bulk parameters and biomarkers

The TOC profile of core Amvr13 increased slightly from 1.3 to 2.7 wt% towards the top of the core (Fig. 5.5). TN and $\delta^{15}\text{N}$ values and chlorin concentrations also increased (Fig. 5.5). The CI decreased towards the top of the core (Fig. 5.5). The C/N ratio was ≤ 9 (Fig. 5.5). Total nitrogen contents were below the detection limit in 18-20 cm (1985-1988) and 2-3 cm (2006-2008), which hindered the calculation of the C/N ratios. $\delta^{13}\text{C}_{\text{TOC}}$ values ranged between -23 to -22‰ throughout the core.

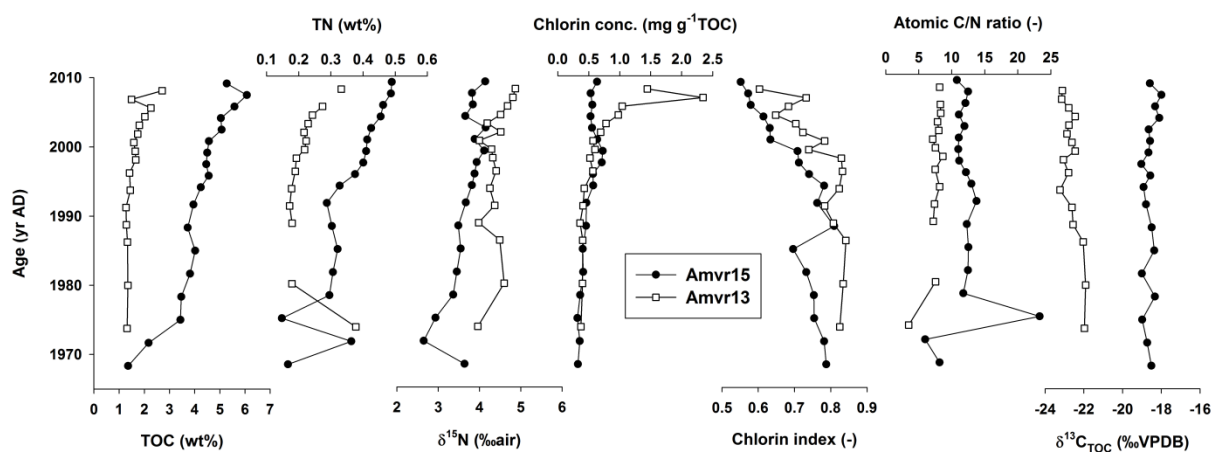


Fig. 5.5. Bulk parameters of cores Amvr13 and Amvr15 plotted vs. age (yr AD), including the concentrations of total organic carbon (TOC), total nitrogen (TN), nitrogen isotopic composition ($\delta^{15}\text{N}$, ‰air), chlorin concentrations (mg g^{-1} TOC), chlorin index (CI), the C/N ratio and the TOC isotopic composition ($\delta^{13}\text{C}_{\text{TOC}}$, ‰VPDB).

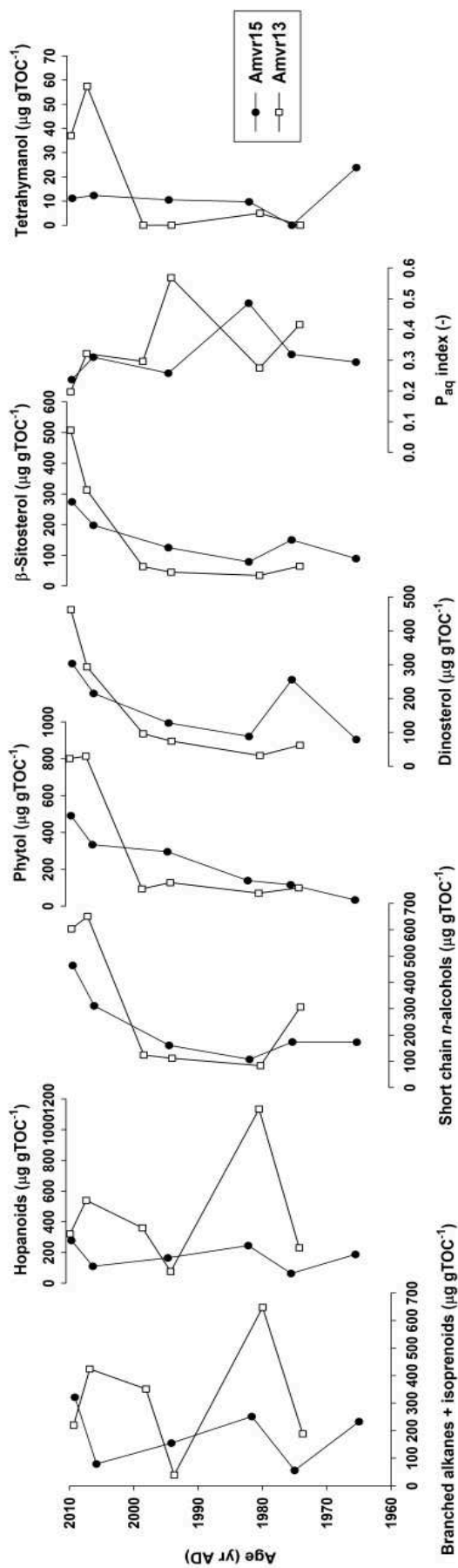


Fig. 5.6. Concentrations ($\mu\text{g g}^{-1}$ TOC) of the sums of branched alkanes/isoprenoids, hopanoids, short chain n -alcohols (C_{11} - C_{20}), phytol, dinosterol, β -sitosterol, P_{aq} index (by Ficken et al., 2000) and tetrahymanol plotted vs. age (yr AD).

The concentrations of branched alkanes, isoprenoids and hopanoids (Fig. 5.6) were highest in 28-29 cm (1974-1975) and in the upper 10 cm (since about 1998). In contrast, they were lowest in 12-14 cm (1993-1995) (Fig. 5.6). Short chain *n*-alcohols, phytol, dinosterol (4,23,24-trimethylcholest-22E-en-3 β -ol, 4-Me30 Δ 22), β -sitosterol (24-ethylcholest-7-en-3 β -ol, C_{29:1} Δ 7) and tetrahymanol increased towards the surface sediment (Fig. 5.6). The P_{aq} proxy is an indicator of macrophytes (Ficken et al., 2000) and ranged between 0.2 and 0.6 in both cores (Fig. 5.6). After hydrogenation, traces of isorenieratane and chlorobactane were found. Only in the lowermost sample of this core chlorobactane could not be detected. Lycopane concentrations and the (lycopane + C₃₅ *n*-alkane) / C₃₁ *n*-alkane ratio increased with depth (Fig. 5.7). The alkenone-based UK'₃₇ index (Me C_{37:2}/[Me C_{37:2}+Me C_{37:3}]; by Prahl and Wakeham, 1987) increased from 0.63 to 0.78 at the sediment surface (Fig. 5.8).

In core Amvr15, the TOC increased from 1.4 in the lowermost part to 6.1 wt% in the surface sediment (Fig. 5.5). TN and $\delta^{15}\text{N}$ values also increased (Fig. 5.5). Chlorin concentrations remained constant throughout the core with about 0.5 mg g⁻¹ TOC (Fig. 5.5). The CI decreased towards the top of the core (Fig. 5.5). The C/N ratio was ≥ 10 , but below 20 cm (before 1977) C/N values ranged between 6 and 23 (Fig. 5.5). $\delta^{13}\text{C}_{\text{TOC}}$ values ranged between -19 to -18‰ throughout the core.

The concentrations of branched alkanes, isoprenoids and hopanoids were relatively constant throughout core Amvr15 (Fig. 5.6). Short chain *n*-alcohols, phytol, dinosterol and β -sitosterol increased quite continuously towards the surface sediment (Fig. 5.6). The P_{aq} proxy is an indicator of macrophytes (Ficken et al., 2000) and ranged between 0.2 and 0.6 in both cores (Fig. 5.6). After hydrogenation, traces of isorenieratane and chlorobactane were found throughout the core.

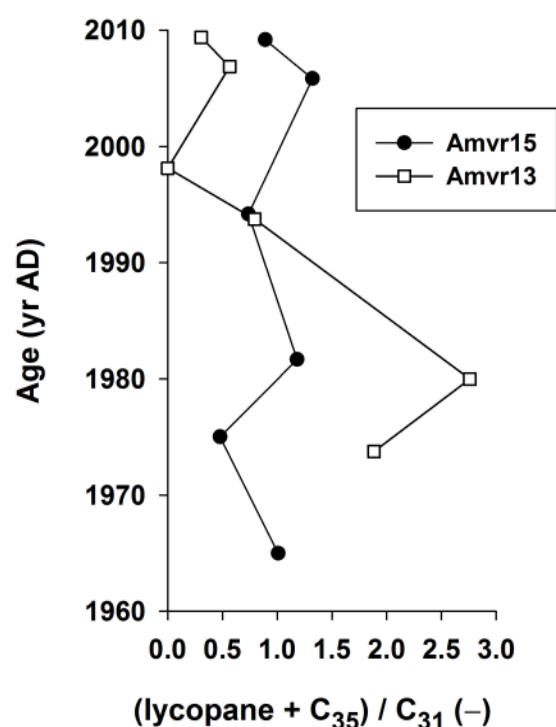


Fig. 5.7. Profiles of (lycopane + C₃₅ *n*-alkane) / C₃₁ *n*-alkane ratio vs. age (yr AD).

Tetrahymanol and lycopane concentrations and the (lycopane + C₃₅ *n*-alkane) / C₃₁ *n*-alkane ratio remained constant in core Amvr15 (Fig. 5.6, 5.7). The alkenone-based UK'₃₇ index (Me C_{37:2}/[Me C_{37:2}+Me C_{37:3}]; by Prahl and Wakeham, 1987) increased towards the surface sediment from 0.61 to 0.84 (Fig. 5.8).

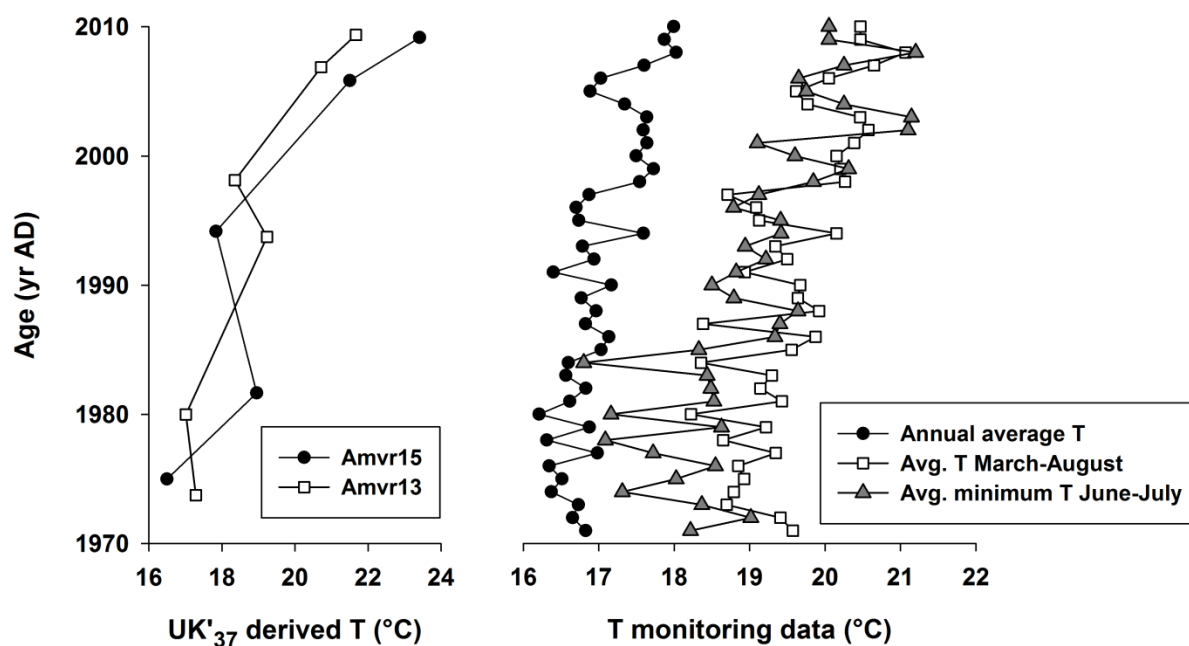


Fig. 5.8. UK'₃₇ index-derived surface water temperatures (left) according to the correlation of Müller et al. (1998), $UK'_{37} = 0.033 T + 0.069$ ($R^2=0.981$) with T = mean annual sea surface temperature, plotted vs. age (yr AD). For comparison, air temperature data (°C) between 1970 and 2010 from the meteorological station Preveza (Aktio) were added (data from the Hellenic National Meteorological Service and <http://www.weatheronline.co.uk>): Annual average air temperatures, average air temperatures of March-August, average minimum air temperatures of June-July.

5.5 Discussion

5.5.1 Benthic foraminifera abundance

In core Amvr15, epifauna species dominated the benthic assemblages between 20 and 42 cm (1940-1977) (Fig. 5.3) suggesting adequate oxygen levels of the bottom water (Murray, 2006). The increased participation of diverse *Quinqueloculina spp*, *Rosalina spp*, *Cibicides spp*. together with *Planorbulina mediterranensis* and other epifauna species may also be attributed to the presence of seagrass meadows colonized locally on the coring site (Murray, 2001; Mateu-Vicens et al., 2010). Furthermore, the presence of *Cibicides spp* could also be related to the hydrodynamic regime at the coring site since high abundances of these taxa are related to high current velocities (Szarek et al., 2006). Infaunal species showed increased abundances in the upper 20 cm (since ca. 1977) indicating reduced oxygen levels in the bottom water (Murray, 2006). In this interval *Bulimina aculeata* dominated the benthic assemblages with up to 40% of the total association (Fig. 5.3). This taxon occurs predominantly surficial and reacts quickly to labile OM supply (Mojtahid et al., 2010).

In core Amvr13 the higher abundance of shallow and deep infaunal species indicated less favourable oxygenated conditions in relation to those of core Amvr15. All the dominant species in the benthic foraminiferal assemblages of this core (*Bulimina elongata*, *Bulimina aculeata*, *Bolivina dilatata*, *Bolivina spathulata*, *Hopkinsina pacifica*, *Ammonia tepida*, *Nonionella turgida* and *N. bradii*) have been reported as common in shelf environments, associated with high contents of OM, and being stress-tolerant taxa (Jorissen, 1987; Barmawidjaja et al., 1995; van der Zwaan, 2000; Mendes et al., 2004; Murray, 2006).

5.5.2 Benthic foraminifera clusters

Cluster analysis (R-mode) revealed four clusters (Fig. 5.9). Cluster I was composed of *Bulimina elongata*, *Nonionella turgida*, *Textularia agglutinans* and *Ammonia tepida* (Fig. 5.9). In many studies *Nonionella turgida* appears as the most tolerant species to oxygen

depletion and its increase in abundance is associated with enhanced OM supply (Sen Gupta and Machain-Castillo, 1993; Blackwelder et al., 1996), usually of terrestrial origin (Mojtahid et al., 2010; Goineau et al., 2011). *Ammonia tepida* is considered as a species that is tolerant to large environmental variations (Almogi-Labin et al., 1992; Debenay and Guillou, 2002), including hypoxia (Blackwelder et al., 1996) and anthropogenic pollution (Debenay et al., 2005). *Bulimina elongata* is associated with food-enriched sediments related to river plumes (Guadiana River, Iberia; Mendes et al., 2004), closed embayment regimes (Yugoslavia; Murray, 2001) and fish farming products (Croatia; Vidović et al., 2009). *Textularia agglutinans* is an opportunistic species and exhibits a preference for food-enriched conditions and a tolerance to oxygen deficiency (Barmawidjaja et al., 1995). Furthermore, *Nonionella turgida* (as *N. opima*) and *Textularia agglutinans* are major species correlated with a high OM content in areas influenced by the Po River to the Adriatic Sea (Jorissen, 1987; Murray, 2001).

Cluster II was composed of *Hopkinsina pacifica*, *Bolivina dilatata* and *Bolivina spathulata* (Fig. 5.9). All these species are known to occur in benthic assemblages of oxygen-poor and organic rich environments (Sen Gupta and Machain-Castillo, 1993; Mendes et al., 2004; Murray, 2006). However, their low degree of opportunism (Barmawidjaja et al., 1995) in combination with their presence in areas of a river-influenced outer shelf (*Bolivina spp.*; Goineau et al., 2011) and of well-oxygenated substrates (Hyams-Kaphzan et al., 2009) suggests that Cluster II should represent benthic foraminiferal associations in lower stress environments than these of Cluster I.

Cluster III was composed of *Quinqueloculina spp.*, *Miliolinella spp.*, other porcelaneous species, *Textularia conica* and *Planorbulina mediterranensis* (Fig. 5.9). High abundances of *Quinqueloculina spp.* and in general Miliolids were found in oligotrophic environments and at sufficient bottom water oxygen concentrations (Blackwelder et al., 1996; Murray, 2006; Hyams-Kaphzan et al., 2009). Furthermore, the reduction in abundance of both porcelaneous and agglutinated groups of benthic foraminifera was used to trace palaeo-hypoxic evolution (Platon et al., 2005).

Cluster IV was composed of *Cassidulina spp.*, *Nonion spp.*, *Cibicides spp.*, *Rosalina spp.*, *Bulimina aculeata* and *Ammonia beccarii* (Fig. 5.9). Species belonging to the genera of

Cibicides, *Rosalina*, *Nonion* and *Ammonia* are known as epiphytic in the Mediterranean Sea (Murray, 2001; Mateu-Vicens et al., 2010). However, *Bulimina aculeata* (Goineau et al., 2011) and *Ammonia beccarii* (Debenay et al., 2005) have been reported in high abundances on the seaward part of shelves with high OM supply. A similar trend exhibited species belonging to the genera of *Cibicides* and *Rosalina*, which have been reported in high abundances seaward on shelves under the influence of aquaculture products (Croatia; Vidović et al., 2009).

The downcore fluctuations in the abundance of the benthic species of Cluster I compared to the upper core could be used to trace high OM supply and oxygen depletion. Cluster II would represent similar environments, but under lower stress conditions. The abundances of the benthic foraminifera species of Cluster III could be used to trace environments of well-oxygenated conditions and those of Cluster IV of similar environments, but most likely influenced by higher marine OM input and/or seagrass development.

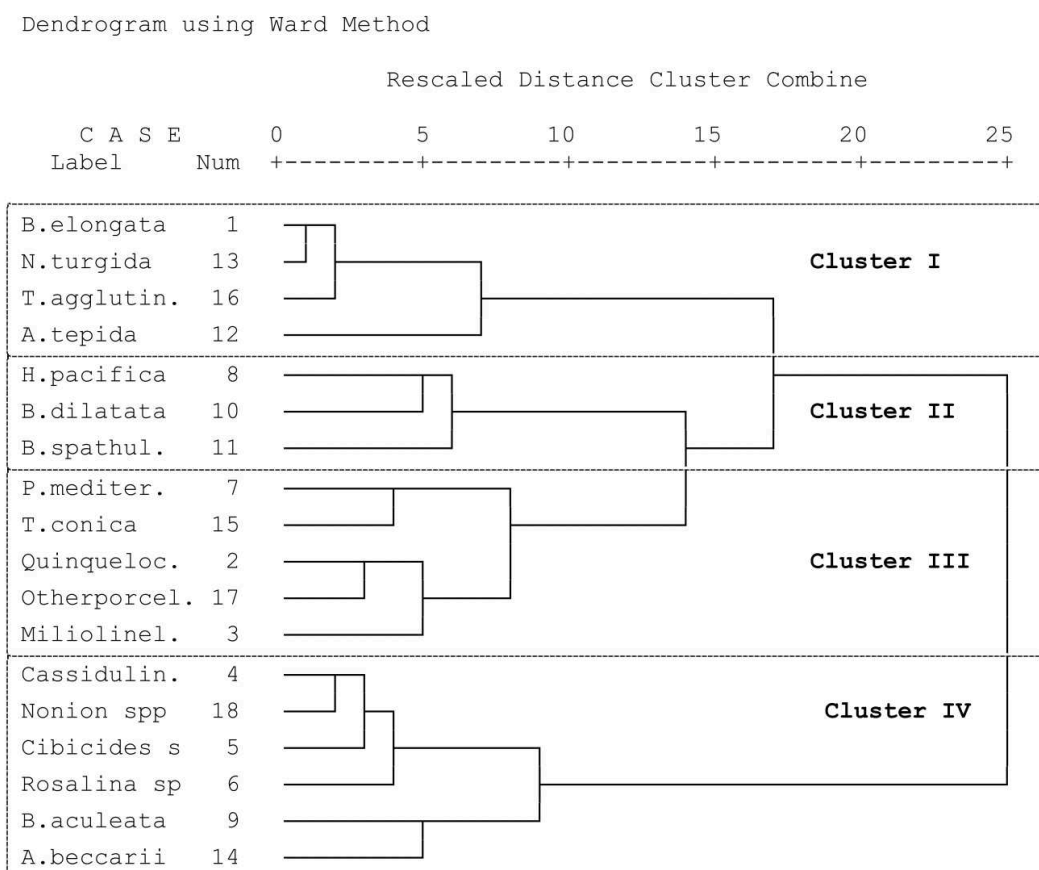


Fig. 5.9. R-mode cluster analysis for the entire dataset of the two cores.

5.5.3 Eutrophication, productivity and OM sources

The TOC increased in both cores with time (Fig. 5.5), which explains the darker colour in the top part of the core. This can be explained by an increased productivity and a higher OM supply recently, which is also supported by the increase in TN values in both cores (Fig. 5.5). On the other hand the decrease of TOC and TN with depth could also be the result of progressive remineralisation within the sediment. However, the higher abundance of foraminiferal species belonging to Cluster I in core Amvr13 and Cluster IV species in core Amvr15 suggests a larger OM input (Fig. 5.10) (Sen Gupta and Machain-Castillo, 1993; Blackwelder et al., 1996; Debenay et al., 2005; Goineau et al., 2011). Also other processes like oxygen availability or degree of opportunism can affect the abundance of these species (Sen Gupta and Machain-Castillo, 1993; Barmawidjaja et al., 1995; Murray, 2006), which might explain that species belonging to Cluster II did not increase. Many biomarkers also traced an enhanced productivity with time, for instance by the increase in short chain *n*-alcohols, phytol and dinosterol towards the uppermost sediment in both cores (Fig. 5.6). These markers indicated an increased abundance of primary producers (Meyers and Ishiwatari, 1993; Rontani and Volkman, 2003; Volkman, 2003). Dinosterol is of diatom origin in Amvrakikos Gulf, because C_{22:6} FA, which would hint to dinoflagellates as the source organisms (Withers, 1983; Volkman, 2003), is absent. The higher productivity is a direct result of progressive eutrophication in the gulf, as suggested by increasing $\delta^{15}\text{N}$ values, which have been used to reconstruct sewage supply and eutrophication in other settings (Cole et al., 2004; Wu et al., 2006). The higher chlorin concentrations in core Amvr13 within the most recent decade (Fig. 5.5) agree with this explanation. In contrast, the constant chlorin levels throughout core Amvr15 indicated that productivity hardly changed at this site.

The C/N ratio below 10 (Fig. 5.5) indicated that the OM in core Amvr13 mainly originated from algal sources, in agreement with observations in other settings (Meyers and Ishiwatari, 1993). In contrast, the higher C/N ratios in core Amvr15 suggested significant supply of terrestrial vascular plant-derived OM sources (Fig. 5.5). The constant $\delta^{13}\text{C}_{\text{TOC}}$ values throughout both cores indicated that the OM source remained constant during the last decades. The $\delta^{13}\text{C}_{\text{TOC}}$ values in Amvr15 (average: -18.6‰; Fig. 5.5) are typical of marine OM, whereas terrigenous OM sources average at -26‰ (Sackett, 1964; Jasper and Gagosian,

1990). The lower $\delta^{13}\text{C}_{\text{TOC}}$ values in Amvr13 (average: -22.6‰; Fig. 5.5) might indicate mixed marine and terrigenous sources, but this explanation disagrees with the low C/N values (Fig. 5.5), which are characteristic of a predominantly marine OM origin (Meyers and Ishiwatari, 1993). Therefore, the lower $\delta^{13}\text{C}_{\text{TOC}}$ values in Amvr13 were more likely the result of mixing and uptake of dissolved inorganic carbon derived from OM degradation, which can lead to isotopic shifts towards depleted values in eutrophic systems (van Breugel et al., 2006). This would mean that Amvrakikos Gulf is not in equilibrium with the atmosphere. Therefore, complicating factors that can affect the $\delta^{13}\text{C}_{\text{TOC}}$ like the Suess effect (McCarroll and Loader, 2004; Meyers, 2006) are expected to be of minor importance in Amvrakikos Gulf.

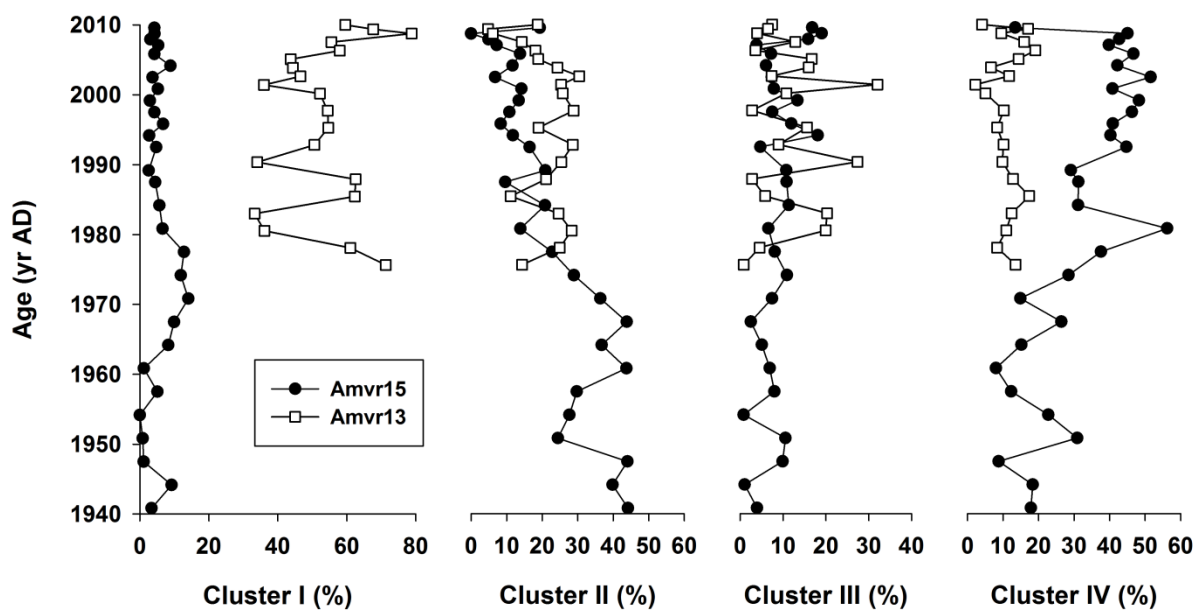


Fig. 5.10. Downcore variations of the sum abundances of the benthic foraminifera clusters (I-IV) in cores Amvr13 and Amvr15 vs. age (yr AD).

The relatively enriched $\delta^{13}\text{C}_{\text{TOC}}$ values in core Amvr15 most likely resulted from additional OM input by seagrass meadows, which were present at this sampling location. In the western Mediterranean Sea, it was shown that the presence of seagrass meadows led to an overprint of the OM in the sediment (Papadimitriou et al., 2005). $\delta^{13}\text{C}_{\text{TOC}}$ values were enriched at sites with seagrass meadows compared to sites with predominantly phytoplankton derived OM

sources by 4-6‰, which is well within the observed offset between cores Amvr15 and Amvr13. Furthermore, seagrass meadows can lead to 2-3‰ depleted $\delta^{15}\text{N}$ values (Papadimitriou et al., 2005), which would also explain lower $\delta^{15}\text{N}$ values in Amvr15.

β -Sitosterol is the major sterol of emerged macrophytes (Volkman, 1986). Therefore, seagrass might be a main source of this marker at least in Amvr15 (Fig. 5.6). The high P_{aq} index above 0.2 in both cores (Fig. 5.6) traced the predominance of mid-chain over long chain *n*-alkanes (Ficken et al., 2000), which indicated that macrophytes are predominant lipid sources compared to higher land plant sources.

The disagreement between constant chlorin concentrations and the increase of many lipid biomarkers in Amvr15 (for instance short chain *n*-alcohols, phytol, dinosterol, β -sitosterol; Fig. 5.5, 5.6) indicated that degradation also affected the biomarker profiles. The CI is an estimate of the OM freshness (Schubert et al., 2005). CI values obtained in the gulf sediment indicated a lower degree of degradation in the uppermost part of both cores (Fig. 5.5). The CI values were higher in core Amvr13 (Fig. 5.5), indicating higher degradation rates at this location. These results suggest that the increase in concentration of many biomarkers (for instance short chain *n*-alcohols, phytol, dinosterol, β -sitosterol; Fig. 5.6) is also affected by degradation. In agreement with the constant chlorin concentrations in Amvr15 (Fig. 5.5), the slight biomarker concentration decrease in this core might be due to degradation. But the much higher increase in biomarker concentrations in Amvr13 (for instance short chain *n*-alcohols, phytol, dinosterol, β -sitosterol; Fig. 5.6) must be mainly due to a higher productivity, which is supported by the increase in chlorin concentrations in this core (Fig. 5.5).

5.5.4 Impact of eutrophication on benthic foraminifera and bacteria – Hypoxia reconstructions in the gulf

The increase in population of benthic foraminiferal assemblages was associated with a decreasing diversity as depicted by the high negative correlation between the H(s) and the benthic productivity indices (Pearson coefficient $r=-0.71$, $p<0.01$) for the entire dataset of the cores. This is in contrast to the usual trend of microfauna, which appeared less diverse and

less abundant in stressful, fluctuating environments (Blackwelder et al., 1996). However, the sediments of the gulf are under the influence of fish farming and urban waste. Eutrophication can lead to an increase in benthic foraminifera density (Angel et al., 2000) in conjunction with a decrease of diversity where the opportunistic species are dominant (Debenay et al., 2005). Therefore, the summed abundances of the benthic species of Clusters I and II showed high positive correlation with the benthic productivity index (Pearson coefficient $r=0.83$, $p<0.01$) and high negative correlation with the diversity index ($r=-0.87$, $p<0.01$) for the entire dataset. The opposite trend represents the summed abundances of the benthic species of Clusters III and IV, which showed high positive correlation with the diversity index (Pearson coefficient $r=0.72$, $p<0.01$) and negative correlation with the benthic productivity index ($r=-0.74$, $p<0.01$) for the entire dataset.

The benthic foraminifera in core Amvr13 represent low diversity, but high abundance assemblages (Fig. 5.10). The coring site of core Amvr13 is under the influence of large OM supply and stratified water masses promoting the development of low oxygen bottom water. This bottom-water environment is suggested by the dominance of species of Cluster I and II compared to those of Cluster III and IV. Furthermore, fluctuations in the abundances of the four clusters in conjunction with fluctuations in the benthic abundance and diversity index indicate fluctuating sea bottom environmental changes for the last 35 years. The development of more unfavourable benthic environments occurred at around 1985-1988, 1994-1997 and after 2000, as shown by the decreasing abundances of species belonging to Cluster III, whereas the number of species of Cluster I increased (Fig. 5.10).

Branched alkanes, isoprenoids and hopanoids are bacterial biomarkers (Rohmer et al., 1984; Summons et al., 2007). These compounds indicated a higher bacterial biomass around 1980 and since the end of the 1990s in core Amvr13 (Fig. 5.6). The profiles of these markers were especially similar to *Bulimina aculeata* (Fig. 5.3), which is indicative of a higher supply of OM and severe oxygen depletion. These results suggest that the higher supply of OM has led to increased OM mineralisation and oxygen consumption rates. These developments might be related to aquacultures, which started around 1980 and excessively supplied nutrients and OM to the gulf (Ferentinos et al., 2010; Kountoura and Zacharias, 2011). Furthermore, mass mortality events of fish and reduction of fish populations in aquaculture rafts were observed between 1988 and 1997 (Ferentinos et al., 2010).

The most stressful conditions started at around 2000, as recorded by a gradual increase in the abundance of species of Cluster I together with decreasing abundances of Cluster III species. These conditions peaked with the almost absence of species that belong to Cluster III in 2008 at the time of the recently recorded seasonal hypoxic event in the gulf. However, the rapid increase of Cluster III species and the H(s) index shortly after the event suggests a fast recovery of the benthic environment (Fig. 5.10). These conditions starting at around 2000 and peaking in 2008 were already indicated by higher concentrations of bacterial biomarkers since the mid/late 1990s (Fig. 5.6). These increased concentrations were in good agreement with the intensified productivity (section 5.5.3) and the resulting higher OM supply to the sediment, which had the same implications as during the 1980s.

In contrast, the constant abundance of chlorins and lower concentrations of bacterial markers throughout core Amvr15 indicated less severe conditions than at site Amvr13 without significant changes in productivity and OM supply (Fig. 5.5, 5.6). Benthic assemblages at site Amvr15 appeared to be less productive and more diversified than those of core Amvr13. The dominance of species belonging to Cluster III and IV (Fig. 5.10) suggested lower OM supply, hence, higher sea floor oxygenation. This can be attributed to the location of site Amvr15 at the entrance of the gulf characterized by sufficient oxygen supply due to the water replenishment from the Ionian Sea (Ferentinos et al., 2010). Tziavos and Vouloumanos (1994) also reported a reduction of the benthic diversity eastwards in the surface sediments of the gulf. The observation of seagrass meadows at site Amvr15 and their absence at site Amvr13 further supports the lower impact of eutrophication (Green and Short, 2003).

More opportunistic species of Cluster IV replaced Cluster III species at site Amvr15 during times of nutrient enrichment and oxygen depletion (Fig. 5.10). This was especially the case between 1976 and 1980, the time interval when aquaculture development started. However, the reduction of species of both Clusters III and IV at 1985-1987 and 1995-1997 (Fig. 5.10) and a higher bacterial biomass around 1980 (Fig. 5.6) coincided with relative changes at site Amvr13, which suggested similar control mechanisms and time synchronicity in the bottom water oxygen regime between the two coring sites. Furthermore, similar to site Amvr13, the most severe sea floor conditions with respect to oxygen at site Amvr15 appeared in 2008 as suggested by the almost absence of species belonging to Cluster III and a higher bacterial biomass around that time (Fig. 5.6, 5.10). This indicates that the effects of that hypoxic event

did not only influence the benthic fauna of the inner part of the gulf, but were also spread in areas which are considered as throughout the year being well oxygenated. However, the impact of hypoxia on the benthic microfauna at the bottom of the gulf entrance was less intense than that occurred in the inner part of the gulf, since species considered being sensitive to hypoxia (Cluster IV) were still highly abundant (Fig. 5.10) and seagrass meadows were also present at this site.

Furthermore, the more severe oxygen depletion at Amvr13 compared to Amvr15 was also indicated by the increase of the (lycopane + C₃₅ *n*-alkane) / C₃₁ *n*-alkane ratio with depth (Fig. 5.7). Although the source of lycopane is unknown, it has been used to reconstruct palaeo-redox conditions in the bottom water in marine settings (Wakeham et al., 1993; Sinninghe Damsté et al., 2003). In contrast, the quite constant ratio in core Amvr15 (Fig. 5.7) suggested enhanced oxygen concentrations.

Isorenieratane and chlorobactane are tracers for phototrophic sulfur bacteria (Chlorobiaceae) and hence phototrophic zone euxinia and anoxia (Brocks and Summons, 2003). The observation of these carotenoids throughout both cores indicated regularly occurring developments of anoxic and euxinic conditions reaching into the photic zone at both sites. The monitoring data showed that oxygen depletion has occurred seasonally during summer and fall in the western part of the gulf (Ferentinis et al., 2010; Kountoura and Zacharias, 2011). Due to the low concentrations of these pigments in the sediment of both cores, only the existence of photic zone anoxia but no temporal changes could be reconstructed.

5.5.5 Impact of climate on stratification and oxygen replenishment

Stratification is another key factor in the oxygen budget of the gulf water column, because oxygen is resupplied by mixing. A repeatedly used indicator for stratification, stagnation and/or salinity is tetrahymanol, which is found in bacteriovoric ciliates (Sinninghe Damsté et al., 1995; Thiel et al., 1997; Bechtel and Schubert, 2009). The relatively constant tetrahymanol concentrations in core Amvr15 (Fig. 5.6) suggested that stratification did not change since the 1970s. In contrast, the increase of tetrahymanol in the uppermost part of core Amvr13 (Fig. 5.6) clearly showed a higher stratification and stagnation, probably due to

higher water temperatures and/or salinities in the gulf. To prove these relationships, sedimentary proxies were compared with monitoring data.

The UK'₃₇ index ($\text{Me C}_{37:2}/[\text{Me C}_{37:2}+\text{Me C}_{37:3}]$; by Prahl and Wakeham, 1987) is an alkenone-based proxy, which is highly correlated with mean annual sea surface temperatures (Prahl et al., 1988; Müller et al., 1998). Alkenones are specific for haptophyte algae (Herbert, 2003). The temperature calibration of Prahl et al. (1988) yielded values between 16.9 and 23.6°C and between 17.4 and 21.9°C in cores Amvr15 and Amvr13, respectively. For comparison, the temperature calibration by Müller et al. (1998), which is based on sediment core top samples worldwide, yielded very similar results (16.5-23.4°C in core Amvr15 and 17.0-21.7°C in Amvr13; Fig. 5.8). The difference between estimated surface water temperatures using both calibrations was only up to 0.4°C.

The temperature estimates from both cores indicated a trend with increased surface water temperatures, which matched well with increasing air temperatures observed at the Preveza (Aktio) weather station during the last decades (Fig. 5.8). The UK'₃₇-derived surface water temperatures in both cores (16.5-23.4°C, 1974-2010; Fig. 5.8) were within the range of monitored average annual minimum and maximum air temperatures with values between about 12 and 22°C (1970-2010), except the uppermost part of core Amvr15 with larger UK'₃₇ temperature estimates. The annual average air temperatures ranged between 16.2 and 18.0°C (1970-2010), and were lower than estimated UK'₃₇ temperatures (Fig. 5.8). Although the timing of blooms of the source organisms is unknown for Amvrakikos Gulf, the best agreement between UK'₃₇-derived and monitored temperatures was obtained by using the average temperature of March until August. The air temperatures ranged from 18.2 to 21.1°C (1970-2010; Fig. 5.8; data from the Hellenic National Meteorological Service and <http://www.weatheronline.co.uk>). The monitoring data showed that especially the annual minimum temperatures increased during the last decades, whereas the annual maximum temperatures hardly increased. By using only monthly average minimum temperature data, the best fit was obtained with the average minimum temperature data of June and July with a range of 16.8-21.2°C (Fig. 5.8). These results indicated that alkenones might have captured the lowermost surface water temperatures during June and July. In contrast, this and other calibrations showed strong correlations either with annual average temperatures or seasonal average temperatures at times of blooms (Prahl et al., 1988; Müller et al., 1998; Herbert,

2003). Therefore, a shift of the time of blooms from spring towards summer is more likely, which would also explain the large increase in estimated temperatures during the last decades.

Nonetheless, the warming trend of UK₃₇-derived temperatures together with the monitoring data indicated that the surface water temperatures in Amvrakikos Gulf increased during the last decades. Previous studies showed that steep temperature gradients separate surface and bottom waters (Ferentinos et al., 2010). Higher temperatures in the surface water may further increase these differences, which can explain the observation of a higher stratification during the last years.

Furthermore, also salinity controls stratification by steep salinity gradients in the water column due to the inflow of high salinity water masses through the Preveza Strait from the Ionian Sea and brackish water outflow (Ferentinos et al., 2010). This circulation pattern is similar to the Black Sea; however, the reduced outflow of the Black Sea prevents the reduction of its permanent stratification (Ozsoy and Unluata, 1997; Murray et al., 2007), which is not the case for Amvrakikos Gulf (Ferentinos et al., 2010). However, the similar developments regarding circulation patterns, eutrophication and temperature have led to a strong decrease in oxygen concentrations, which resulted in mass mortality events and ecosystem collapse in both settings (Lancelot et al., 2002; Mee et al., 2005; Ferentinos et al., 2010; Kountoura and Zacharias, 2011).

5.6 Conclusions

The analysis of benthic foraminifera and lipid biomarkers revealed that Amvrakikos Gulf exhibited dramatic environmental changes due to eutrophication during the last decades. The higher productivity and OM supply to the sediment (higher concentrations of chlorins, TOC, TN and $\delta^{15}\text{N}$ values) led to a higher abundance of tolerant and opportunistic benthic species and bacteria, whereas the benthic species density decreased. Especially the increased abundance of species from Cluster I (*Bulimina elongata*, *Nonionella turgida*, *Textularia agglutinans*, *Ammonia tepida*) together with a decreasing abundance of Cluster III species (*Quinqueloculina* spp, *Miliolinella* spp, other porcelaneous, *Textularia conica*, *Planorbulina*

mediterraneensis) indicated more severe OM supply and oxygen depletion in 1976, 1980, 1985-1987, 1995-1997, 2000 and 2008. Cluster III and IV species (Cluster IV: *Cassidulina* spp., *Nonion* spp., *Cibicides* spp, *Rosalina* spp, *Bulimina aculeata*, *Ammonia beccarii*) rapidly recovered after environmental disturbances. In core Amvr15 the benthic assemblages appeared to be less productive and more diversified with a dominance of species of Clusters III and IV under conditions of lower OM supply and higher bottom water oxygen concentrations than in core Amvr13. The presence of seagrass at site Amvr15 largely influenced the values of $\delta^{13}\text{C}_{\text{TOC}}$, C/N ratio and mid-chain *n*-alkanes. Nonetheless, the presence of isorenieratane and chlorobactane in both cores traced temporarily euxinic conditions in the photic zone throughout the gulf. The increasing air temperatures have led to stronger stratification and hence oxygen depletion during the last decade.

5.7 Acknowledgements

This study was funded by the European Union project “Hypox – In situ monitoring of oxygen depletion in hypoxic ecosystems of coastal and open seas and land-locked water bodies“ (EC grant 226213). Karl Schubert is thanked for support during sampling. Marie-Eve Randlett (Eawag) is thanked for help with the analysis and data interpretation of alkenones. The article benefitted substantially from the critical review of H. Filipsson and an anonymous reviewer.

Chapter 6: Conclusions and Outlook

This thesis provides a contribution to the interpretation of organic and inorganic proxies in respect to palaeoxygen reconstructions. As a major improvement, the manganese to iron ratio (Mn/Fe ratio) could be used to reconstruct bottom water oxygen concentrations in the Swiss Lake Zurich. Furthermore, the previous chapters have emphasised the use of lipid biomarkers and trace metals to reconstruct eutrophication and microbial community changes, to distinguish between aquatic and terrigenous OM sources and to characterise chlorophyll/chlorin degradation. In the following, the most important achievements of this thesis are presented.

Oxygen reconstructions

The major aim of this thesis was to reconstruct relative and absolute changes of oxygen with lipid biomarker and trace metal proxies in the sediments of selected Swiss lakes and the Black Sea. The pigment isorenieratane and Me,*n*-Pr and Me,*i*-Bu maleimides were robust indicators for the presence of Chlorobiaceae and therefore photic zone euxinia and anoxia in Rotsee and the Black Sea. Similarly, okenone evidenced that Chromatiaceae have occurred in the Rotsee chemocline, also tracing oxygen depletion in the photic zone. Relative changes of these markers in the sediment of Rotsee were clearly related to community shifts between Chlorobiaceae and Chromatiaceae rather than changes in oxygen concentrations. Oxygen depletion is strongly coupled to eutrophication, in the way that increased productivity results in higher mineralisation rates and microbial oxygen consumption. This process can also lead to a higher abundance of methanogenic archaea and increased methane production. The increase of tetrahymanol indicated that lake stratification increased during eutrophication, which reduced mixing and oxygen replenishment of the hypolimnion. Although a major limitation of biomarker proxies is their dependence on additional factors, such as production/preservation and community changes of their source organisms, lipid biomarkers can be useful indicators for interpretations of relative oxygen depletion.

The manganese to iron ratio (Mn/Fe ratio) was used to reconstruct maximum bottom water oxygen reconstructions in Lake Zurich. This achievement was possible due to the precise age model, the high resolution XRF core scanning and long-term monthly oxygen monitoring data since 1936. On this basis, the proxy could be calibrated and used for semi-quantitative reconstructions of bottom water oxygenation back until 1895 in the deepest core. However, it has to be kept in mind that geochemical and sediment focusing, but also sedimentological factors can limit the applicability of this proxy for quantitative estimates of water column oxygen levels.

Eutrophication, remediation measures and the reconstruction of changes of microbial and foraminifera communities

Lipid biomarkers can be used to reconstruct eutrophication and relative changes of productivity and microbial communities. The high resolution sedimentary biomarker record was used to study short-term changes of environmental parameters and microbial biomass in Rotsee. Rotsee was an ideal site to study an anthropogenically altered ecosystem, in order to examine the causes, processes and effects of eutrophication. The strong sewage supply since the 1850s led to two productivity events in the time intervals 1918-1921 and 1958-1972. The former event caused a radiation of primary producers (especially diatoms) and methanogens, whereas in the latter event especially primary producers, bacteria and macrophytes increased. The construction of a mechanical sewage treatment plant might be the reason for enhanced bacterial biomass in 1933. Therefore, both eutrophication and historical remediation measures strongly affected many microbial groups, which reacted with abundance and/or community shifts to changed environmental conditions. The supply of fossil OM and/or petroleum contamination ended with the constructions of an interceptor sewer and a mechanical treatment plant in 1969 and 1974, respectively. These measures resulted in a progressively lower productivity due to reduced nutrient supply. Apart from the reconstruction of environmental changes and developments in the lake, it was observed that the diatom *Stephanodiscus parvus* was the dominant source of dinosterol and 24-methylcholesterol. In contrast, *Cyclotella radiosa* and *Asterionella formosa* were the predominant source organisms of C_{18:2(9,12)}, C_{18:3(5,9,12)} and C_{20:5(5,8,11,14,17)} FAs. The abundance of methanogenic archaea

could be traced with GDGT-0 during the last 150 years in Rotsee ($0.5\text{--}1.8 \times 10^9$ cells g⁻¹ dry sediment).

Amvrakikos Gulf has been strongly affected since the 1970s by eutrophication due to extensive agriculture, aquaculture and urban development, the construction of two dams, which control the run-off of the Arachthos River, and the establishment of oil stations along the southern border of the gulf. As a result, the system changed to a fluctuating and increasingly stressful environment, which suffers from oxygen depletion and have led episodically to massive fish mortality events. Also in Amvrakikos Gulf, the productivity increased, together with a higher bacterial biomass. Benthic foraminifera assemblages in the Gulf shifted towards opportunistic and tolerant species, whereas the species density decreased. The pigments isorenieratane, chlorobactane and lycopane traced photic zone euxinic and anoxic conditions throughout the gulf. The increase in surface water temperatures and eutrophication led to a reduction in water column mixing and oxygen replenishment to deeper waters.

Aquatic vs. terrigenous OM – BIT_{CH} index

It has been an important issue in organic geochemistry to reveal the different contributions of OM from in-lake production (aquatic sources) and OM originating from the catchment (terrigenous sources). The study of OM sources in Rotsee indicated by TOC/N values, distributions of FAs, *n*-alkanes and *n*-alcohols showed that the organic material is mainly of autochthonous origin. However, the distributions of these lipid groups and the observation of lupeol, β -amyrin and amyrenone suggest contributions from the catchment. The traditional branched and isoprenoid tetraether index (BIT index) indicated a predominance of allochthonous sources in Rotsee, which suggested that this index might be misleading. It was observed that crenarchaeol originates from the water column and/or the sediment, but might mainly be soil derived instead. This suggested that crenarchaeol cannot be used as the aquatic end member in this lake. Therefore, a novel BIT index was proposed (BIT_{CH}), which better estimates aquatic and terrigenous sources as the ratio of the sum of branched and isoprenoid glycerol dialkyl glycerol tetraethers (GDGTs). While this index decreased with time before about 1920, it remained constant afterwards. The same pattern was found for the relative

contents of iron, potassium and titanium. The covariance between the BIT_{CH} index and these trace metals indicated that branched GDGTs could be considered to be of terrigenous/catchment soil origin, despite the observation that the branched GDGTs are also produced partly in the water column (at least GDGT-III-a). The new index is most likely a tracer for the dilution of terrigenous material as a result of the higher in-lake OM production. The enhanced supply of aquatic OM resulted from eutrophication and related higher productivity, whereas the fluxes of terrigenous material may have remained constant over time. Therefore, the BIT_{CH} index might be a valuable proxy for estimating the relative contributions of aquatic and terrigenous OM in lakes.

OM degradation

It is an important prerequisite for reliable palaeoenvironmental reconstructions to understand the effects of degradation on lipid biomarker profiles. Therefore, the relative degree of degradation on labile OM was estimated with the chlorin index. However, this proxy lost its sensitivity already in about 50 year old Rotsee sediment, which suggests that this index is only applicable for relatively young sediments. In contrast, the novel maleimide based degradation indices proposed in this thesis were applicable for more than 100 years (Me,Me index) and for almost 1000 years (Me,Et index) in Rotsee. In contrast to Rotsee, in the Black Sea their application limit is ca. 7700 yr and 42 ka for the Me,Me and Me,Et indices, respectively. The new indices have improved the interpretability of sedimentary records regarding the degradation degree of labile OM, i.e. chlorophylls, within the sediment. Both maleimide indices might be universally applicable, but this must be further evaluated in other systems.

Perspectives for further research

This thesis gives new insights into the use of organic and inorganic proxies regarding the reconstruction of oxygen depletion, eutrophication, microbial community changes, the determination of OM origin and OM degradation. Possible future research topics could be:

- This thesis showed how biomarker proxies can trace relative changes of past oxygen in the water column. However, it was not possible to assess information on the amount of oxygen. This issue remains to be solved in the future.
- The development of the BIT_{CH} index is a new approach to distinguish between aquatic and terrigenous lipid sources. But there is still a need to prove the robustness of this indicator and other (maybe new) proxies, which might enable unambiguous determinations of the origin of lipids and/or OM.
- More work is needed to determine the origin of some maleimides, because the source pigments of some maleimides are unknown based on structural reasons. Further analysis might reveal transformation processes of chlorophylls and chlorins prior to maleimide formation. The novel maleimide indices need to be further applied to prove their potential for estimating relative OM degradation.
- The Mn/Fe ratio as a proxy for semi-quantitative reconstructions of past bottom water oxygenation in lakes needs to be further tested in other lakes and other aquatic settings. For this purpose, more details about short-term dynamics of Mn and Fe are necessary. Another problem to be solved is the clear separation between redox-sensitive and detrital sources of trace metals.

Acknowledgements

I would like to thank the advisors / referees of my dissertation, Carsten J. Schubert, Rolf Kipfer and Bernhard Wehrli (all Eawag) for their discussions, comments, suggestions and all their support during my PhD project.

Furthermore, I am grateful to Rienk Smittenberg (University of Stockholm, Sweden), Adrian Gilli and Francien Peterse (both ETH), Philippe Schaeffer and Pierre Adam (both University of Strasbourg, France) and Helge Niemann (University of Basel) for support with data interpretation, helpful discussions, ideas and suggestions that improved the work and outcome of this PhD. Additionally, I would like to thank Ryan North, Dörte Carstens, Marie-Eve Randlett, Yama Tomonaga and Prosper Zigah (all Eawag) for their help and support during my PhD. Regarding the study of Amvrakikos Gulf, I would like to thank Maria Geraga, George Papatheodorou George Ferentinos (all University of Patras, Greece) and Heleni Kaberi (Hellenic Centre for Marine Research, Anavyssos, Greece). Furthermore, I thank Emi Kirilova and Andy Lotter for diatom analysis in Rotsee sediment.

For field support, I would like to acknowledge Alois Zwyssig (Eawag), but also Ulrike van Raden and Stefanie Wirth (both ETH) for supporting me on Swiss lakes. For the work on the Black Sea, I am grateful to Jana Friedrich (Helmholtz Centre Geesthacht, Germany), but also to Marian-Trajan Gomoiu, Dan Secrieru, Sorin Balan, Remzi Bectas (all GeoEcoMar, Constanta, Romania) and the whole Mare Nigrum team for all their help during the cruises.

For help in the lab and on the analytical instruments, I appreciated the great support of Gijs Nobbe (Eawag). Gaby Schmitt and Celine Munsch (University of Strasbourg, France) are thanked for pigment analysis and support in the lab during my stay in Strasbourg.

Additionally, I would like to thank all the other colleagues at Eawag, which supported me during my PhD project in many different ways, especially to mention here David Livingstone, Flavio Anselmetti and Beat Müller (all Eawag).

I am grateful for funding by the European Union project “Hypox – In situ monitoring of oxygen depletion in hypoxic ecosystems of coastal and open seas and land-locked water

bodies“ (EC grant 226213). Additional funds came from the Eawag PhD mobility support grant, enabling me to spend two months at the University of Strasbourg.

Finally and most important, I would like to express my deepest gratitude to my family for their support during all of my life, which cannot be evaluated with any words.

Bibliography

- Adrian, R., O'Reilly, C.M., Zagarese, H., Baines, S.B., Hessen, D.O., Keller, W., Livingstone, D.M., Sommaruga, R., Straile, D., Van Donk, E., Weyhenmeyer, G.A., Winder, M., 2009. Lakes as sentinels of climate change. *Limnology and Oceanography* 54, 2283-2297.
- Airolidi, L., Beck, M.W., 2007. Loss, status and trends for coastal marine habitats of Europe. *Oceanography and marine biology: an annual review* 45, 345-405.
- Airs, R.L., Jie, C., Keely, B.J., 2000. A novel sedimentary chlorin: structural evidence for a chlorophyll origin for aetioporphyrins. *Organic Geochemistry* 31, 1253-1256.
- Almogi-Labin, A., Perelis-Grossovicz, L., Raab, M., 1992. Living ammonia from a hypersaline inland pool, Dead Sea area, Israel. *Journal of Foraminiferal Research* 22, 257-266.
- Anastasakis, G., Piper, D.J.W., Tziavos, C., 2007. Sedimentological response to neotectonics and sea-level change in a delta-fed, complex graben: Gulf of Amvrakikos, western Greece. *Marine Geology* 236, 27-44.
- Angel, D.L., Verghese, S., Lee, J.J., Saleh, A.M., Zuber, D., Lindell, D., Symons, A., 2000. Impact of a net cage fish farm on the distribution of benthic foraminifera in the Northern Gulf of Eilat (Aqaba, Red Sea). *Journal of Foraminiferal Research* 30, 54-65.
- Appleby, P.G., Oldfield, F., 1978. The calculation of lead-210 dates assuming a constant rate of supply of unsupported ^{210}Pb to the sediment. *Catena* 5, 1-8.
- Arthur, M.A., Dean, W.E., 1998. Organic-matter production and preservation and evolution of anoxia in the Holocene Black Sea. *Paleoceanography* 13, 395-411.
- Bachmann, H., 1931. Hydrobiologische Untersuchungen am Rotsee. *Aquatic Sciences* 5, 39-81.

- Baker, E.W., Louda, J.W., 1986. Porphyrin geochemistry of Atlantic Jurassic-Cretaceous black shales. *Organic Geochemistry* 10, 905-914.
- Bale, N.J., Airs, R.L., Llewellyn, C.A., 2011. Type I and Type II chlorophyll-a transformation products associated with algal senescence. *Organic Geochemistry* 42, 451-464.
- Baltenweck-Guyot, R., Ocampo, R., 2007. Identification of a novel 7-desmethyl-7-acetonyl bacteriopheophorbide c series in a recent sediment. *Organic Geochemistry* 38, 1580-1584.
- Barmawidjaja, D.M., van der Zwaan, G.J., Jorissen, F.J., Puskaric, S., 1995. 150 years of eutrophication in the northern Adriatic Sea - Evidence from a benthic foraminiferal record. *Marine Geology* 122, 367-384.
- Barwise, A.J.G., Roberts, I., 1984. Diagenetic and catagenetic pathways for porphyrins in sediments. *Organic Geochemistry* 6, 167-176.
- Battarbee, R.W., Jones, V.J., Flower, R.J., Cameron, N.G., Bennion, H., Carvalho, L., Juggins, S., 2002. Diatoms tracking environmental change using lake sediments. In: Smol, J.P., Birks, H.J.B., Last, W.M., Bradley, R.S., Alverson, K. (Eds.), *Developments in Paleoenvironmental Research*, Springer, The Netherlands, pp. 155-202.
- Bechtel, A., Schubert, C.J., 2009. A biogeochemical study of sediments from the eutrophic Lake Lugano and the oligotrophic Lake Brienz, Switzerland. *Organic Geochemistry* 40, 1100-1114.
- Bechtel, A., Smittenberg, R.H., Bernasconi, S.M., Schubert, C.J., 2010. Distribution of branched and isoprenoid tetraether lipids in an oligotrophic and a eutrophic Swiss lake: Insights into sources and GDGT-based proxies. *Organic Geochemistry* 41, 822-832.
- Behrens, A., Wilkes, H., Schaeffer, P., Clegg, H., Albrecht, P., 1998. Molecular characterization of organic matter in sediments from the Keg River formation (Elk

- Point group), western Canada sedimentary basin. *Organic Geochemistry* 29, 1905-1920.
- Belt, S.T., Masse, G., Allard, W.G., Robert, J.M., Rowland, S.J., 2001. Identification of a C₂₅ highly branched isoprenoid triene in the freshwater diatom *Navicula sclesvicensis*. *Organic Geochemistry* 32, 1169-1172.
- Bianchi, T.S., Canuel, E.A., 2011. *Chemical Biomarkers in Aquatic Ecosystems*. Princeton University Press, Princeton, USA.
- Blackwelder, P., Hood, T., Alvarez-Zarikian, C., Nelsen, T.A., McKee, B., 1996. Benthic foraminifera from the NECOP study area impacted by the Mississippi River plume and seasonal hypoxia. *Quaternary International* 31, 19-36.
- Blaga, C.I., Reichart, G.J., Heiri, O., Sinninghe Damsté, J.S., 2009. Tetraether membrane lipid distributions in water-column particulate matter and sediments: A study of 47 European lakes along a north-south transect. *Journal of Paleolimnology* 41, 523-540.
- Bloesch, J., 1974. Sedimentation und Phosphorhaushalt im Vierwaldstättersee (Horwer Bucht) und im Rotsee. *Aquatic Sciences* 36, 71-186.
- Bloesch, J., 2007. Sedimentation and lake sediment formation. In: O'Sullivan, P., Reynolds, C. (Ed.), *The Lakes Handbook*, Volume 1. Blackwell Science Ltd, Oxford, pp. 197-229.
- Blumenberg, M., Seifert, R., Reitner, J., Pape, T., Michaelis, W., 2004. Membrane lipid patterns typify distinct anaerobic methanotrophic consortia. *Proceedings of the National Academy of Sciences USA* 101, 11111-11116.
- Boetius, A., Ravensschlag, K., Schubert, C.J., Rickert, D., Widdel, F., Gieseke, A., Amann, R., Jorgensen, B.B., Witte, U., Pfannkuche, O., 2000. A marine microbial consortium apparently mediating anaerobic oxidation of methane. *Nature* 407, 623-626.

- Boreham, C.J., Fookes, C.J.R., Popp, B.N., Hayes, J.M., 1989. Origins of etioporphyrins in sediments: Evidence from stable carbon isotopes. *Geochimica et Cosmochimica Acta* 53, 2451-2455.
- Bossard, P., Gammeter, S., Lehmann, C., Schanz, F., Bachofen, R., Burgi, H.R., Steiner, D., Zimmermann, U., 2001. Limnological description of the Lakes Zurich, Lucerne, and Cadagno. *Aquatic Sciences* 63, 225-249.
- Brassell, S.C., Eglinton, G., 1983. Steroids and triterpenoids in deep sea sediments as environmental and diagenetic indicators. In: Bjørøy, M.E.A., et al. (Eds.), *Advances in Organic Geochemistry*, Wiley, Chichester, pp. 684-697.
- Bray, E.E., Evans, E.D., 1961. Distribution of n-paraffins as a clue to recognition of source beds. *Geochimica et Cosmochimica Acta* 22, 2-15.
- Brocks, J.J., Love, G.D., Summons, R.E., Knoll, A.H., Logan, G.A., Bowden, S.A., 2005. Biomarker evidence for green and purple sulphur bacteria in a stratified Palaeoproterozoic sea. *Nature* 437, 866-870.
- Brocks, J.J., Summons, R.E., 2003. Sedimentary hydrocarbons, biomarkers for early life. In: Holland, H.D., Turekian, K. (Ed.), *Treatise in Geochemistry*. Elsevier, Oxford, pp. 65-115.
- Brown, S.B., Houghton, J.D., Vernon, D.I., 1990. New trends in photobiology biosynthesis of phycobilins. Formation of the chromophore of phytochrome, phycocyanin and phycoerythrin. *Journal of Photochemistry and Photobiology B: Biology* 5, 3-23.
- Brown, S.B., Smith, K.M., Bisset, G.M.F., Troxler, R.F., 1980. Mechanism of photo-oxidation of bacteriochlorophyll c derivatives - a possible model for natural chlorophyll breakdown. *Journal of Biological Chemistry* 255, 8063-8068.
- Bull, I.D., Lockheart, M.J., Elhmmali, M.M., Roberts, D.J., Evershed, R.P., 2002. The origin of faeces by means of biomarker detection. *Environment International* 27, 647-654.

- Buzas, M.A., Gibson, T.G., 1969. Species diversity: Benthonic foraminifera in western North Atlantic. *Science* 163, 72-75.
- Callot, H.J., 1991. Geochemistry of chlorophylls. In: Scheer, H. (Ed.), *Chlorophylls*. CRC Press, pp. 339–364.
- Calvert, S.E., Pedersen, T.F., 2007. Elemental proxies for palaeoclimatic and palaeoceanographic variability in marine sediments: Interpretation and application. In: Hillaire-Marcel, C., De Vernal, A. (Ed.), *Developments in Marine Geology*, Volume 1. Elsevier, pp. 567-644.
- Canfield, D.E., Kristensen, E., Thamdrup, B., 2005. *Aquatic Geomicrobiology*. Elsevier Academic Press, San Diego.
- Canfield, D.E., Thamdrup, B., 2009. Towards a consistent classification scheme for geochemical environments, or, why we wish the term 'suboxic' would go away. *Geobiology* 7, 385-392.
- Casagrande, D.J., Hodgson, G.W., 1976. Geochemistry of porphyrins: the observation of homologous tetrapyrroles in a sediment sample from the Black Sea. *Geochimica et Cosmochimica Acta* 40, 479-482.
- Cole, M.L., Valiela, I., Kroeger, K.D., Tomasky, G.L., Cebrian, J., Wigand, C., McKinney, R.A., Grady, S.P., Carvalho da Silva, M.H., 2004. Assessment of a $\delta^{15}\text{N}$ isotopic method to indicate anthropogenic eutrophication in aquatic ecosystems. *Journal of Environment Quality* 33, 124-132.
- Conley, D.J., Carstensen, J., Vaquer-Sunyer, R., Duarte, C.M., 2009. Ecosystem thresholds with hypoxia. *Hydrobiologia* 629, 21-29.
- Cordeiro, L.G.S.M., Carreira, R.S., Wagener, A.L.R., 2008. Geochemistry of fecal sterols in a contaminated estuary in southeastern Brazil. *Organic Geochemistry* 39, 1097-1103.

- Cuven, S., Francus, P., Lamoureux, S.F., 2010. Estimation of grain size variability with micro X-ray fluorescence in laminated lacustrine sediments, Cape Bounty, Canadian High Arctic. *Journal of Paleolimnology* 44, 803-817.
- Davison, W., 1993. Iron and manganese in lakes. *Earth-Science Reviews* 34, 119-163.
- Dean, W., Doner, L., 2012. A Holocene record of endogenic iron and manganese precipitation and vegetation history in a lake-fen complex in northwestern Minnesota. *Journal of Paleolimnology* 47, 29-42.
- Debenay, J.P., Guillou, J.J., 2002. Ecological transitions indicated by foraminiferal assemblages in paralic environments. *Estuaries* 25, 1107-1120.
- Debenay, J.P., Millet, B., Angelidis, M.O., 2005. Relationships between foraminiferal assemblages and hydrodynamics in the Gulf of Kalloni, Greece. *Journal of Foraminiferal Research* 35, 327-343.
- Diaz, R.J., 2001. Overview of hypoxia around the world. *Journal of Environmental Quality* 30, 275-281.
- Diaz, R.J., Rosenberg, R., 2008. Spreading dead zones and consequences for marine ecosystems. *Science* 321, 926-929.
- Diem, D., 1983. Die Oxydation von Mangan (II) im See. PhD thesis. ETH Zurich, Switzerland.
- Diem, D., Stumm, W., 1984. Is dissolved Mn^{2+} being oxidized by O_2 in absence of Mn-bacteria or surface catalysts? *Geochimica et Cosmochimica Acta* 48, 1571-1573.
- Engstrom, D.R., Wright, H.E., 1984. Chemical stratigraphy of lake sediments as a record of environmental change. In: Haworth, E.Y., Lund, J.W.G. (Ed.), *Lake Sediments and Environmental History*. Leicester University Press, Leicester, pp. 11-67.
- Ellsworth, R.K., 1970. Gas chromatographic determination of some maleimides produced by the oxidation of heme and chlorophyll a. *Journal of Chromatography A* 50, 131-134.

- Falz, K.Z., Holliger, C., Grosskopf, R., Liesack, W., Nozhevnikova, A.N., Muller, B., Wehrli, B., Hahn, D., 1999. Vertical distribution of methanogens in the anoxic sediment of Rotsee (Switzerland). *Applied and Environmental Microbiology* 65, 2402-2408.
- Ferentinos, G., Papatheodorou, G., Geraga, M., Iatrou, M., Fakiris, E., Christodoulou, D., Dimitriou, E., Koutsikopoulos, C., 2010. Fjord water circulation patterns and dysoxic/anoxic conditions in a Mediterranean semi-enclosed embayment in the Amvrakikos Gulf, Greece. *Estuarine, Coastal and Shelf Science* 88, 473-481.
- Ficken, K.J., Li, B., Swain, D.L., Eglinton, G., 2000. An *n*-alkane proxy for the sedimentary input of submerged/floating freshwater aquatic macrophytes. *Organic Geochemistry* 31, 745-749.
- Fietz, S., Martínez-García, A., Huguet, C., Rueda, G., Rosell-Melé, A., 2011. Constraints in the application of the Branched and Isoprenoid Tetraether index as a terrestrial input proxy. *Journal of Geophysical Research* 116, C10032.
- Filipsson, H.L., Nordberg, K., 2004. A 200-year environmental record of a low-oxygen fjord, Sweden, elucidated by benthic foraminifera, sediment characteristics and hydrographic data. *Journal of Foraminiferal Research* 34, 277-293.
- Foley, B., Jones, I.D., Maberly, S.C., Rippey, B., 2012. Long-term changes in oxygen depletion in a small temperate lake: effects of climate change and eutrophication. *Freshwater Biology* 57, 278-289.
- Folly, P., Engel, N., 1999. Chlorophyll b to chlorophyll a conversion precedes chlorophyll degradation in *Hordeum vulgare* L. *Journal of Biological Chemistry* 274, 21811-21816.
- Frey, O., 1907. Talbildung und glaziale Ablagerungen zwischen Emme und Reuss. Zücher and Furrer.
- Friedl, G., Wehrli, B., Manceau, A., 1997. Solid phases in the cycling of manganese in eutrophic lakes: New insights from EXAFS spectroscopy. *Geochimica et Cosmochimica Acta* 61, 275-290.

- Garcia, H.E., Locarnini, R.A., Boyer, T.P., Antonov, J.I., Baranova, O.K., Zweng, M.M., Johnson, D.R., 2010. World Ocean Atlas 2009, Volume 3: Dissolved Oxygen, Apparent Oxygen Utilization, and Oxygen Saturation. In: Levitus, S. (Ed.), NOAA Atlas NESDIS 70. U.S. Government Printing Office, Washington, pp. 344.
- Garrett, C., 1990. The role of secondary circulation in boundary mixing. *Journal of Geophysical Research* 95, 3181-3188.
- Gilbert, D., Rabalais, N.N., Díaz, R.J., Zhang, J., 2010. Evidence for greater oxygen decline rates in the coastal ocean than in the open ocean. *Biogeosciences* 7, 2283-2296.
- Giovanoli, R., Brüttsch, R., Diem, D., Osman-Sigg, G., Sigg, L., 1980. The composition of settling particles in Lake Zürich. *Aquatic Sciences* 42, 89-100.
- Glazer, A.N., Apell, G.S., Hixson, C.S., Bryant, D.A., Rimon, S., Brown, D.M., 1976. Biliproteins of cyanobacteria and Rhodophyta: Homologous family of photosynthetic accessory pigments. *Proceedings of the National Academy of Sciences of the USA* 73, 428-431.
- Goineau, A., Fontanier, C., Jorissen, F.J., Lansard, B., Buscail, R., Mouret, A., Kerhervé, P., Zaragosi, S., Ernoult, E., Artéro, C., Anschutz, P., Metzger, E., Rabouille, C., 2011. Live (stained) benthic foraminifera from the Rhone prodelta (Gulf of Lion, NW Mediterranean): Environmental controls on a river-dominated shelf. *Journal of Sea Research* 65, 58-75.
- Gooday, A.J., Jorissen, F., Levin, L.A., Middelburg, J.J., Naqvi, S.W.A., Rabalais, N.N., Scranton, M., Zhang, J., 2009. Historical records of coastal eutrophication-induced hypoxia. *Biogeosciences* 6, 1707-1745.
- Granina, L., Müller, B., Wehrli, B., 2004. Origin and dynamics of Fe and Mn sedimentary layers in Lake Baikal. *Chemical Geology* 205, 55-72.
- Gray, J.S., Wu, R.S.S., Or, Y.Y., 2002. Effects of hypoxia and organic enrichment on the coastal marine environment. *Marine Ecology-Progress Series* 238, 249-279.

- Green, E.P., Short, F.T., 2003. World Atlas of Seagrasses. University of California Press, Berkeley.
- Grice, K., 1995. Distributions and stable carbon isotopic compositions of individual biological markers from the Permian Kupferschiefer (Lower Rhine Basin, N.W. Germany). PhD thesis. University of Bristol, UK.
- Grice, K., Gibbison, R., Atkinson, J.E., Schwark, L., Eckardt, C.B., Maxwell, J.R., 1996. Maleimides (1*H*-pyrrole-2,5-diones) as molecular indicators of anoxygenic photosynthesis in ancient water columns. *Geochimica et Cosmochimica Acta* 60, 3913-3924.
- Grice, K., Schaeffer, P., Schwark, L., Maxwell, J.R., 1997. Changes in palaeoenvironmental conditions during deposition of the Permian Kupferschiefer (Lower Rhine Basin, northwest Germany) inferred from molecular and isotopic compositions of biomarker components. *Organic Geochemistry* 26, 677-690.
- Grossart, H.P., Wurzbacher, C.M., Barlocher, F., 2010. Fungi in lake ecosystems. *Aquatic Microbial Ecology* 59, 125-149.
- Harris, P.G., Zhao, M., Rosell-Melé, A., Tiedemann, R., Sarnthein, M., Maxwell, J.R., 1996. Chlorin accumulation rate as a proxy for Quaternary marine primary productivity. *Nature* 383, 63-65.
- Harvey, H.R., Fallon, R.D., Patton, J.S., 1986. The effect of organic matter and oxygen on the degradation of bacterial membrane lipids in marine sediments. *Geochimica et Cosmochimica Acta* 50, 795-804.
- Hasler, A.D., 1947. Eutrophication of lakes by domestic drainage. *Ecology* 28, 383-395.
- Hauke, V., Graff, R., Wehrung, P., Trendel, J.M., Albrecht, P., Riva, A., Hopfgartner, G., Gülaçar, F.O., Buchs, A., Eakin, P.A., 1992. Novel triterpene-derived hydrocarbons of the arborane/fernane series in sediments: Part II. *Geochimica et Cosmochimica Acta* 56, 3595-3602.

- Heaton, T.H.E., 1986. Isotopic studies of nitrogen pollution in the hydrosphere and atmosphere - a review. *Chemical Geology* 59, 87-102.
- Hebting, Y., Schaeffer, P., Behrens, A., Adam, P., Schmitt, G., Schneckenburger, P., Bernasconi, S.M., Albrecht, P., 2006. Biomarker evidence for a major preservation pathway of sedimentary organic carbon. *Science* 312, 1627-1631.
- Herbert, T.D., 2003. Alkenone Paleotemperature Determinations. In: Heinrich, D.H., Karl, K.T. (Ed.), *Treatise on Geochemistry*. Pergamon, Oxford, pp. 391-432.
- Hinrichs, K.U., Summons, R.E., Orphan, V., Sylva, S.P., Hayes, J.M., 2000. Molecular and isotopic analysis of anaerobic methane-oxidizing communities in marine sediments. *Organic Geochemistry* 31, 1685-1701.
- Hinrichs, K.U., Hmelo, L.R., Sylva, S.P., 2003. Molecular fossil record of elevated methane levels in Late Pleistocene coastal waters. *Science* 299, 1214-1217.
- Hodgson, G.W., Hitchon, B., Taguchi, K., Baker, B.L., Peake, E., 1968. Geochemistry of porphyrins, chlorins and polycyclic aromatics in soils, sediments and sedimentary rocks. *Geochimica et Cosmochimica Acta* 32, 737-772.
- Hoefs, J., 2009. *Stable isotope geochemistry*, 6th edition. Springer, Heidelberg.
- Hoefs, M.J.L., Rijpstra, W.I.C., Sinninghe Damsté, J.S., 2002. The influence of oxic degradation on the sedimentary biomarker record I: Evidence from Madeira Abyssal Plain turbidites. *Geochimica et Cosmochimica Acta* 66, 2719-2735.
- Hofmann, A.F., Peltzer, E.T., Walz, P.M., Brewer, P.G., 2011. Hypoxia by degrees: Establishing definitions for a changing ocean. *Deep Sea Research Part I: Oceanographic Research Papers* 58, 1212-1226.
- Holt, A.S., Purdie, J.W., Wasley, J.W.F., 1966. Structures of *Chlorobium* chlorophylls (660). *Canadian Journal of Chemistry* 44, 88-93.
- Hopmans, E.C., Schouten, S., Pancost, R.D., van der Meer, M.T.J., Sinninghe Damsté, J.S., 2000. Analysis of intact tetraether lipids in archaeal cell material and sediments by

- high performance liquid chromatography/atmospheric pressure chemical ionization mass spectrometry. *Rapid Communications in Mass Spectrometry* 14, 585-589.
- Hopmans, E.C., Weijers, J.W.H., Schefuss, E., Herfort, L., Sinninghe Damsté, J.S., Schouten, S., 2004. A novel proxy for terrestrial organic matter in sediments based on branched and isoprenoid tetraether lipids. *Earth and Planetary Science Letters* 224, 107-116.
- Huguet, C., Hopmans, E.C., Febo-Ayala, W., Thompson, D.H., Sinninghe Damsté, J.S., Schouten, S., 2006. An improved method to determine the absolute abundance of glycerol dibiphytanyl glycerol tetraether lipids. *Organic Geochemistry* 37, 1036-1041.
- Huguet, C., Urakawa, H., Martens-Habben, W., Truxal, L., Stahl, D.A., Ingalls, A.E., 2010. Changes in intact membrane lipid content of archaeal cells as an indication of metabolic status. *Organic Geochemistry* 41, 930-934.
- Hyams-Kaphzan, O., Almogi-Labin, A., Benjamini, C., Herut, B., 2009. Natural oligotrophy vs. pollution-induced eutrophy on the SE Mediterranean shallow shelf (Israel): Environmental parameters and benthic foraminifera. *Marine Pollution Bulletin* 58, 1888-1902.
- IPCC, 2007. *Climate Change 2007: The Physical Science Basis. Contribution of Working Group I to the Fourth Assessment Report of the Intergovernmental Panel on Climate Change*. In: Solomon, S., Qin, D., Manning, M., Chen, Z., Marquis, M., Averyt, K.B., Tignor, M., Miller, H.L. (Ed.). Cambridge University Press, Cambridge, UK, and New York, USA.
- Jaffé, R., Hausmann, K.B., 1995. Origin and early diagenesis of arborinone/isoarborinol in sediments of a highly productive freshwater lake. *Organic Geochemistry* 22, 231-235.
- Jasper, J.P., Gagosian, R.B., 1990. The sources and deposition of organic matter in the Late Quaternary Pigmy Basin, Gulf of Mexico. *Geochimica et Cosmochimica Acta* 54, 1117-1132.

- Jen, J.J., MacKinney, G., 1970. On photodecomposition of chlorophyll in vitro-II. Intermediates and breakdown products. *Photochemistry and Photobiology* 11, 303-308.
- Jorissen, F.J., 1987. The distribution of benthic foraminifera in the Adriatic Sea. *Marine Micropaleontology* 12, 21-48.
- Joyce, S., 2000. The dead zones: oxygen-starved coastal waters. *Environmental Health Perspectives* 108, A120-A125.
- Kapsimalis, V., Pavlakis, P., Poulos, S.E., Alexandri, S., Tziavos, C., Sioulas, A., Filippas, D., Lykousis, V., 2005. Internal structure and evolution of the Late Quaternary sequence in a shallow embayment: The Amvrakikos Gulf, NW Greece. *Marine Geology* 222, 399-418.
- Keeling, R.F., Kortzinger, A., Gruber, N., 2010. Ocean deoxygenation in a warming world. *Annual Review of Marine Science* 2, 199-229.
- Keely, B.J., Harris, P.G., Popp, B.N., Hayes, J.M., Meischner, D., Maxwell, J.R., 1994. Porphyrin and chlorin distributions in a Late Pliocene lacustrine sediment. *Geochimica et Cosmochimica Acta* 58, 3691-3701.
- Kelts, K., 1978. Geological and sedimentary evolution of Lakes Zurich and Zug, Switzerland. PhD thesis. ETH Zurich, Switzerland.
- Kohler, H.P., Ahring, B., Albella, C., Ingvorsen, K., Keweloh, H., Laczko, E., Stupperich, E., Tomei, F., 1984. Bacteriological studies on the sulfur cycle in the anaerobic part of the hypolimnion and in the surface sediments of Rotsee in Switzerland. *FEMS Microbiology Letters* 21, 279-286.
- Kohnen, M.E.L., Schouten, S., Sinninghe Damsté, J.S., de Leeuw, J.W., Merritt, D.A., Hayes, J.M., 1992. Recognition of paleobiochemicals by a combined molecular sulfur and isotope geochemical approach. *Science* 256, 358-362.

- Koinig, K.A., Shotyk, W., Lotter, A.F., Ohlendorf, C., Sturm, M., 2003. 9000 years of geochemical evolution of lithogenic major and trace elements in the sediment of an alpine lake - the role of climate, vegetation, and land-use history. *Journal of Paleolimnology* 30, 307-320.
- Kountoura, K., Zacharias, I., 2011. Temporal and spatial distribution of hypoxic/seasonal anoxic zone in Amvrakikos Gulf, Western Greece. *Estuarine, Coastal and Shelf Science* 94, 123-128.
- Kozono, M., Nomoto, S., Mita, H., Ishiwatari, R., Shimoyama, A., 2002. 2-Ethyl-3-methylmaleimide in Tokyo Bay sediments providing the first evidence for its formation from chlorophylls in the present photic and oxygenic zone. *Bioscience Biotechnology and Biochemistry* 66, 1844-1847.
- Kozono, M., Nomoto, S., Mita, H., Shimoyama, A., 2001. Detection of maleimides and their characteristics in Neogene sediments of the Shinjo basin, Japan. *Geochemical Journal* 35, 225-236.
- Lancelot, C., Martin, J.M., Panin, N., Zaitsev, Y., 2002. The north-western Black Sea: A pilot site to understand the complex interaction between human activities and the coastal environment. *Estuarine, Coastal and Shelf Science* 54, 279-283.
- Lehmann, M.F., Reichert, P., Bernasconi, S.M., Barbieri, A., McKenzie, J.A., 2003. Modelling nitrogen and oxygen isotope fractionation during denitrification in a lacustrine redox-transition zone. *Geochimica et Cosmochimica Acta* 67, 2529-2542.
- Levin, L.A., Ekau, W., Gooday, A.J., Jorissen, F., Middelburg, J.J., Naqvi, S.W.A., Neira, C., Rabalais, N.N., Zhang, J., 2009. Effects of natural and human-induced hypoxia on coastal benthos. *Biogeosciences* 6, 2063-2098.
- Lipp, J.S., Morono, Y., Inagaki, F., Hinrichs, K.-U., 2008. Significant contribution of Archaea to extant biomass in marine subsurface sediments. *Nature* 454, 991-994.

- Livingstone, D.M., 1997. An example of the simultaneous occurrence of climate-driven "sawtooth" deep-water warming/cooling episodes in several Swiss lakes. *Proceedings of the International Association of Theoretical and Applied Limnology* 26, 822-828.
- Livingstone, D.M., 2003. Impact of secular climate change on the thermal structure of a large temperate central European lake. *Climatic Change* 57, 205-225.
- Loizeau, J.L., Span, D., Coppee, V., Dominik, J., 2001. Evolution of the trophic state of Lake Annecy (eastern France) since the last glaciation as indicated by iron, manganese and phosphorus speciation. *Journal of Paleolimnology* 25, 205-214.
- Lotter, A.F., 1989. Subfossil and modern diatom plankton and the paleolimnology of Rotsee (Switzerland) since 1850. *Aquatic Sciences* 51, 338-350.
- Louda, J.W., Li, J., Liu, L., Winfree, M.N., Baker, E.W., 1998. Chlorophyll-*a* degradation during cellular senescence and death. *Organic Geochemistry* 29, 1233-1251.
- Löwemark, L., Chen, H.F., Yang, T.N., Kylander, M., Yu, E.F., Hsu, Y.W., Lee, T.Q., Song, S.R., Jarvis, S., 2011. Normalizing XRF-scanner data: A cautionary note on the interpretation of high-resolution records from organic-rich lakes. *Journal of Asian Earth Sciences* 40, 1250-1256.
- Magness, S.L., 2001. Distributions and stable isotope characteristics of maleimides (1-*H*-pyrrole-2,5-diones). PhD thesis. University of Bristol, UK.
- Massé, G., Belt, S.T., Allard, W.G., Lewis, A.C., Wakeham, S.G., Rowland, S.J., 2004a. Occurrence of novel monocyclic alkenes from diatoms in marine particulate matter and sediments. *Organic Geochemistry* 35, 813-822.
- Massé, G., Belt, S.T., Rowland, S.J., 2004b. Biosynthesis of unusual monocyclic alkenes by the diatom *Rhizosolenia setigera* (Brightwell). *Phytochemistry* 65, 1101-1106.
- Mateu-Vicens, G., Box, A., Deudero, S., Rodriguez, B., 2010. Comparative analysis of epiphytic foraminifera in sediments colonized by seagrass *Posidonia oceanica* and invasive macroalgae *Caulerpa spp.* *Journal of Foraminiferal Research* 40, 134-147.

- Matzinger, A., Muller, B., Niederhauser, P., Schmid, M., Wuest, A., 2010. Hypolimnetic oxygen consumption by sediment-based reduced substances in former eutrophic lakes. *Limnology and Oceanography* 55, 2073-2084.
- McCarroll, D., Loader, N.J., 2004. Stable isotopes in tree rings. *Quaternary Science Reviews* 23, 771–801.
- Mee, L.D., Friedrich, J., Gomoiu, M.T., 2005. Restoring the Black Sea in times of uncertainty. *Oceanography* 18, 32-43.
- Melles, M. et al., 2012. 2.8 Million years of Arctic climate change from Lake El'gygytgyn, NE Russia. *Science* 337, 315-320.
- Mendes, I., Gonzalez, R., Dias, J.M.A., Lobo, F., Martins, V., 2004. Factors influencing recent benthic foraminifera distribution on the Guadiana shelf (Southwestern Iberia). *Marine Micropaleontology* 51, 171-192.
- Mermoud, F., Gulacar, F.O., Buchs, A., 1985. 5- α (H)-Cholestan-3- α -ol in sediments - characterization and geochemical significance. *Geochimica et Cosmochimica Acta* 49, 459-462.
- Meyers, P.A., 2006. An overview of sediment organic matter records of human eutrophication in the Laurentian Great Lakes region. *Water, Air, and Soil Pollution: Focus* 6, 453–463.
- Meyers, P.A., Ishiwatari, R., 1993. Lacustrine organic geochemistry - an overview of indicators of organic matter sources and diagenesis in lake sediments. *Organic Geochemistry* 20, 867-900.
- Middelburg, J.J., Levin, L.A., 2009. Coastal hypoxia and sediment biogeochemistry. *Biogeosciences* 6, 1273-1293.
- Mille-Lindblom, C., von Wachenfeldt, E., Tranvik, L.J., 2004. Ergosterol as a measure of living fungal biomass: Persistence in environmental samples after fungal death. *Journal of Microbiological Methods* 59, 253-262.

- Minder, L., 1938. Der Zürichsee als Eutrophierungsphänomen: Summarische Ergebnisse aus 50 Jahren Zürichseeforschung. *Geologie der Meere und Binnengewässer* 2, 284-299.
- Mojtahid, M., Jorissen, F., Lansard, B., Fontanier, C., 2010. Microhabitat selection of benthic foraminifera in sediments off the Rhone River mouth (NW Mediterranean). *Journal of Foraminiferal Research* 40, 231-246.
- Müller, B., Wang, Y., Wehrli, B., 2006. Cycling of calcite in hard water lakes of different trophic states. *Limnology and Oceanography* 51, 1678-1688.
- Müller, P.J., Kirst, G., Ruhland, G., von Storch, I., Rosell-Melé, A., 1998. Calibration of the alkenone paleotemperature index UK'37 based on core-tops from the eastern South Atlantic and the global ocean (60°N-60°S). *Geochimica et Cosmochimica Acta* 62, 1757-1772.
- Müller, B., Bryant, L.D., Matzinger, A., Wüest, A., 2012. Hypolimnetic oxygen depletion in eutrophic lakes. *Environmental Science and Technology* 46, 9964-9971.
- Munro, A.W., Girvan, H.M., McLean, K.J., Cheesman, M.R., Leys, D., 2009. Heme and Hemoproteins. In: Warren, M.J., Smith, A.G. (Eds.), *Tetrapyrroles: Birth, Life and Death*. Springer, New York, USA, pp. 160-183.
- Murray, J.W., 2001. *Ecology and Palaeoecology of Benthic Foraminifera*. Longman Scientific and Technical, New York.
- Murray, J.W., 2006. *Ecology And Applications of Benthic Foraminifera*. Cambridge University Press, Cambridge.
- Murray, J.W., Stewart, K., Kassakian, S., Krynytzky, M., DiJulio, D., 2007. Oxic, Suboxic and Anoxic Conditions in the Black Sea. In: Yanko-Hombach, V., Gilbert, A.S., Panin, N., Dolukhanov, P.M. (Ed.), *The Black Sea Food Question: Changes in Coastline, Climate and Human Settlement*. Springer, pp. 1-22.
- Naeher, S., Smittenberg, R.H., Gilli, A., Kirilova, E.P., Lotter, A.F., Schubert, C.J., 2012a. Impact of recent lake eutrophication on microbial community changes as revealed by

- high resolution lipid biomarkers in Rotsee (Switzerland). *Organic Geochemistry* 49, 86-95.
- Naylor, C.C., Keely, B.J., 1998. Sedimentary purpurins: oxidative transformation products of chlorophylls. *Organic Geochemistry* 28, 417-422.
- Nealson, K.H., Saffarini, D., 1994. Iron and Manganese in Anaerobic Respiration - Environmental Significance, Physiology, and Regulation. *Annual Review of Microbiology* 48, 311-343.
- Niessen, F., Sturm, M., 1987. Die Sedimente des Baldeggersees (Schweiz) - Ablagerungsraum und Eutrophierungsentwicklung während der letzten 100 Jahre. *Archiv für Hydrobiologie* 108, 365-383.
- Niessen, F., Wick, L., Bonani, G., Chondrogianni, C., Siegenthaler, C., 1992. Aquatic system response to climatic and human changes: Productivity, bottom water oxygen status, and sapropel formation in Lake Lugano over the last 10 000 years. *Aquatic Sciences* 54, 257-276.
- Nipkow, H.F., 1927. Über das Verhalten der Skelette planktischer Kieselalgen im geschichteten Tiefenschlamm des Zürich- und Baldeggersees. PhD thesis. ETH Zurich, Switzerland.
- Ocampo, R., Repeta, D.J., 1999. Structural determination of purpurin-18 (as methyl ester) from sedimentary organic matter. *Organic Geochemistry* 30, 189-193.
- Ohkouchi, N., Nakajima, Y., Ogawa, N.O., Chikaraishi, Y., Suga, H., Sakai, S., Kitazato, H., 2008. Carbon isotopic composition of the tetrapyrrole nucleus in chloropigments from a saline meromictic lake: A mechanistic view for interpreting the isotopic signature of alkyl porphyrins in geological samples. *Organic Geochemistry* 39, 521-531.
- Omlin, M., Brun, R., Reichert, P., 2001. Biogeochemical model of Lake Zürich: sensitivity, identifiability and uncertainty analysis. *Ecological Modelling* 141, 105-123.

- Orcutt, D.M., Patterson, G.W., 1975. Sterol, fatty acid and elemental composition of diatoms grown in chemically defined media. *Comparative Biochemistry and Physiology B - Biochemistry & Molecular Biology* 50, 579-583.
- Ormerod, J.G., 1983. *The Phototrophic bacteria: anaerobic life in the light*. Blackwell Science Ltd.
- O'Sullivan, P.E., Reynolds, C.S., 2005. *The Lakes Handbook: Lake restoration and rehabilitation*. Blackwell Science, Oxford.
- Otte, S.C.M., Meent, E.J., Veelen, P.A., Pundsnes, A.S., Amesz, J., 1993. Identification of the major chlorosomal bacteriochlorophylls of the green sulfur bacteria *Chlorobium vibrioforme* and *Chlorobium phaeovibrioides*; their function in lateral energy transfer. *Photosynthesis Research* 35, 159-169.
- Ozsoy, E., Unluata, U., 1997. Oceanography of the Black Sea: a review of some recent results. *Earth-Science Reviews* 42, 231-272.
- Pancost, R.D., Boot, C.S., Aloisi, G., Maslin, M., Bickers, C., Ettwein, V., Bale, N., Handley, L., 2009. Organic geochemical changes in Pliocene sediments of ODP Site 1083 (Benguela Upwelling System). *Palaeogeography, Palaeoclimatology, Palaeoecology* 280, 119-131.
- Pancost, R.D., Crawford, N., Magness, S., Turner, A., Jenkyns, H.C., Maxwell, J.R., 2004. Further evidence for the development of photic-zone euxinic conditions during Mesozoic oceanic anoxic events. *Journal of the Geological Society* 161, 353-364.
- Pancost, R.D., Crawford, N., Maxwell, J.R., 2002. Molecular evidence for basin-scale photic zone euxinia in the Permian Zechstein Sea. *Chemical Geology* 188, 217-227.
- Paoli, M., Marles-Wright, J., Smith, A., 2002. Structure-function relationships in heme-proteins. *DNA and Cell Biology* 21, 271-280.
- Papadimitriou, S., Kennedy, H., Kennedy, D.P., Duarte, C.M., Marba, N., 2005. Sources of organic matter in seagrass-colonized sediments: A stable isotope study of the silt and

- clay fraction from *Posidonia oceanica* meadows in the western Mediterranean. *Organic Geochemistry* 36, 949-961.
- Pease, T.K., Van Vleet, E.S., Barre, J.S., Dickins, H.D., 1998. Simulated degradation of glyceryl ethers by hydrous and flash pyrolysis. *Organic Geochemistry* 29, 979-988.
- Peeters, F., Livingstone, D.M., Goudsmit, G.H., Kipfer, R., Forster, R., 2002. Modeling 50 years of historical temperature profiles in a large central European lake. *Limnology and Oceanography* 47, 186-197.
- Peters, K.E., Walters, C.C., Moldowan, J.M., 2006. *The Biomarker Guide*. Cambridge University Press, Cambridge.
- Pfennig, N., 1978. General physiology and ecology of photosynthetic bacteria. In: Clayton, R.K., Sistrom, W.R. (Ed.), *Photosynthetic Bacteria*. Plenum Press, pp. 3-16.
- Pfister, C., 1999. *Wetternachhersage - 500 Jahre Klimavariationen und Naturkatastrophen (1496-1995)*. Verlag Paul Haupt, Bern.
- Pickering, M.D., Keely, B.J., 2011. Low temperature abiotic formation of mesopyrophaeophorbide *a* from pyrophaeophorbide *a* under conditions simulating anoxic natural environments. *Geochimica et Cosmochimica Acta* 75, 533-540.
- Pihl, L., Baden, S.P., Diaz, R.J., 1991. Effects of periodic hypoxia on distribution of demersal fish and crustaceans. *Marine Biology* 108, 349-360.
- Piiper, J., 1982. Respiratory gas exchange at lungs, gills and tissues: mechanisms and adjustments. *Journal of Experimental Biology* 100, 5-22.
- Piper, D.Z., Calvert, S.E., 2011. Holocene and late glacial palaeoceanography and palaeolimnology of the Black Sea: Changing sediment provenance and basin hydrography over the past 20,000 years. *Geochimica et Cosmochimica Acta* 75, 5597-5624.
- Pitcher, A., Hopmans, E.C., Mosier, A.C., Park, S.-J., Rhee, S.-K., Francis, C.A., Schouten, S., Sinninghe Damste, J.S., 2011. Core and intact polar glycerol dibiphytanyl glycerol

- tetraether lipids of ammonia-oxidizing archaea enriched from marine and estuarine sediments. *Applied and Environmental Microbiology* 77, 3468-3477.
- Platon, E., Sen Gupta, B.K., Rabalais, N.N., Turner, R.E., 2005. Effect of seasonal hypoxia on the benthic foraminiferal community of the Louisiana inner continental shelf. The 20th century record. *Marine Micropaleontology* 54, 263-283.
- Posch, T., Köster, O., Salcher, M.M., Pernthaler J., 2012. Harmful filamentous cyanobacteria favoured by reduced water turnover with lake warming. *Nature Clim. Change*, doi:10.1038/nclimate1581
- Prahl, F.G., Muehlhausen, L.A., Zahnle, D.L., 1988. Further evaluation of long-chain alkenones as indicators of paleoceanographic conditions. *Geochimica et Cosmochimica Acta* 52, 2303-2310.
- Prahl, F.G., Wakeham, S.G., 1987. Calibration of unsaturation patterns in long-chain ketone compositions for palaeotemperature assessment. *Nature* 330, 367-369.
- Quirke, E., Shaw, G.J., Soper, P.D., Maxwell, J.R., 1980. Petroporphyrins-II. The presence of porphyrins with extended alkyl substituents. *Tetrahedron* 36, 3261-3267.
- Raederstorff, D., Rohmer, M., 1987. Sterol biosynthesis via cycloartenol and other biochemical features related to photosynthetic phyla in the amoebae *Naegleria lovaniensis* and *Naegleria gruberi*. *European Journal of Biochemistry* 164, 427-434.
- Rempfer, J., Livingstone, D.M., Forster, R., Blodau, C., 2009. Response of hypolimnetic oxygen concentrations in deep Swiss perialpine lakes to interannual variations in winter climate. *International Association of Theoretical and Applied Limnology*, Vol 30, Pt 5, Proceedings 30, 717-721.
- Repeta, D.J., 1993. A high-resolution historical record of Holocene anoxygenic primary production in the Black Sea. *Geochimica et Cosmochimica Acta* 57, 4337-4342.

- Repeta, D.J., Simpson, D.J., 1991. The distribution and recycling of chlorophyll, bacteriochlorophyll and carotenoids in the Black Sea. *Deep Sea Research Part I: Oceanographic Research Papers* 38, Supplement 2, S969-S984.
- Repeta, D.J., Simpson, D.J., Jorgensen, B.B., Jannasch, H.W., 1989. Evidence for anoxygenic photosynthesis from the distribution of bacteriochlorophylls in the Black Sea. *Nature* 342, 69-72.
- Rezanka, T., Vokoun, J., Slavicek, J., Podojil, M., 1983. Determination of fatty acids in algae by capillary gas chromatography mass spectrometry. *Journal of Chromatography* 268, 71-78.
- Richter, T.O., van der Gaast, S., Koster, B., Vaars, A., Gieles, R., de Stigter, H.C., de Haas, H., van Weering, T.C.E., 2006. The Avaatech XRF core scanner: technical description and applications to NE Atlantic sediments. In: Rothwell, G. (Ed.), *New Techniques in Sediment Core Analysis*, Geological Society London Special Publications 267, pp. 39-50.
- Rohmer, M., Bouviernave, P., Ourisson, G., 1984. Distribution of hopanoid triterpenes in prokaryotes. *Journal of General Microbiology* 130, 1137-1150.
- Rontani, J.-F., Volkman, J.K., 2003. Phytol degradation products as biogeochemical tracers in aquatic environments. *Organic Geochemistry* 34, 1-35.
- Rontani, J.F., Baillet, G., Aubert, C., 1991. Production of acyclic isoprenoid compounds during the photodegradation of chlorophyll-a in seawater. *Journal of Photochemistry and Photobiology A: Chemistry* 59, 369-377.
- Ross, D.A., Degens, E.T., 1974. Recent sediments of the Black Sea. In: Ross, D.A., Degens, E.T. (Ed.), *The Black Sea - Geology, Chemistry and Biology*. American Association of Petroleum Geologists Memoirs, Tulsa, pp. 183-199.
- Sackett, W.M., 1964. The depositional history and isotopic organic carbon composition of marine sediments. *Marine Geology* 2, 173-185.

- Saliot, A., Parrish, C.C., Sadouni, N., Bouloubassi, I., Fillaux, J., Cauwet, G., 2002. Transport and fate of Danube Delta terrestrial organic matter in the Northwest Black Sea mixing zone. *Marine Chemistry* 79, 243-259.
- Schaeffer, P., Adam, P., Wehrung, P., Albrecht, P., 1997. Novel aromatic carotenoid derivatives from sulfur photosynthetic bacteria in sediments. *Tetrahedron Letters* 38, 8413-8416.
- Schaller, T., Wehrli, B., 1996. Geochemical focusing of manganese in lake sediments - An indicator of deep-water oxygen conditions. *Aquatic Geochemistry* 2, 359-378.
- Scheer, H., 2006. An overview of chlorophylls and bacteriochlorophylls: Biochemistry, biophysics, functions and applications. In: Grimm, B., Porra, R.J., Rüdiger, W., Scheer, H. (Ed.), *Advances in Photosynthesis and Respiration*, 25. Springer, The Netherlands, pp. 1-26.
- Scheffer, M., 2009. *Critical transitions in nature and society*. Princeton University Press.
- Scheffer, M., 2010. Complex systems: Foreseeing tipping points. *Nature* 467, 411-412.
- Sherwin, M.R., Van Vleet, E.S., Fossato, V.U., Dolci, F., 1993. Coprostanol (5 β -cholestan-3 β -ol) in lagoonal sediments and mussels of Venice, Italy. *Marine Pollution Bulletin* 26, 501-507.
- Schmocker-Fackel, P., Naef, F., 2010. Changes in flood frequencies in Switzerland since 1500. *Hydrology and Earth System Sciences* 14, 1581-1594.
- Schouten, S., Rijpstra, W.I.C., Kok, M., Hopmans, E.C., Summons, R.E., Volkman, J.K., Sinninghe Damsté, J.S., 2001. Molecular organic tracers of biogeochemical processes in a saline meromictic lake (Ace Lake). *Geochimica et Cosmochimica Acta* 65, 1629-1640.
- Schouten, S., Hopmans, E.C., van der Meer, J., Mets, A., Bard, E., Bianchi, T.S., Diefendorf, A., Escala, M., Freeman, K.H., Furukawa, Y., Huguet, C., Ingalls, A., Ménot-Combes, G., Nederbragt, A.J., Oba, M., Pearson, A., Pearson, E.J., Rosell-Melé, A., Schaeffer,

- P., Shah, S.R., Shanahan, T.M., Smith, R.W., Smittenberg, R., Talbot, H.M., Uchida, M., Van Mooy, B.A.S., Yamamoto, M., Zhang, Z., Sinninghe Damsté, J.S., 2009. An interlaboratory study of TEX₈₆ and BIT analysis using high-performance liquid chromatography mass spectrometry. *Geochemistry Geophysics Geosystems* 10, Q03012, doi:10.1029/2008GC002221.
- Schubert, C.J., Lucas, F., Durisch-Kaiser, E., Stierli, R., Diem, T., Scheidegger, O., Vazquez, F., Müller, B., 2010. Oxidation and emission of methane in a monomictic lake (Rotsee, Switzerland). *Aquatic Sciences* 72, 455-466.
- Schubert, C.J., Niggemann, J., Klockgether, G., Ferdelman, T.G., 2005. Chlorin Index: A new parameter for organic matter freshness in sediments. *Geochemistry Geophysics Geosystems* 6, Q03005, doi:10.1029/2004GC000837.
- Schubert, C.J., Villanueva, J., Calvert, S.E., Cowie, G.L., von Rad, U., Schulz, H., Berner, U., Erlenkeuser, H., 1998. Stable phytoplankton community structure in the Arabian Sea over the past 200,000 years. *Nature* 394, 563-566.
- Scott, D.B., Piper, D.J.W., Panagos, A.G., 1979. Recent saltmarsh and intertidal mudflat foraminifera from the western coast of Greece. *Rivista Italiana de Paleontologia e Stratigrafia* 85, 243-266.
- Seifert, W.K., Moldowan, J.M., 1978. Applications of steranes, terpanes and monoaromatics to the maturation, migration and source of crude oils. *Geochimica et Cosmochimica Acta* 42, 77-95.
- Sen Gupta, B.K., Machain-Castillo, M.L., 1993. Benthic foraminifera in oxygen-poor habitats. *Marine Micropaleontology* 20, 183-201.
- Shanchun, J., O'Leary, T., Volkman, J.K., Huizhi, Z., Rongfen, J., Suhua, Y., Yan, W., Zuofeng, L., Zuoqing, S., Ronghua, J., 1994. Origins and simulated thermal alteration of sterols and keto-alcohols in deep-sea marine sediments of the Okinawa Trough. *Organic Geochemistry* 21, 415-422.

- Shankle, A.M., Goericke, R., Franks, P.J.S., Levin, L.A., 2002. Chlorin distribution and degradation in sediments within and below the Arabian Sea oxygen minimum zone. *Deep Sea Research Part I: Oceanographic Research Papers* 49, 953-969.
- Shannon, C.E., 1948. A mathematical theory of communication. *Bell System Technical Journal* 27, 379-423.
- Shimkus, K.M., Trimonis, E.S., 1974. Modern Sedimentation in Black Sea: Sediments. In: Degens, E.T., Ross, D.A. (Ed.), *The Black Sea - geology, chemistry, and biology*, 20. American Association of Petroleum Geologists, pp. 249-278.
- Shimoyama, A., Kozono, M., Mita, H., Nomoto, S., 2001. Maleimides in the Cretaceous/Tertiary boundary sediments at Kwaruppu, Hokkaido, Japan. *Geochemical Journal* 35, 365-375.
- Sigg, L., Sturm, M., Kistler, D., 1987. Vertical transport of heavy metals by settling particles in Lake Zurich. *Limnology and Oceanography* 32, 112-130.
- Sinninghe Damsté, J.S., Irene, W., Rijpstra, C., de Leeuw, J.W., Schenck, P.A., 1988. Origin of organic sulphur compounds and sulphur-containing high molecular weight substances in sediments and immature crude oils. *Organic Geochemistry* 13, 593-606.
- Sinninghe Damsté, J.S., Kenig, F., Koopmans, M.P., Koster, J., Schouten, S., Hayes, J.M., de Leeuw, J.W., 1995. Evidence for gammacerane as an indicator of water column stratification. *Geochimica et Cosmochimica Acta* 59, 1895-1900.
- Sinninghe Damsté, J.S., Kuypers, M.M.M., Schouten, S., Schulte, S., Rullkötter, R., 2003. The lycopane/C₃₁ *n*-alkane ratio as a proxy to assess palaeoacidity during sediment deposition. *Earth and Planetary Science Letters* 209, 215-226.
- Sinninghe Damsté, J.S., Rijpstra, W.I.C., Hopmans, E.C., Prahl, F.G., Wakeham, S.G., Schouten, S., 2002. Distribution of membrane lipids of planktonic Crenarchaeota in the Arabian Sea. *Applied and Environmental Microbiology* 68, 2997-3002.

- Sinninghe Damsté, J.S., Wakeham, S.G., Kohnen, M.E.L., Hayes, J.M., de Leeuw, J.W., 1993. A 6,000-year sedimentary molecular record of chemocline excursions in the Black Sea. *Nature* 362, 827-829.
- Smith, K.M., Bushell, M.J., Rimmer, J., Unsworth, J.F., 1980. Bacteriochlorophylls *c* from *Chloropseudomonas ethylicum*. Composition and NMR studies of the pheophorbides and derivatives. *Journal of the American Chemical Society* 102, 2437-2448.
- Smith, K.M., Goff, D.A., Fajer, J., Barkigia, K.M., 1983. Isolation and characterization of two new bacteriochlorophylls *d* bearing neopentyl substituents. *Journal of the American Chemical Society* 105, 1674-1676.
- Smith, V.H., Tilman, G.D., Nekola, J.C., 1999. Eutrophication: Impacts of excess nutrient inputs on freshwater, marine and terrestrial ecosystems. *Environmental Pollution* 100, 179-196.
- Smittenberg, R.H., Pancost, R.D., Hopmans, E.C., Paetzel, M., Sinninghe Damsté, J.S., 2004. A 400-year record of environmental change in an euxinic fjord as revealed by the sedimentary biomarker record. *Palaeogeography Palaeoclimatology Palaeoecology* 202, 331-351.
- Spitzer, V., 1997. Structure analysis of fatty acids by gas chromatography low resolution electron impact mass spectrometry of their 4,4-dimethyloxazoline derivatives - A review. *Progress in Lipid Research* 35, 387-408.
- Squier, A.H., Hodgson, D.A., Keely, B.J., 2002. Sedimentary pigments as markers for environmental change in an Antarctic lake. *Organic Geochemistry* 33, 1655-1665.
- Stadelmann, P., 1980. Der Zustand des Rotsees bei Luzern. In: Quartierverein Maihof (Ed.), *Geschichte und Eigenart eines Quartiers*, Quartierverein Maihof, Luzern, pp. 54-61.
- Stein, R., 1991. *Accumulation of organic carbon in marine sediments*, Springer, Heidelberg.

- Strasser, M., Schindler, C., Anselmetti, F.S., 2008. Late pleistocene earthquake-triggered moraine dam failure and outburst of Lake Zurich, Switzerland. *Journal of Geophysical Research* 113, F02003, doi:10.1029/2007JF000802.
- Stumm, W., 1985. Chemical processes in lakes. Wiley, New York.
- Summerhayes, C.P., Kroon, D., Rosell-Melé, A., Jordan, R.W., Schrader, H.J., Hearn, R., Villanueva, J., Grimalt, J.O., Eglinton, G., 1995. Variability in the Benguela Current upwelling system over the past 70,000 years. *Progress in Oceanography* 35, 207-251.
- Summons, R.E., Jahnke, L.L., Simoneit, B.R.T., 2007. Lipid Biomarkers for Bacterial Ecosystems: Studies of Cultured Organisms, Hydrothermal Environments and Ancient Sediments, Ciba Foundation Symposium 202 - Evolution of Hydrothermal Ecosystems on Earth and Mars. John Wiley and Sons, Chichester, pp. 174-197.
- Szarek, R., Kuhnt, W., Kawamura, H., Kitazato, H., 2006. Distribution of recent benthic foraminifera on the Sunda Shelf (South China Sea). *Marine Micropaleontology* 61, 171-195.
- Tchobanoglous, G., Burton, F.L., Metcalf, Eddy, Stensel, H.D., 2004. Wastewater engineering: Treatment and reuse. McGraw-Hill.
- Thamdrup, B., Fossing, H., Jørgensen, B.B., 1994. Manganese, iron and sulfur cycling in a coastal marine sediment, Aarhus bay, Denmark. *Geochimica et Cosmochimica Acta* 58, 5115-5129.
- Thiel, V., Jenisch, A., Landmann, G., Reimer, A., Michaelis, W., 1997. Unusual distributions of long-chain alkenones and tetrahymanol from the highly alkaline Lake Van, Turkey. *Geochimica et Cosmochimica Acta* 61, 2053-2064.
- Tjallingii, R., Rohl, U., Kolling, M., Bickert, T., 2007. Influence of the water content on X-ray fluorescence core-scanning measurements in soft marine sediments. *Geochemistry Geophysics Geosystems* 8, Q02004, doi:10.1029/2006GC001393.

- Treibs, A., 1936. Chlorophyll and heme derivatives in organic mineral materials. *Angewandte Chemie* 49, 0682-0686.
- Tribovillard, N., Algeo, T.J., Lyons, T., Riboulleau, A., 2006. Trace metals as paleoredox and paleoproductivity proxies: An update. *Chemical Geology* 232, 12-32.
- Tsabaris, C., Evangeliou, N., Fillis-Tsirakis, E., Sotiropoulou, M., Patiris, D.L., Florou, H., 2011. Distribution of natural radioactivity in sediment cores from Amvrakikos gulf (Western Greece) as a part of IAEA's campaign in the Adriatic and Ionian Seas. *Radiation Protection Dosimetry*, 1–14.
- Tziavos, C., Vouloumanos, N., 1994. Microfaunal distribution in the surface sediments of Amvrakikos Gulf (Western Greece). *Bulletin of the Geological Society of Greece* 30, 429-436.
- van Bentum, E.C., Hetzel, A., Brumsack, H.J., Forster, A., Reichart, G.J., Sinninghe Damsté, J.S., 2009. Reconstruction of water column anoxia in the equatorial Atlantic during the Cenomanian-Turonian oceanic anoxic event using biomarker and trace metal proxies. *Palaeogeography Palaeoclimatology Palaeoecology* 280, 489-498.
- van Breugel, Y., Schouten, S., Paetzel, M., Sinninghe Damsté, J.S., 2006. Seasonal variation in the stable carbon isotopic composition of algal lipids in a shallow anoxic fjord: Evaluation of the effect of recycling of respired CO₂ on the $\delta^{13}\text{C}$ of organic matter. *American Journal of Science* 306, 367-387.
- van der Zwaan, G.J., 2000. Variation in Natural vs. Anthropogenic Eutrophication of Shelf Areas in Front of Major Rivers. In: Martin, R.E. (Ed.), *Environmental Micropaleontology*. Kluwer, New York, pp. 385–404.
- Vidović, J., Čosović, V., Juračić, M., Petricioli, D., 2009. Impact of fish farming on foraminiferal community, Drvenik Veliki Island, Adriatic Sea, Croatia. *Marine Pollution Bulletin* 58, 1297-1309.

- Villanueva, J., Hastings, D.W., 2000. A century-scale record of the preservation of chlorophyll and its transformation products in anoxic sediments. *Geochimica et Cosmochimica Acta* 64, 2281-2294.
- Vitousek, P.M., Mooney, H.A., Lubchenco, J., Melillo, J.M., 1997. Human domination of earth's ecosystems. *Science* 277, 494-499.
- Volkman, J.K., 1986. A review of sterol markers for marine and terrigenous organic matter. *Organic Geochemistry* 9, 83-99.
- Volkman, J.K., 2003. Sterols in microorganisms. *Applied Microbiology and Biotechnology* 60, 495-506.
- Volkman, J.K., Barrett, S.M., Blackburn, S.I., Mansour, M.P., Sikes, E.L., Gelin, F., 1998. Microalgal biomarkers: A review of recent research developments. *Organic Geochemistry* 29, 1163-1179.
- Volkman, J.K., Barrett, S.M., Dunstan, G.A., Jeffrey, S.W., 1992. C₃₀-C₃₂ alkyl diols and unsaturated alcohols in microalgae of the class Eustigmatophyceae. *Organic Geochemistry* 18, 131-138.
- Volkman, J.K., Barrett, S.M., Dunstan, G.A., Jeffrey, S.W., 1993. Geochemical significance of the occurrence of dinosterol and other 4-methylsterols in a marine diatom. *Organic Geochemistry* 20, 7-15.
- Volkman, J.K., Johns, R.B., Gillan, F.T., Perry, G.J., Bavor, H.J., 1980. Microbial lipids of an inter-tidal sediment - I. Fatty acids and hydrocarbons. *Geochimica et Cosmochimica Acta* 44, 1133-1143.
- Wakeham, S.G., Amann, R., Freeman, K.H., Hopmans, E.C., Jorgensen, B.B., Putnam, I.F., Schouten, S., Sinninghe Damsté, J.S., Talbot, H.M., Woebken, D., 2007. Microbial ecology of the stratified water column of the Black Sea as revealed by a comprehensive biomarker study. *Organic Geochemistry* 38, 2070-2097.

- Wakeham, S.G., Freeman, K.H., Pease, T.K., Hayes, J.M., 1993. A photoautotrophic source for lycopane in marine water columns. *Geochimica et Cosmochimica Acta* 57, 159-165.
- Weijers, J.W.H., Schouten, S., van den Donker, J.C., Hopmans, E.C., Sinninghe Damsté, J.S., 2007. Environmental controls on bacterial tetraether membrane lipid distribution in soils. *Geochimica et Cosmochimica Acta* 71, 703-713.
- Weltje, G.J., Tjallingii, R., 2008. Calibration of XRF core scanners for quantitative geochemical logging of sediment cores: Theory and application. *Earth and Planetary Science Letters* 274, 423-438.
- Wieland, E., Lienemann, P., Bollhalder, S., Lück, A., Santschi, P.H., 2001. Composition and transport of settling particles in Lake Zurich: relative importance of vertical and lateral pathways. *Aquatic Sciences* 63, 123-149.
- Wilson, M.A., Hodgson, D.A., Keely, B.J., 2004. Structural variations in derivatives of the bacteriochlorophylls of Chlorobiaceae: impact of stratigraphic resolution on depth profiles as revealed by methanolysis. *Organic Geochemistry* 35, 1299-1307.
- Wilson, M.A., Hodgson, D.A., Keely, B.J., 2005. Atmospheric pressure chemical ionisation liquid chromatography/multistage mass spectrometry for assignment of sedimentary bacteriochlorophyll derivatives. *Rapid Communications in Mass Spectrometry* 19, 38-46.
- Withers, N., 1983. Dinoflagellate sterols. In: P. Scheuer (Eds.), *Marine Natural Products: Chemical and Biological Perspectives*. Academic Press, New York, pp. 87-130.
- Wu, J., Lin, L., Gagan, M., Schleser, G., Wang, S., 2006. Organic matter stable isotope ($\delta^{13}\text{C}$, $\delta^{15}\text{N}$) response to historical eutrophication of Lake Taihu, China. *Hydrobiologia* 563, 19-29.
- Wu, J.M., Hu, R.K., Yue, J.Q., Yang, Z.G., Zhang, L.F., 2009. Determination of fecal sterols by gas chromatography-mass spectrometry with solid-phase extraction and injection-port derivatization. *Journal of Chromatography A* 1216, 1053-1058.

- Wuchter, C., 2006. Ecology and Membrane Lipid Distribution of Marine Crenarchaeota: Implications for TEX86 Paleothermometry, PhD thesis. University of Utrecht, The Netherlands.
- Zapata, M., Garrido, J.L., Jeffrey, S.W., 2006. Chlorophyll c Pigments: Current Status. In: Grimm, B., Porra, R.J., Rüdiger, W., Scheer, H. (Eds.), Chlorophylls and Bacteriochlorophylls - Biochemistry, Biophysics, Functions and Applications, 25, Advances in Photosynthesis and Respiration. Springer, The Netherlands, pp. 39-53.
- Zhang, J., Gilbert, D., Gooday, A.J., Levin, L., Naqvi, S.W.A., Middelburg, J.J., Scranton, M., Ekau, W., Peña, A., Dewitte, B., Oguz, T., Monteiro, P.M.S., Urban, E., Rabalais, N.N., Ittekkot, V., Kemp, W.M., Ulloa, O., Elmgren, R., Escobar-Briones, E., Van der Plas, A.K., 2010. Natural and human-induced hypoxia and consequences for coastal areas: synthesis and future development. *Biogeosciences* 7, 1443-1467.
- Züllig, H., 1984. Preliminary report on the occurrence of the pigment okenone originating from purple bacteria in lake sediments. *Schweizerische Zeitschrift für Hydrologie-Swiss Journal of Hydrology* 46, 297-300.
- Züllig, H., 1985a. Carotenoids from plankton and purple sulfur bacteria in lake sediments as indicators of changes in the environment. *Experientia* 41, 533-534.
- Züllig, H., 1985b. Pigmente phototropher Bakterien in Seesedimenten und ihre Bedeutung für die Seenforschung. *Aquatic Sciences* 47, 87-126.

Curriculum vitae

Personal details

Name: Sebastian Näher

Date of birth: July, 26th, 1984

Place of birth: D-55765 Birkenfeld, Germany

Nationality: German

Education

- | | |
|-------------------|---|
| 08/2009 – 10/2012 | Doctoral candidate at Eawag Kastanienbaum (Swiss Federal Institute of Aquatic Science and Technology), Department of Surface Waters – Research and Management, and ETH Zurich, Institute for Biogeochemistry and Pollution Dynamics |
| 12/2008 – 05/2009 | Diploma thesis at Johannes Gutenberg University in Mainz and IWW Rhine-Main in Biebesheim/Rhein, Germany (degree: Dipl.-Geol.) |
| 10/2007 – 05/2009 | Undergraduate in geology in the Institute of Geosciences, Johannes Gutenberg University of Mainz, Germany |
| 10/2006 – 10/2007 | Undergraduate in geology in the Department of Earth Sciences, ETH Zurich, Switzerland, with an Erasmus studentship of European Union |
| 04/2004 – 10/2006 | Undergraduate in geology and chemistry in the Institutes of Geosciences and Chemistry, Johannes Gutenberg University of Mainz, Germany |
| 03/2004 | Abitur at Gymnasium Hermeskeil, Germany |